R.A. Schalk

Data Analytics for RCF Damages on the Dutch HSL Track

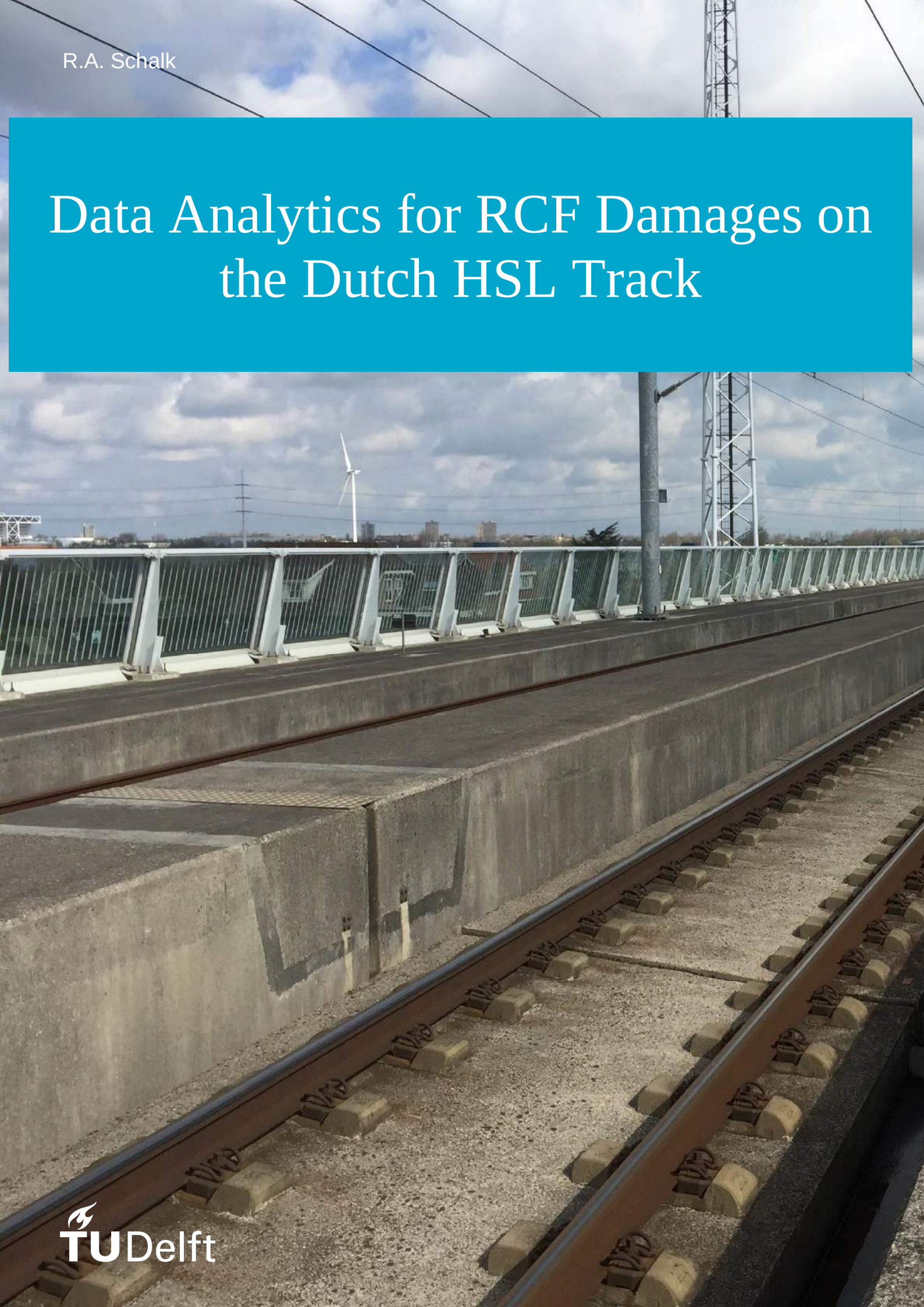

TU Delft

Data Analytics for RCF Damages on the Dutch HSL Track

By

R.A. Schalk

in partial fulfilment of the requirements for the degree of

Master of Science
in Construction, Management and Engineering

at the Delft University of Technology,
to be defended publicly on Friday September 23, 2016 at 15:00.

Supervisor:	Dr. ir. Arjen Zoeteman	TU Delft
Thesis committee:	Prof. dr. ir. Rogier Wolfert,	TU Delft
	Dr. Alfredo Núñez Vicencio,	TU Delft
	Ir. Aad Hertogs,	Infraspeed

An electronic version of this thesis is available at http://repository.tudelft.nl/.

TU Delft

Preface

This master thesis is the result of a study regarding damages related to rolling contact fatigue at the HSL-South in the Netherlands. The study has been executed during an internship period at Infraspeed Maintenance B.V. which is the rail infrastructure manager for the HSL-South. The sections of integral design and management and railway engineering have taken care of the supervision at the Delft University of Technology. The focus of this study was to propose an integrated method to evaluate rail conditions by using measurements and data analysis in order to be able to see which characteristics have an influence on the occurrence of rolling contact fatigue.

I would like to thank Arjen Zoeteman for his help during the process and his constructive review of my work. Also I would like to thank Prof. Wolfert for his valuable advices and suggestions. Also many thanks to Alfredo Núñez to whom I could always come for questions and helped me on track as a newcomer to railway engineering. Also Aad Hertogs, thank you for the experience at Infraspeed and the opportunities which have been created there for my research. Last but not least I would like to thank my family and friends for their support during the study.

Ricks August Schalk

Delft, September 2016

Abstract

Data analytics are today a common way to process available data and gain valuable insights in the connections between the data to support decision making. The aim of this study is to show how data analytics can help rail infra managers in supporting coping with different problems. In this thesis the use of data analytics will be demonstrated for rolling contact fatigue (RCF) damages, affecting a railway track. RCF is an issue affecting the integrity of the rails and influences the safety and availability of the tracks. However, as RCF can appear in different forms and have different causes it is not always clear what the influencing factors are regarding RCF at a specific track or track sections. The focus of this study was to be able to determine influencing parameters regarding RCF damages for a railway track. Two approaches and a combined approach are proposed in this thesis in order to determine these influencing parameters. These approaches have been developed to be used after rail condition measurements and interpret this data. Eddy current inspection has been chosen to evaluate rail conditions as this method is currently the standard technology to detect and measure early cracks. The use of these approaches has been demonstrated at a case study for the HSL-South in the Netherlands.

The rail condition has been approached as the interaction between track geometry, rolling material and maintenance parameters. The parameters used, have been selected according a literature study regarding the root causes of RCF. These root causes have been interpreted and processed into a series of relevant parameters, which are both quantitative and qualitative. The parameters are being used to evaluate the whole track by partitioning. For the HSL-South partitions of 500m have been evaluated, which proved an appropriate length to provide enough detailed information.

In order to evaluate the rail conditions, eddy current measurements have been transformed into a numerical parameter which represents the rail conditions. This numerical parameter has been named: intensity. The intensity was processed to give a numerical representation of both the number of defects and the depth of defects for a track partition. The intensity has proven its value as it was able to accurately show the hotspots at the HSL-south.

The first approach presented in this thesis is the bottom-up approach (B-U approach), which is designed to evaluate the worst affected areas at a railway track (hotspots). The hotspots had been defined using certain characteristics for identification. In this approach these hotspots are evaluated using several data processing techniques like, identifying similar parameter values and clustering into types of hotspots. These types of hotspots are defined according sets of characteristic parameter values. These characteristic parameter values are then interpreted on how they can be related to the RCF at these hotspots. Accordingly, this will then be evaluated using literature and developed into a hypothesis for each hotspot type. The last step in the B-U approach is testing the rest of the track for this set of characteristic parameter values and see whether these are to be found and whether RCF also occurs among these areas. The B-U approach proved to be valuable in the case of the HSL-South, two types of hotspots had been identified as the ‘open track hotspot’ and the ‘entry zone hotspot’. Also influencing parameters like cant excess, 350HT rail grade and cant excess through curves had been identified. It also showed clearly that the rail damages are related to the use TRAXX locomotives which drive below design speed.

The second approach which has been introduced was the Top-Down approach (T-D approach). This approach, opposed to the B-U approach, evaluates the measurements for the whole track. The T-D approach is based on the intensity and how it relates to other parameters with respect to the whole track. The main aim of the T-D approach is to be able to mark significant relations and to rank them in order to evaluate which are the main influencing parameters. The technique which has been used here regarding quantitative parameters was the introduction of Pearson’s correlation which enables to see linear relations between two parameters. For the qualitative parameters, visual data techniques like bar graphs and boxplots have been used to evaluate how the intensities relate to qualitative parameter values. The T-D approach was able to find most of the same influential parameters for the HSL-South as the B-U approach and was able to find significant correlations regarding the traction of the TRAXX and intensities.

Also a combined approach is proposed which uses the findings of the B-U approach to evaluate certain track parts with the techniques of the T-D approach. Here the characteristic parameter values regarding the hotspot types can be used in order to check the hypothesis regarding the hotspot types. Which mostly verified the initial findings regarding the open track and entry zone hotspot types.

List of figures

List of tables

Table of contents

1. Introduction

Rail infrastructure maintenance companies cope with several issues to keep their tracks at top condition in order to provide safe and comfortable traffic conditions regarding their tracks. One of these issues is coping with rolling contact fatigue (RCF) which is an issue related to the small wheel-rail contact area where the loads of the train are being transferred to the rails. Every cycle of a train wheel will result in a stress cycle in both the wheel- and rail materials, this will eventually lead to material fatigue during its lifetime (Dollevoet, 2010). This material fatigue can be visible as cracks in the rails which can lead to various problems like delays or even rail breaks. Therefore its desirable to control the rail conditions, detect early defects and treat them before they grow into serious defects. An example of RCF damage at the HSL-South can be seen in Figure 2.

Figure 2: Example of RCF at a rail, which is visible as small cracks at the rail surface.

Many railways are being used by different types of rolling stock, i.e. normal-, high-speed passenger traffic or freight traffic. Different types of rolling stock behave differently regarding rail-vehicle interaction. It is therefore desirable to know for each type of rolling stock how it interacts with the rail structure and to what extent each type contributes to the RCF issues for a certain track. Also the track geometry and rail maintenance actions influence the wheel-rail interface. However, it is often unclear which of these factors contributes at which extend to the formation of RCF damages at a certain track- or track partition. This thesis will present two approaches to evaluate rail conditions and relate them to parameters influencing these conditions. The research question for this thesis will therefore be:

How can data analysis be used to find influencing parameters regarding root causes for RCF damages for a railway track?

In order to answer this question a set of sub-questions is formulated which will help to be able to investigate the main research question:

- *What kind of RCF damages affect rails?*
- *What are the root causes for RCF damages?*
- *Which track parts are most vulnerable to RCF damages?*
- *Are the current rail monitoring practices sufficient to detect RCF damages timely?*
- *Which data analysis techniques can be used to determine influencing parameters?*

The set-up of the report is shown in Figure 3. The second chapter will provide the theoretical background regarding railway design, RCF damages and maintenance and monitoring techniques for this study. For this chapter a literature study has been conducted by the author which aims at answering the first four sub-questions.

The methodology chapter will provide the data analysis techniques which will be used to develop two approaches to find influencing parameters for RCF damages on a railway track. In this chapter, the last sub question will be answered and the approaches are presented stepwise.

Also a case study has been done in order to demonstrate the use of the two approaches and the combined approach and to see how their results compare. The case study has been done for the HSL-South in the Netherlands.

The final chapter will discuss the results for this study also recommendations for future research will be presented. In the Appendix additional information is presented regarding the use of each the parameters, also additional data in the form of figures and measurements can be seen here.

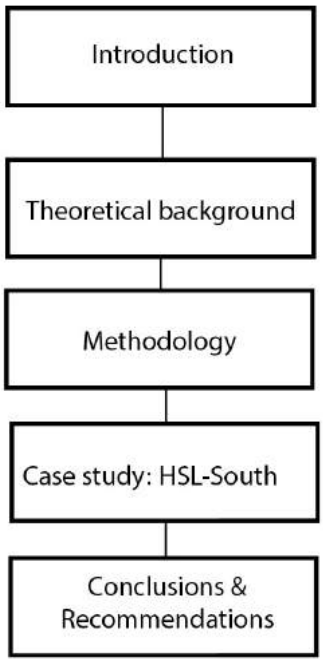

Figure 3: Schematic representation of the structure of this thesis.

2. Theoretical background

This chapter will discuss the theoretical background of this thesis. The general characteristics for track geometry, vehicle rail interaction, rail defects and rail maintenance and monitoring techniques will be described. This in order to provide adequate information for answering some of the sub questions. This will eventually result in a selection of parameters which will be used in the third chapter. A literature study has been the basis for this chapter. The most basic track geometry definitions are shown in A.2. Track geometry.

2.1. Rail-vehicle interaction

2.1.1. Rail profile parts

The different rail components are presented in Figure 4. These names will be used often in the discussions regarding the contact positions and at what areas the forces are being transferred to the rails.

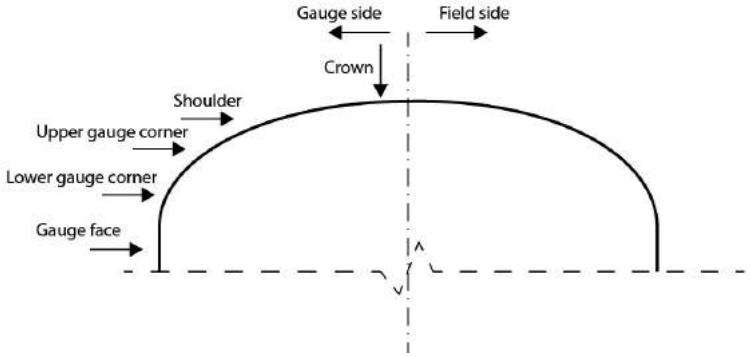

Figure 4: Names of the rail profile components.

2.1.2. Static forces on the rail

There are four types of static forces on the track, namely: vertical forces, longitudinal forces, acceleration and breaking forces and lateral forces. In this section each will be briefly described. An overview of the forces on the rail is shown in Figure 5.

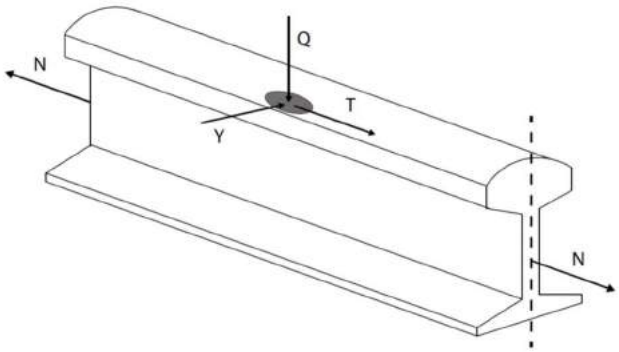

Figure 5: Overview of the forces on the rail.

Vertical forces

Vertical forces (Q) are the consequence of the loads transmitted through the wheels at the rail surface. Though these vertically transmitted loads can vary due to different circumstances like: irregularities in the railhead and in curves due to free lateral acceleration (Lichtberger, 2005). Also for different types of tracks different axle loads are used, for high-speed traffic the typical axle load is 200kN at maximum.

Longitudinal forces

Longitudinal forces (T) may occur on the track in several occasions (Lichtberger, 2005):

- Due to the change of length in the rails caused by temperature (N).
- Longitudinal forces caused by acceleration and braking.
- Due to the internal stresses in the rail after welding.
- Due to rail creep.

Acceleration and braking forces

Driven axles have the effect of generating additional longitudinal forces on the rails due to friction at the wheel-rail interface. Also resulting in tension in front of the driven axle and compression behind the driven axle (Lichtberger, 2005). The impact of these longitudinal forces generated by acceleration depends on the wheel forces and the friction coefficient. When trains brake, another effect occurs namely that the compression takes place in front of the braking wheelset. Also in this case longitudinal forces are being executed on the tracks.

Lateral forces

A moving vehicle also generates lateral forces (Y) at the wheel-rail interface which stresses the rail horizontally and at a right angle to the track axis. This force may be split into a centrally acting part *Q*, a torsional moment *M* and a lateral force *Y* (Lichtberger, 2005). The amount of lateral forces excited at the wheel-rail interface depend on vehicle specific and geometric characteristics like axle loads, wheelbase, bogie design, curvature and speed.

2.1.3. Dynamic forces on the rail

Traction

High traction and breaking efforts are known to raise maximum shear stresses from the subsurface of the rails to the surface of the rail (Z Li, 2009).

An effect related to traction in curves is that when a vehicle drives through a curve at or above the balance speed (cant deficiency) the traction ratio is greater at the high rail than low rail. Therefore, plastic flow is expected to occur more often on the higher rails in the curves (Grassie & Kalousek, 1993). The situation would be different for a vehicle driving under cant excess through a curve, here the traction ratio on the lower rail increases. This occurs often when the leading wheelset shifts to the high rail and the trailing wheelsets to the low rail.

Adhesion

Adhesion, or the coefficient of friction between the rail and wheel is regarded as an important issue for safe, reliable and efficient railway operations. For braking it is a safety issue, regarding traction it is more a performance issue. It is also important to notice that whenever tractive or breaking efforts exceed the available adhesion, slipping occurs and temperature rises at the wheel-rail interface which can cause metallurgical transformation of both wheel and rail (Tanvir, 1980).

Friction

The definition for friction force is the resistance encountered by one body moving over another, this goes for both sliding and rolling bodies (Lewis & Olofsson, 2009). Pure rolling (without traction) always involves some sliding. Acceleration and breaking require a coefficient of friction at the wheel-rail interface which is the ratio of the tangential load to the normal load. This ratio is usually around 0.2 (Olofsson, 2009). The friction forces always operate in the direction parallel to the motion of the wheel.

Inadequate friction coefficients also lead to poor adhesion, resulting in larger stopping distances and affect traction limiting the tangential forces which can be developed in curves (Olofsson, 2009). Lubricants or friction modifiers can be used to avoid too large contact stresses which cause excessive wear to the rails and wheels (G. Evans, 2013).

Figure 6 shows the wheel-rail interface at the rail as an ellipsoid. This area can be divided in two regions, namely the stick and slip regions. At the slip regions longitudinal creep and lateral forces arise in the trailing region of the contact area. In Figure 6, it can be seen that when the tangential forces increase also the slip region at the contact area increase and the stick decreases. This results in rolling and sliding at the contact area (Olofsson, 2009). The maximum level of tangential forces depends on capacity at the interface to absorb the adhesion.

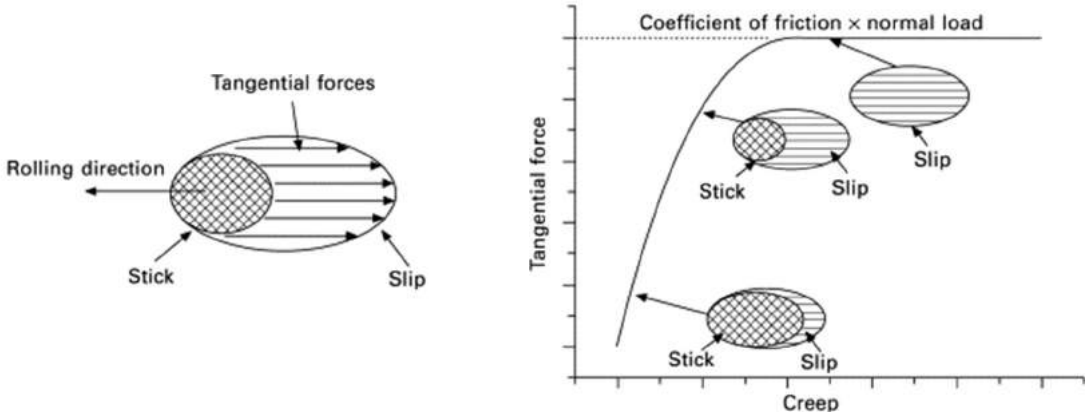

Figure 6: The relationship between tangential forces and creep at the wheel-rail interface. Source: Olofsson, 2009, Adhesion and friction modification

2.1.4. Wheel-rail contact positions

There are different contact situations at the wheel rail interface as shown in Figure 7. Though, it seems this contact occurs in points, in reality the stress distribution occurs in ellipsoids. Situation (A) shows single point contact at the gauge face. Situation (B) shows single point contact at the gauge corner. Situation (C) shows single point contact at the head of the rail. In these three situations both tangential and vertical forces are transmitted to the rail at a single ellipsoid area when the wheel is in motion. Situation (D) shows a dual contact situation which also occurs often, here the contact points are at the rail head and gauge face. In this situation the lateral forces are transmitted through the gauge face and the vertical forces at the rail head. This situation occurs for example when the first axle enters a curve. Not that dual contact also results in a difference in rolling radius for these contact positions which can cause slip at either one of them.

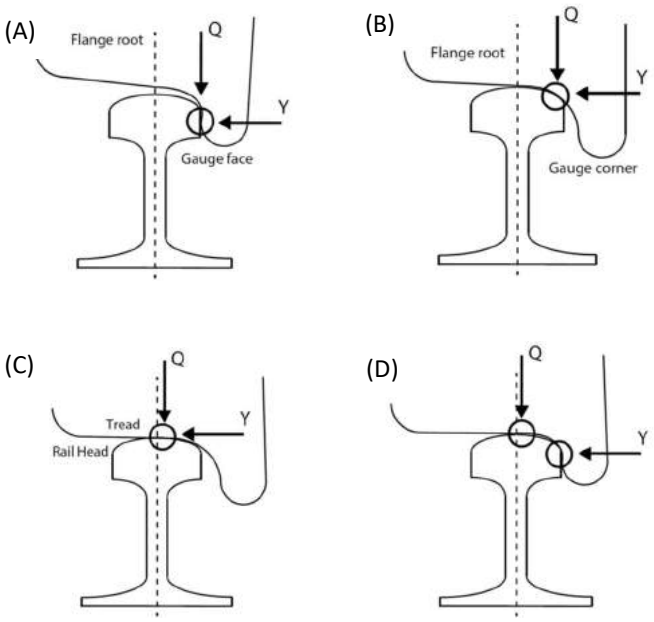

Figure 7: Different contact positions for the wheel and rail.

2.1.5. Cant Deficiency

The ideal cant applies only for a small speed range. Therefore, uniform traffic for railways is recommended. The ideal cant deficiency lies between 20-40mm, which ensures stable driving conditions for the trains and being led by the outer leg in the curve (AM Architectuur en Techniek, 2015).

The general situation of a train in a curve is shown in Figure 8. In this figure a train runs through a curve with radius R and cant h with a constant speed v. The resultant of the non-compensated lateral acceleration on the vehicle has been described by (Esveld, 2001) as:

$$a_d = \frac{v^2}{R} - \frac{gh}{s}$$

In which:

a_d: Resultant non-compensated lateral acceleration
v: Running speed [m/s]
R: Curve radius
g: Acceleration due to gravity $[= 9{,}81 m/s^2]$
h: Cant [mm]
s: Track width [=1500mm]

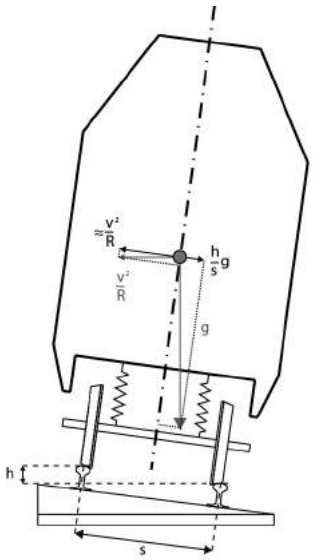

Figure 8: Situation of a train in a curve.

Cant deficiency h_d is the difference between the theoretical cant and the actual cant, and is formulated as (Esveld, 2001):

$$h_d(x,t) = \frac{sv(x,t)^2}{gR} - h$$

In which:

h_d: cant deficiency [mm]
x: location
t: moment in time
v: running speed [m/s]
R: curve radius [m]
g: acceleration due to gravity (=9,81m/s²)
h: cant [mm]
s: track width (=1500mm)

The cant deficiency must satisfy the following condition:

$$h_d(x,t) = 11{,}8 * \frac{V_{\max}^2(x,t)}{R} - h < \bar{h}_d$$

$\bar{h}_d$: maximum cant deficiency by norms [mm]
V_{max} : maximum running speed [km/h]

The norms for allowed cant deficiencies vary among different organizations. ProRail, the Dutch government and the European government handle different norms for their allowed cant deficiencies. These norms have been set, because too high cant deficiencies can have bad consequences as it can cause excessive wear to the outer leg (and wheel), discomfort for passengers and even derailment is a risk. ProRail handles their own norms and exceptional value for their tracks and can be found in Table 1 (AM Architectuur en Techniek, 2015).

The Dutch regulations for cant deficiencies were replaced in 2012 where they implemented the European Union regulations (Schultz van Haegen-Maas Geesteranus, 2012). Though during the period of 2005-2012 there were regulations regarding maximum cant deficiencies (Minister van Verkeer en Waterstaat, 2005).

The European norms regarding cant deficiencies are stipulated in INF – TSI 1299 which became applicable from November 2014 ("INF - TSI 1299/2014/EU," 2014).

Table 1: Norms and values for allowable cant deficiencies as prescribed by different organizations.

	ProRail		**Dutch Government**	**European Union**
Speed limits (km/h)	200<	200-300	200<	160-300
Norm Value (mm)	100	80	150	153
Exceptional Value (mm)	120	100	-	-

In general, in curves the wheels roll in the direction they are facing, the leading wheelset tends to roll to the outside of the curve whereas the trailing wheelset tends to roll to the inside of the curve (J. Evans & Iwnicki, 2002). This causes some effects in the curves, regarding the coning of the wheels, as both wheels have the same rotational speed they will have contact under different wheel radiuses. The larger wheel radius will attempt to roll further than the inner wheel thus the steering moment will follow the curve. Therefore during design small cant deficiencies are desired. Too big differences in rolling radius can cause wheel slip. And zero cant deficiency (within theoretical cant) causes no lateral acceleration in the curve, which causes the vehicle to theoretically react to any irregularity and unstable behaviour.

2.1.6. Cant Excess

Cant excess can occur when low running speeds are reached and therefore the train moves to the direction of the lower rail in the curve. Substantial cant excess can cause a high load on the low rail in the curve (Esveld, 2001). Cant excess can be calculated using the following formula:

$$h_e(x,t) = h - 11{,}8 * \frac{V_{min}^2(x,t)}{R}$$

In which:

h_e: cant excess [mm]
x: location
t: moment in time
h: canting [mm]
V_{min}: minimum speed [km/h]
R: curve radius [m]

For the maximum cant excess there are less legal regulations, because when the train is shifting towards the lower leg, there is no risk for derailment. Though large cant excess can cause passenger discomfort and damages due to high loading to the rails also excessive wear to the inner leg (and wheel) is one of its effects.

The maximum allowed cant excess is formulated as:

$$h_e(x,t) = h - 11{,}8 * \frac{V_{min}^2(x,t)}{R} < \bar{h}_e$$

In which:

h_e: cant excess [mm] $\bar{h}_e$: maximum cant excess norms [mm]

Regarding the regulations, ProRail has its own norms and exceedance values concerning allowed cant excess, as can be viewed in Table 2. The Dutch government and European Union have since 2012 no regulations regarding cant excess, as there are no regulations in the applicable INF-TSI 1299. Before this, the Dutch government handled a maximum value of 90mm (Minister van Verkeer en Waterstaat, 2005). To have an international comparison between Dutch and international regulations, the values the Deutsche Bahn handles for speeds over 250km/h have been included in Table 2 (Esveld, 2001).

Table 2: Regulations from different institutions regarding cant excess.

	ProRail		Dutch Government	Deutsche Bahn
Speed limits (km/h)	200<	200-300	200<	>250
Norm Value (mm)	70	50	90	50
Exceptional Value (mm)	90	70	-	70

Cant excess results into some undesired effects, one being the different steering moment through the curve as shown in Figure 9. Where for cant deficiency a steering moment along the direction of the curve is created. For cant excess the steering moment is opposed to the direction of the curve.

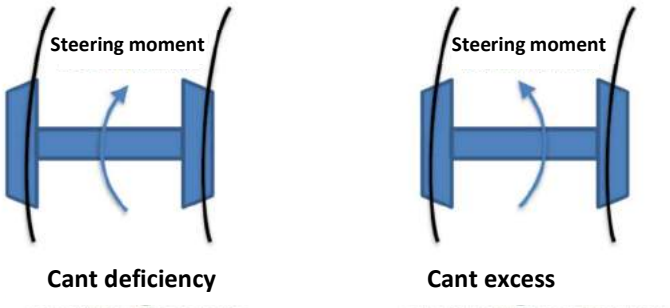

Figure 9: Different steering moments in a curve for cant excess and cant deficiency.

Another effect of cant excess is the different distribution of the vertical loads on the legs as shown in Figure 10. For cant excess more loads are transferred to the inner leg of the curve. The train will shift to the inner leg when the lateral acceleration to the lower leg exceeds the shear resistance.

Figure 10: Different distribution of the vertical loads in a curve on the rails for cant excess and cant deficiency.

2.1.7. Surface waves

Regarding a moving train vibration is generated by two mechanisms according to (Thompson & Jones, 2009):

- The movement of a quasi-static load along the track on the ground surface.
- Excitation due to roughness of the wheel and rail surfaces, in the same way as for rolling noise.

When dynamic track loads are considered, it usually assumes the track load is stationary. However, the running speed has an influence on the dynamic interaction between track and vehicle. Therefore it is important regarding track design to take the speed range into account. As different track and subsurface stiffness's should be taken into account.

This situation is modelled based on a moving vertical constant load on a single beam on an elastic foundation with damping as shown in Figure 11:

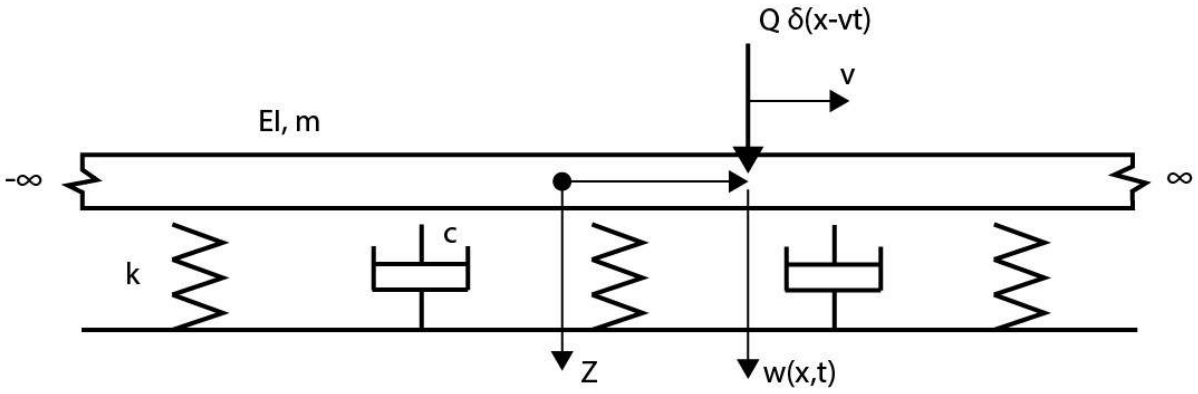

Figure 11: The elastic beam-model with a moving load. In which: EI [Nm2], m [kg/m], c [Ns/m2], k [N/m2], q [N/m], Q [N], v [m/s], x [m], t [s], w [m].

This is the system as proposed by (Esveld, 2001). This can be reduced to the following equation regarding the track, using Esveld's formulas and equations:

$$EI\frac{\partial^4 w(x,t)}{\partial x^4} + m\frac{\partial^2 w(x,t)}{\partial t^2} + c\frac{\partial w(x,t)}{\partial t} + k\,w(x,t) = 0$$

Introducing a new dimensionless variable s and λ, the inverse of the static characteristic of the length of the track $(1/L)$ indicating a moving set of variables:

$$s = \lambda(x - vt), where: \lambda = \left(\frac{k}{4EI}\right)^{\frac{1}{4}} = 1/L$$

After substitution the following equations are obtained:

$$\frac{\partial w}{\partial x} = \lambda \frac{dw}{ds}; \frac{\partial w}{\partial t} = -\lambda \frac{dw}{ds}, etc.$$

The homogenous normal differential equation regarding variable s now gives the following equation:

$$\frac{d^4w}{ds^4}(s) + 4\alpha^2 \frac{d^2w}{ds^2}(s) - 8\alpha\beta \frac{dw}{ds}(s) + 4w(s) = 0$$

in which the resonance α (ratio between actual speed and critical speed) is:

$$\alpha = \frac{v}{2\lambda}\left(\frac{m}{EI}\right)^{\frac{1}{2}}$$

And the ratio between actual and critical damping β is:

$$\beta = \frac{c}{2m}\left(\frac{m}{k}\right)^{\frac{1}{2}}$$

The highest mechanical loading at the track takes places when trains reach the so-called critical speed. Which can be calculated according the following equation:

$$V_{cr}^2 = \frac{2}{m}\sqrt{kEI}$$

In which:

m: rail mass per length EI: bending stiffness

k: Track stiffness

By conventional traffic the critical speed will not be reached as this speed is much higher. Though for high-speed traffic this should be taken into consideration as a design criterion. As the critical speed regarding a certain track is highly influenced by both the soil conditions and the superstructure used, which are used for the critical damping. Basically three situations can occur concerning actual- and critical speed. The first situation is the actual speed being slower than the critical speed. In this situation the load creates an Eigen field with respect to the wave and load velocities as shown in Figure 12 (A). The second situation is when the actual speed exceeds the critical speed then wave radiation with respect to the speed of the surface waves takes place. The speed of the load then exceeds the Raleigh velocity causing wave radiation behind the load as shown in Figure 12 (B).

The third situation occurs when the ratio of the actual speed and critical speed (α) is 1. Here we also have to take into account what kind of damping conditions occur concerning the actual versus the critical damping (β). For undamped cases (β=0) the wave amplitudes will become infinite. For small damped cases (β≈0,1) very large wave amplitudes will occur.

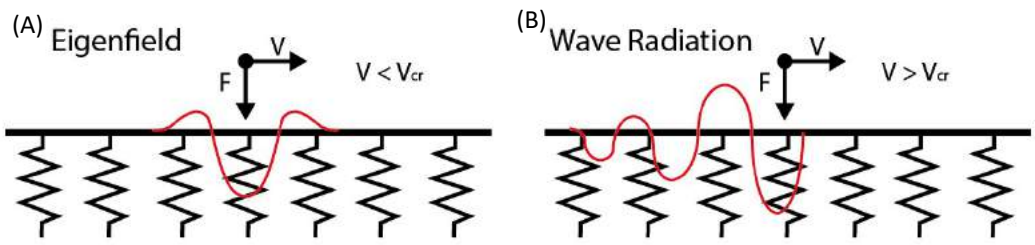

Figure 12: Illustration of two situations regarding surface waves and their relation to the traffic speed. (A) The eigenfield with respect to wave- and load velocity. (B) Wave radiation.

2.2. Rail damage

2.2.1. Squats

Squats occur at the top of the rails within the running band, most commonly in straight track and large curves (Z Li, 2009). They have been found on both ballast and slab-track. They also occur on all different kinds of lines like passenger, mixed traffic, high-speed and metro lines.

Figure 13 shows an example of a squat on a rail. A mature squat usually has a 'two-lung' shape and a widened running band. The cracks are commonly U, V or Y shaped, these cracks can branch down when at a depth of 3-5mm (Dollevoet, 2010).

The causes of squats have been investigated by (Z Li, Zhao, Esveld, Dollevoet, & Molodova, 2008) using a correlation analysis. Concluding squats can be associated with the occurrence of rail surface irregularities like indentations, wheel burns and short-pitch corrugation (Z Li, Zhao, Esveld, et al., 2008). Another theory regarding the initiation of squats is related to the white edging layer at the surface area of the rail (Carroll & Beynon, 2007a). Squats are also often associated with high-speed traffic and areas with high tractive effort (Magel, 2011). Also local stiffness variations are known to play a role in the occurrence of squats. This has been shown in a parameter study by (Z Li, Zhao, Dollevoet, & Molodova, 2008), where deteriorated fishplate insulated joints under well-preloaded conditions showed large contact variations which can initiate squats.

As squats are being associated with high-frequency vibrations of the wheel-rail system which can be registered by axle box acceleration (ABA) measurements, a finite element model has been described by (Molodova, Li, Núñez, & Dollevoet, 2014b), where is shown that (ABA) measurements can be used for the detection and assessment of severity of squats. The early detection of squats has by ABA measurements has been further reported in other papers by the same group (Molodova, Li, & Dollevoet, 2011), (Molodova, Li, Núñez, & Dollevoet, 2014a) and (Z. Li, Molodova, Núñez, & Dollevoet, 2015). Other methods like video images are more prompt to contamination and other effects that compromise the quality of the detection (Faghih-Roohi, Hajizadeh, Núñez, Babuska, & de Schutter, 2016). Squats in rails can be treated by grinding or milling the rails.

Figure 13: Example of a squat on a rail. Source: http://file.scirp.org/Html/4-7401350_31574.htm

2.2.2. Head checks

Head checks can be classified as a group of fine surface cracks which occur at the gauge corner of a rail, the distance between these cracks is generally between 0.5-0.7mm (Larsson-Kråik, 2009). An example of head-checks is shown in Figure 14. Head checks are often found in curves with radii smaller than 3000m and in switches and crossings, at these locations they are found mostly on the outer rail (Dollevoet, 2010).

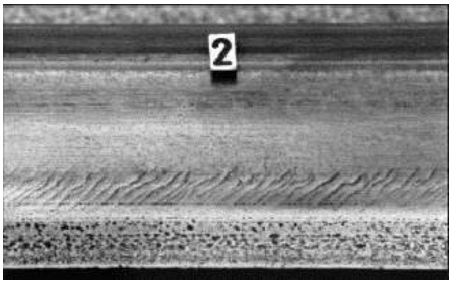

Figure 14: Example of head checks on a rail. Source: http://www.ndt.net/article/v07n06/thomas/thomas.htm

Head checks result from accumulation of ratchetting which exhausts the ductility of the surface material where the first point cracks can initiate. The conditions which are considered to be critical for the initiation of head checks are high loading and friction (Lewis & Olofsson, 2009).

Initially these cracks grow under a shallow angle with the rail surface but at later stages they tend to grow under a more steep angle into the rail (Dollevoet, 2010). The crack growth in the initial phase is driven by ratchetting in the plastically deformed layer. As the crack becomes longer and deeper the growth is driven by the stresses due to repeated contact loading. In the final phase when the crack turns downwards the bending stresses of the rail play a major role (Kapoor, Fletcher, & Franklin, 2003). When head checks reach critical lengths this can result into rail breaks.

2.2.3. Studs (spalling defects)

Studs or spalling defects were only recently reported and are not to be confused with squats, though they share some superficial similarities. An example of the studs which have been found at the HSL is shown in Figure 15. Studs have first been characterised by S.L. Grassie during studies at the London underground tracks. The characteristics of the stud are described by as*: 'a V-shaped surface-breaking crack whose apex pointed to the field side of the rail'*(Grassie, Fletcher, Hernandez, & Summers, 2011). The risk of the stud is that it can spall out when it has been well developed. They initiate at the head of the rail, often towards the gauge corner and then often grow towards the field side of the rail, so they develop across the rail (Grassie, 2015).

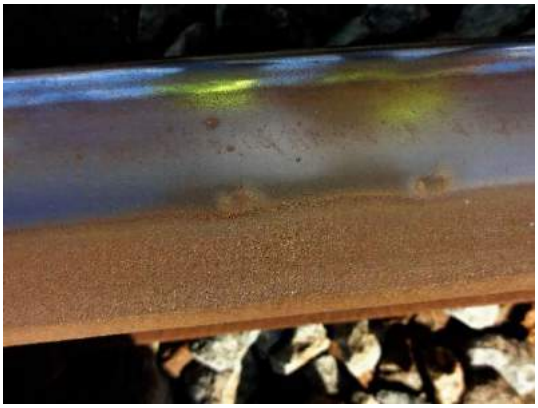

Figure 15: Example of the studs which have been found at the HSL-South.

The studs which have been examined in Grassie's study had some specific characteristics like the occurrence in so-called hotspots where they were found in great numbers. These hotspots occurred mainly in open areas, in several occasions in areas where the trains approach signals and often had to brake or give traction and in areas where a vertical gradient was present and trains are constantly driving under high tractive efforts (Grassie, 2012). Furthermore there is also some evidence from Australian experience that studs seem more prevalent in head-hardened than standard carbon rail (Wilson, Kerr, Marich, & Kaewunruen, 2012).

It also occurs that the studs develop rather quickly compared to other defects like squats. For instance, some studs were found on rails which were placed three months before. They have been found in both curves and straight track. The cause of studs and initiation mechanism is not yet fully understood. Thermally transformed

material had been found in several occasions together with studs and a possible cause could therefore be wheel-slip (Grassie, 2015).

2.2.4. Corrugation

There are many types of corrugation, short- and long pitch corrugation based on the periodicity are some of the most common. Both defects are caused by traffic loads and most often appear in curves, but can also occur in tangent tracks. In corrugated rails, the loads are not evenly distributed among the rail surface. Therefore some areas will occur with higher loads, higher plastic deformation, higher hardening and more wear, while neighbouring areas will have less plastic deformation (Feller & Walf, 1991).

Short-pitch corrugation can be characterized by the irregular sequence of bright ridges and dark hollows which appear at the running surface (Esveld, 2001). An example of short-pitch can be seen in Figure 16. The pitch most often varies between 3- and 8 cm. Short-wave corrugation regarding curves has been reported by (Torstensson & Nielsen, 2009), where is shown that the magnitude of corrugation can vary among the curve after grinding. (Grassie, 1996) reported in a study regarding short-pitch corrugation for the British railways that it is caused by differential wear among the rail surface.

Figure 16: Example of short-pitch wave corrugation at the HSL-Zuid at the Hoofddorp location taken in November 2014.

The difference with long-pitch corrugation is that this corrugation leaves no difference between the appearance of ridges and hollows, the pitch is also longer than the short-pitch and varies between 8 and 30cm (Esveld, 2001). Long pitch corrugation appears mostly on the lower legs in the curves and is found mostly as depressions at the running surface here. For both types, grinding is recommended in the early stages.

However, some more distinctions can be made between corrugation types. There are actually two types of characteristics; the wavelength-fixing mechanism and the damage mechanism (Grassie & Kalousek, 1993). From this a total of six types of corrugation have been described by Grassie and Kalousek as: heavy-haul, light-rail, p2 resonance, rutting, roaring and track form specific corrugation.

2.2.5. White edging layer

White edging layer (WEL) result from changing microstructure of the rail surface material from pearlite to a martensite structure which is extremely brittle and therefore crack initiation occurs more often in this layer (Pyzalla, Wang, Wild, & Wroblewski, 2001). The name 'white edging layer' arises from its resistance to edging through acids during the metallographic preparation and because of its white appearance under an optical microscope (Carroll & Beynon, 2007b).

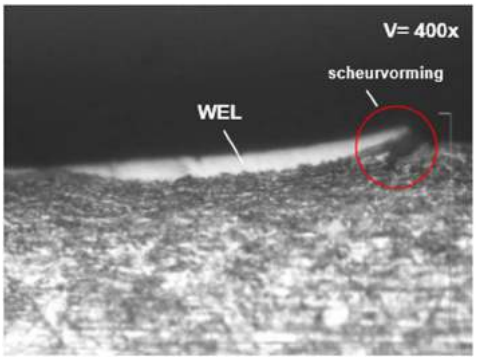

Figure 17: Picture of the WEL at the Hoofddorp hotspot. Source: (van der Stelt, 2015)

White edging layer is a layer formed on the surface of the rail. Because of the loads and the speed of the trains running over the tracks, the contact zone of the rail and the wheel is exposed to mechanical and thermal loading, which leads to changes in the microstructure (Wild & Reimers, 2004). Thus, the wear of the wheel and rail profile does not only develop through the average mechanical and thermal loading but is also time dependent.

White edging layers are zones on the surface which are not etching. These arise when thermal loads lead to transformation of the structure (formation of martensite) or lots of plastic deformation (Carroll & Beynon, 2007a). The depth of the layer commonly found on the rails has a maximum of about 100µm (Carroll & Beynon, 2007a). Because of the transformation by thermal loads the hardness of WEL is much more than that of the rail itself and different types of cracks can initiate in the WEL and eventually grow in the rail (Carroll & Beynon, 2007a). Carrol and Beynon also conclude that '' the WEL makes the rail more vulnerable as the WEL may help to initiate cracks which would not form if the WEL were not present'' (Wild & Reimers, 2004).

As of 2016 a paper by (S. Li et al., 2016), also discusses the findings of another layer (brown edging layer) which is closely related to the WEL. Which thanks its name to the brown appearance after edging. Similar to the WEL also cracks appear to be related to the brown edging layer but penetrate deeper than cracks initiated by WEL.

2.2.6. Growth of cracks

Before discussing the mechanisms under which cracks can grow, it is important to take into account the effect of wear under influence of the wheel at the rail. This because, when a wheel rolls over a crack contributes to the crack growth but at the same time it also causes wear of the rail which again shortens the present crack. Thus there are two conditions possible, the crack growth rate is greater than wear rate and the other one being the wear rate is greater than crack growth rate (Jun, Lee, & Kim, 2015).

There are several mechanisms under which cracks grow into rails, these are presented in Figure 18 and are the standard RCF growth mechanisms (Scott, Fletcher, & Cardwell, 2014). When shear crack growth (a) occurs the crack growth is driven by the shear stresses which occur cyclic at the wheel-rail interface. The other three are crack growth mechanisms in which fluids in the crack play a major role. For the hydraulic crack growth (b) the fluid is trapped in the crack and when the wheel drives over the crack it causes pressure on the fluid, driving the crack growth. The fluid entrapment crack growth mechanism (c) is the mechanism where the crack closes when the wheel passes over it and the fluid is entrapped and pressurized. This causes high pressure at the crack faces and tensile stresses at the tip of the crack causes the growth (Dollevoet, 2010). In the squeezed film crack growth mechanism (d) a fluid is trapped in the crack and growth in the direction of the load motion, the crack mouth

opens under tractive effort, drawing the fluid in where it expands under pressure as the wheel passes over and the crack is closed (Bogdanski, 2002).

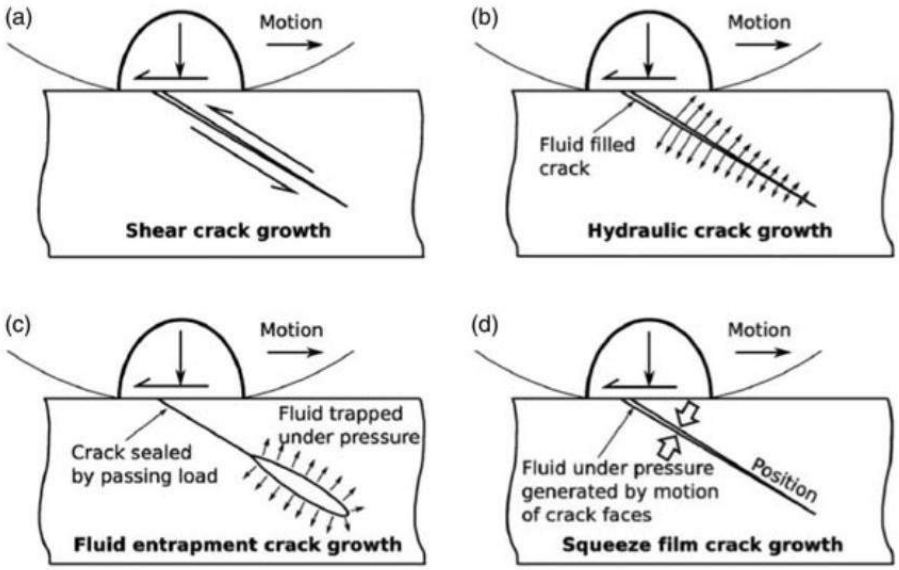

Figure 18: Schematic representation of crack growth mechanisms. Source: Scott, Fletcher and Cardwell, 2012, simulation study of thermally initiated rail defects.

2.3. Maintenance and monitoring techniques

Maintenance actions can be divided as shown in Figure 19. In this paragraph the actions regarding the HSL will be discussed as this is the case which will be evaluated in this thesis. Maintenance techniques like milling and grinding using oscillating stones will therefore not be discussed. The maintenance actions discussed can be used for either preventive maintenance or corrective maintenance. Regarding the occurrence of RCF, grinding actions and renewal are most common to remove the RCF.

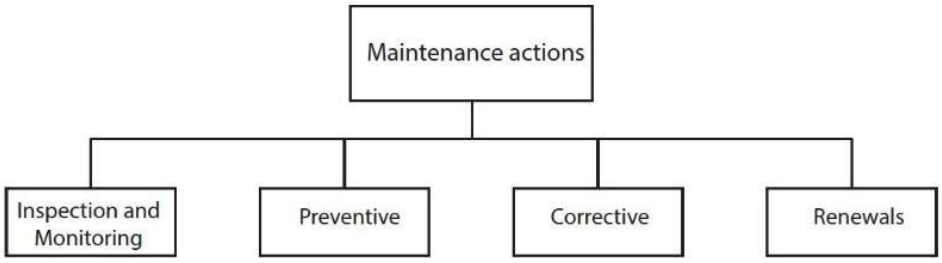

Figure 19: Maintenance actions divided among their categories.

2.3.1. Inspection and monitoring of rails

Visual inspection

The purpose of the visual inspection is to check the mechanical integrity of the track components and to see whether circumstances have arisen which may jeopardize safety or affect the availability of railway traffic (Esveld, 2001). The inspection can be done from the cabin of a rail vehicle (Fassetta) or during a walking inspection along the track.

Camera inspection

Camera inspection for the rails has the same purpose as a visual inspection. With special lighting and digital cameras observations are made by taking pictures of the rail top surface and its surroundings. The inspections

are done by rail vehicles. Camera inspection supports the visual inspections and is more and more supported by video imaging to automatically detect and identify and defaults (Esveld, 2001).

Eddy current measurements

In Figure 20 is shown how the principle of eddy current measuring works. Eddy current is able to detect surface defects like head checks, belgrospis, wheel burns and short-pitch corrugation (Pohl, Erhard, Montag, Thomas, & Wüstenberg, 2004).

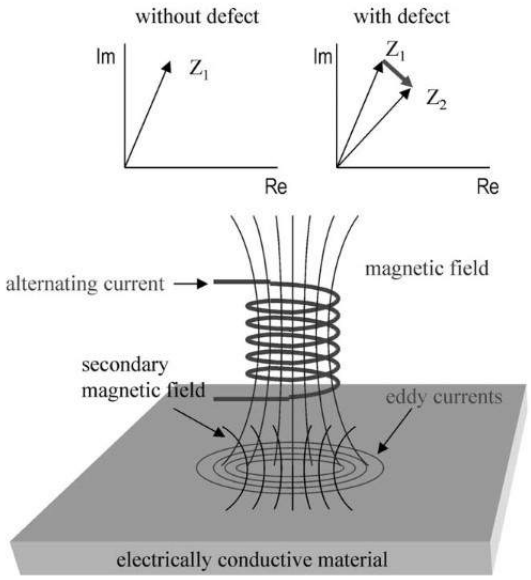

Figure 20: The principle of eddy current testing. The eddy current distribution at the rail surface interacts with any irregularities. If there are irregularities at the rail surface, the electoral impedance changes from Z1 to Z2. Source: (Pohl et al., 2004).

In (Rajamäki, Vippola, Nurmikolu, & Viitala, 2016), it is suggested that eddy current measuring is best used as a tool for maintenance quality control. As overestimating of damages can take place when measuring larger than its penetration depth. Also the eddy current technique measures the length of the crack, the depth can be determined indirectly using different angle values (Popović, Lazarević, Brajović, & Vilotijević, 2015).

The inspection can be done by both rail vehicles and hand measurements, for instance; using the Sperry EC walking sticks. It can accurately measure crack depths between 0.3mm and 5mm.

Ultrasonic measurements

During ultrasonic measurements the whole rail can be evaluated. Ultrasonic measurement, uses a beam of ultrasonic energy, which gets send into the rail. Then transducers are looking for the return of reflected or scattered energy, the difference in time and amplitude of reflections are processed to evaluate the rail (Clark, 2004). However, ultrasonic measurements have not proven accurate for defects close to the rail surface. It is therefore not suitable for the detection of early defects (Popović et al., 2015). The inspection is done by rail vehicles, but can also be done by using hand equipment. It can measure depths 4mm from the rail surface. In Table 3 a comparison is presented for the different measuring and monitoring techniques.

Table 3: Overview of the rail damage monitoring methods.

	Method	What damages	Pros	Cons
Visual inspection	Human eye	Large damages visible on the surface	A trained eye can judge the damages immediately also in relation to the setting Can evaluate the condition of the whole profile	Crack depth is unknown Need of artificial light because the inspections take place by night
Camera inspection	Camera, evaluated by the inspection department at the office	Damages visible on the surface	Not condition bound can evaluate the conditions at any moment Can be used in addition to the measurements to see how a measurement result actually looks Can work with picture recognition	Crack depth is unknown Need of artificial light because most of the inspections take place by night
Ultrasonic measurement	Ultrasonic energy	Cracks larger than 4mm under the surface	Can measure large parts of the track during 1 shift Both available for hand measurements (special structures and evaluation) and complete track measurements Can also measure the web and the part of the foot straight under the web of the rail profile	Cannot measure defects less than 4mm Defect hit-rate of the train turns out very low; about 40% at the HSL. Cannot measure the direction of the crack
Eddy Current measurement	Electrical current, magnetism	Cracks up to 5mm of depth	Can measure early defects from 0,3mm up to 5mm of depth Processed in IRISsys database able to make connections between different parameters	As of 2016 the train measuring the whole railhead is not admissioned for operation. Thus only the walking stick is available making it very labour-intensive to measure large amounts of tracks Cannot measure the direction of the crack, currently all the measurement channels are set upon the algorithm of determining the defects depth as if they are head checks so not secure in determining the depth of other defects Validation of the walking sticks and other equipment of Sperry is ongoing. The accuracy of the measurements are not completely defined at the moment.

2.3.2. Rail maintenance

Two types of rail maintenance are considered in this paragraph, grinding using rotating stones and high-speed grinding, this because both techniques have been used at the HSL-South. These techniques are shown in Figure 21. Other methods for preventive and corrective rail maintenance are: planning, milling and grinding using oscillating stones but will not be extensively evaluated as for the HSL case study these have not been used.

Figure 21: Example of both the rotating stone technique and the high-speed grinding technique. Source: http://www.vossloh-usa.com/en/rail_infrastructure/rail_services/rail_services.html

Grinding using rotating stones

Grinding using rotating stones can be used for both corrective maintenance actions and preventive maintenance actions. Rail grinding using rotating stones is a method effective to remove surface defects and retaining the desired rail profile (Magel & Kalousek, 2002). The rotating stone grinding is done by rail vehicles which carry multiple grinding stones, each covering a certain part of the rail profile. Grinding specifications can be carried out by using different quality stones, number of stones, speeds and number of runs to achieve the desired results according specifications.

High speed grinding

High speed grinding, is a grinding technology based on high working speeds of up to 100km/h. Its main advantage is that grinding can be done without track possessions. Its main purpose is preventive grinding regarding the removal of RCF and corrugation, but can also be used for acoustic grinding (Vossloh). High speed grinding is based on the principle of circumferential grinding, grinding stones are hydraulically pressed on the rail and passively propelled. The material removal is normally achieved using three runs (Vossloh). High speed grinding is a relatively new phenomenon in rail maintenance, but tests with Deutsche Bahn (DB) showed promising results as grinding costs have been halved and rail life been prolonged by early intervention (R Heyder & Hempe, 2009).

In (Hartleben, 2009) the different machining methods regarding rail maintenance have been evaluated which resulted in the overview presented in Figure 22, note that high speed grinding has not been included as the method was still being tested at the time.

	grinding (rotating)	grinding (oscillating)	milling	planing
Machining new rail	●●●	●●	●	●
Preventive machining	●●●	●	●●	-
Maintenance				
-geometrical defects (corrugation)	●●●	●	●●●	●●
-near surface defects (head-checks)	●●●	-	●●●	●●●
Rail machining for acoustic reasons	●	●●●	●	●●
Removal of gauge tightening	●●	-	●●	●●●
Machining of brake shoe tracks	-	-	-	●●●
Reprocessing rails in the tracks	-	-	-	●●●

Figure 22: Overview of the different machine rail maintenance methods, and rating regarding their suitability for certain maintenance actions. The grading was as follows: - =not suitable for a task at all, ●●●=method and task are especially well suited. Source: (Hartleben, 2009)

Rail renewal

Track renewal is usually done when the rails are at the end of their service life. Either because the rails have been worn out, or when its more cost effective regarding maintenance to replace them than to carry out additional maintenance actions. However different principles can be used regarding rail renewal as it is only a component in a track system. One can renew large track sections to avoid quality variabilities or renew only the affected areas.

2.4. Conclusions

The aim of this chapter was to provide the theoretical background regarding track geometry, RCF defects and maintenance and monitoring techniques to answer a set of sub questions which were proposed in the introduction of this thesis. This will result in a selection of parameters which will be used to evaluate the rail conditions.

What kind of RCF damages affect rails?

There are several types of defects, the main ones have been discussed 2.2, these were squats, head checks and studs. Also there are some other effects which can occur at the wheel-interface which should be taken into account like the occurrence of corrugation and white edging layers. The defects differ among their severity, head-checks and squats can cause the most severe problems. Also their location among the rail surface differs, head-checks occur at the gauge corner of the rails whereas studs and squats occur at the rail crown/rail head.

What are the root causes for RCF damages?

The root causes regarding RCF damages have also been discussed in 2.2. For squats there are several mechanisms which play a role: irregularities among the rail surface, high tractive efforts and there are some examples where is shown that white edging layer plays a role as cracks tend to initiate from this layer. For head checks high loading and friction are considered to be essential. In short the fatigue of the material is caused by the high tangential and normal loads at the wheel-rail interface is essential for both head checks and squats (Cannon, Edel, Grassie, & Sawley, 2003).

Which track parts are most vulnerable to RCF damages?

All the RCF defects have been reported mainly in curves and in open areas and tend to be less prone in tunnels. However, typical for head checks is that they occur more on the upper leg in a curve. For studs there are experiences they occur more on head-hardened rails than on softer rail grades. Squats occur in open areas, straight tracks and curves.

Are the current rail monitoring practices sufficient to detect RCF damages timely?

The current monitoring practices regarding rail conditions are visual inspections, camera inspections ultrasonic measurements and eddy current measurements. During ultrasonic measurements the whole rail is evaluated, but has a 'blind zone' for irregularities under 4mm. Eddy current measures the irregularities close to the rail surface and is accurate between 0,3-5mm. Visual and camera inspections are not capable to measure the actual depths of the defects. Concluding, eddy current measurements are thus most suitable as they can measure and detect the smallest crack.

The results from the answers of the set of sub questions will be used to select parameters to evaluate the rail conditions. The rail condition can be approached as shown in Figure 23. Being dependent on the interaction of track geometry, rolling material and maintenance. The characteristics of these will be approximated using parameters. The use of numerous parameters is possible, however the most relevant will be used. Also, the use of parameters is limited to the data available for the rail infra manager. The selection of parameters is presented in Table 4.

A detailed overview of how each parameter for the case study has been evaluated is presented in Appendix A. Parameter overview''. This overview has been done for the case study of the HSL-South; however, the processing of the data has been designed to be appropriate to evaluate any railway track.

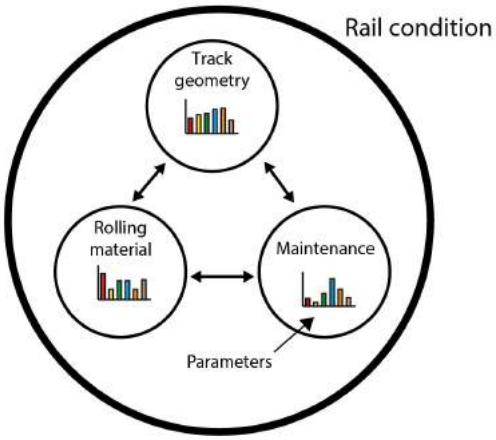

Figure 23: Schematic overview of the rail condition being dependent on sets of parameters, regarding track geometry, rolling material and maintenance.

Table 4: Parameter categories and their variables.

Category	Track	Rolling material	Maintenance	Damage
Parameter	Superstructure (type)	Speed (km/h)	Grinding type (type)	Damage average (mm)
	Rail grade (type)	Traction (% of max)	Grinding depth (mm)	Damage deepest (mm)
	Rail profile (type)	Tonnage cumulative (MGT)	Grinding date (d/m/y)	
	Assets (type)	Tonnage per vehicle (MGT)		
	Design speed (km/h)	Cant deficiency (mm)		
	Curve radius (m)			
	Curve cant (mm)			
	Height difference (m)			

Track parameters

Regarding the track parameters especially curves have been found to be vulnerable places in tracks where RCF often occurs. Curves can be modelled using the radius and canting parameters. Assets are special structures among a railway track, as tunnels proved to be less prone for RCF these will also be modelled. Railways can also have different types of rail grades, rail profiles or superstructures among them, it can be interesting to see whether RCF occurs more on either one type of rail grade, rail profile or superstructure. Furthermore the design speed and height difference have been selected as parameters. The design speed should be taken into account to be able to check whether vehicles behave according design. The height difference should be taken into account to check whether RCF occurs more on for instance ramps where often also traction is present.

Rolling material parameters

For the rolling material parameters the traction is important, as large tractive efforts are known to raise the stresses at the wheel-rail interface. The speed and cant deficiency are also notable parameters. Looking at the speed one can see how the vehicle compares to the design speed and it is also a parameter needed to determine

the cant deficiencies. The cant deficiency tells something about how a train behaves in a curve, large cant deficiencies or cant excesses distribute stresses unevenly among the rails in curves. Regarding the tonnages it is important to know whether a certain track or track partition has been loaded more than others, also the tonnage per vehicle should be taken into account when there are more types of vehicles, this to see how much each of them contributes to the track load.

Maintenance parameters

The parameters which should be taken into account regarding maintenance are all grinding related. Providing for each track partition when it has been ground, how much has been ground and using which technique.

Damage parameters

The parameters for the damages or rail condition can be defined using measurements. As early cracks are most interesting for the infrastructure manager eddy current measurements should be used here. For a track partition the damage average and deepest damage can be used as parameters.

3. Methodology

3.1. Introduction

The previous chapter discussed the theoretical background, using a literature study which resulted in a list of relevant parameters which will be used to evaluate the rail conditions. This chapter will present two approaches how these parameters can be used in order to identify the influencing parameters regarding RCF damages for a railway track.

The first approach is named the bottom-up approach (B-U approach) which is used to evaluate the worst affected areas by RCF on a railway track. This approach will evaluate the so-called hotspots of RCF. The second approach has been named the top-down approach (T-D approach). The top-down approach will be used to evaluate the whole track or certain selected parts of the track. Both methods and a combined approach will be explained step-wise in this chapter.

In Figure 24, the maintenance circle is provided regarding the rails. The highlighted area shows in which stages the methods will be used. This will be: using the data available and evaluate them in order to find damage causes and provide recommendations for future maintenance actions.

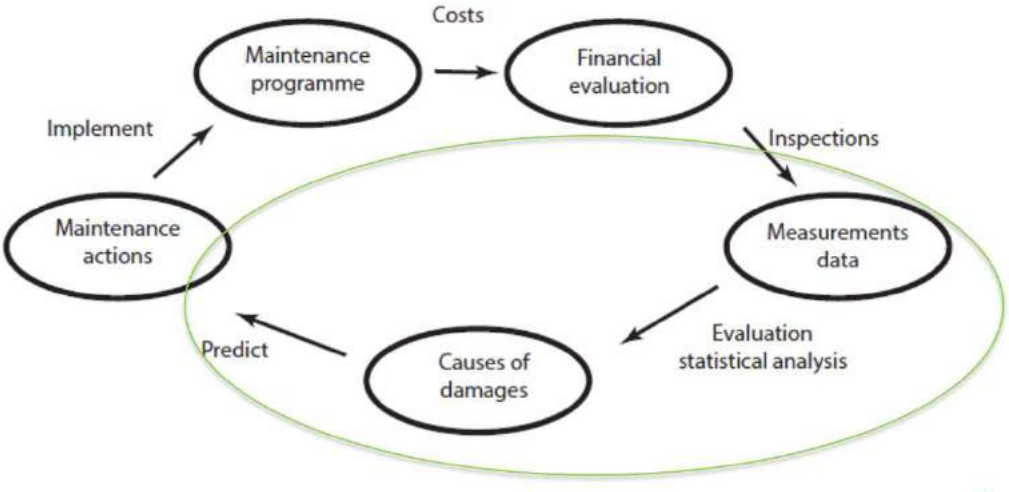

Figure 24: Overview of the maintenance diagram. The marked area shows which areas are covered by the proposed approaches, being evaluating measured data and providing a hypothesis regarding the causes of damage.

Figure 25 shows a schematic representation of the rail condition being dependent on the interaction of three conditions, maintenance, track geometry and rolling material. For this analysis all three will be represented by a number of parameters. What also should be done when evaluating the rail conditions is looking at the visual inspections and reports for pictures and available information to assess the damages whether they are actually rolling contact fatigue.

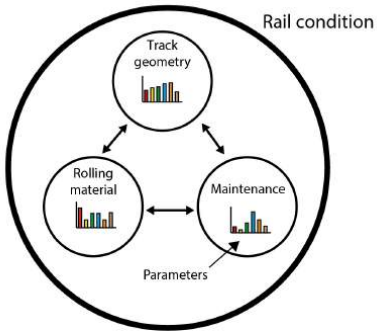

Figure 25: Rail condition will be approached as the interaction between sets of track geometry, rolling material and maintenance parameters.

3.2. Intensity parameter

As the rail conditions are being evaluated in both approaches, a new parameter will be introduced to determine the condition of the rails. The measurements will be transformed into a new numerical parameter, which will function as a key performance indicator (KPI). The definition of good performance indicators is challenge for railway systems. Regarding railways operations, those KPIs will govern the way the maintenance operation are managed, performance indicators have been reported in (Åhrén & Parida, 2009), (Parida & Chattopadhyay, 2007), (Stenström, Norrbin, Parida, & Kumar, 2016) and (Stenström, Parida, Lundberg, & Kumar, 2015).

The way to connect condition measurement with KPI is a difficult task. Using ABA, defined robust and predictive KPIs that consider stochasticity of the defects and prediction over a maintenance time horizon which has been reported in (Jamshidi, Núñez, Li, & Dollevoet, 2015), (Jamshidi, Nunez, & Li, 2015) and (Jamshidi, Núñez, Dollevoet, & Li, 2016). In this thesis for the case study, only one round of valid eddy current measurements is available, so the analysis of robustness and predictive capabilities are part of the further research.

In order to be able to identify the worst affected areas by cracks and to be able to conduct statistical analysis regarding the parameters which have influence on the affected rails. The intensity takes into account both the number of defects as the depth of the defect. The intensity has been calculated for each leg separately.

The steps which are taken to transform the eddy current measurements into the intensity are shown in Figure 26. In this figure, also a numerical example is given for a fictional partition.

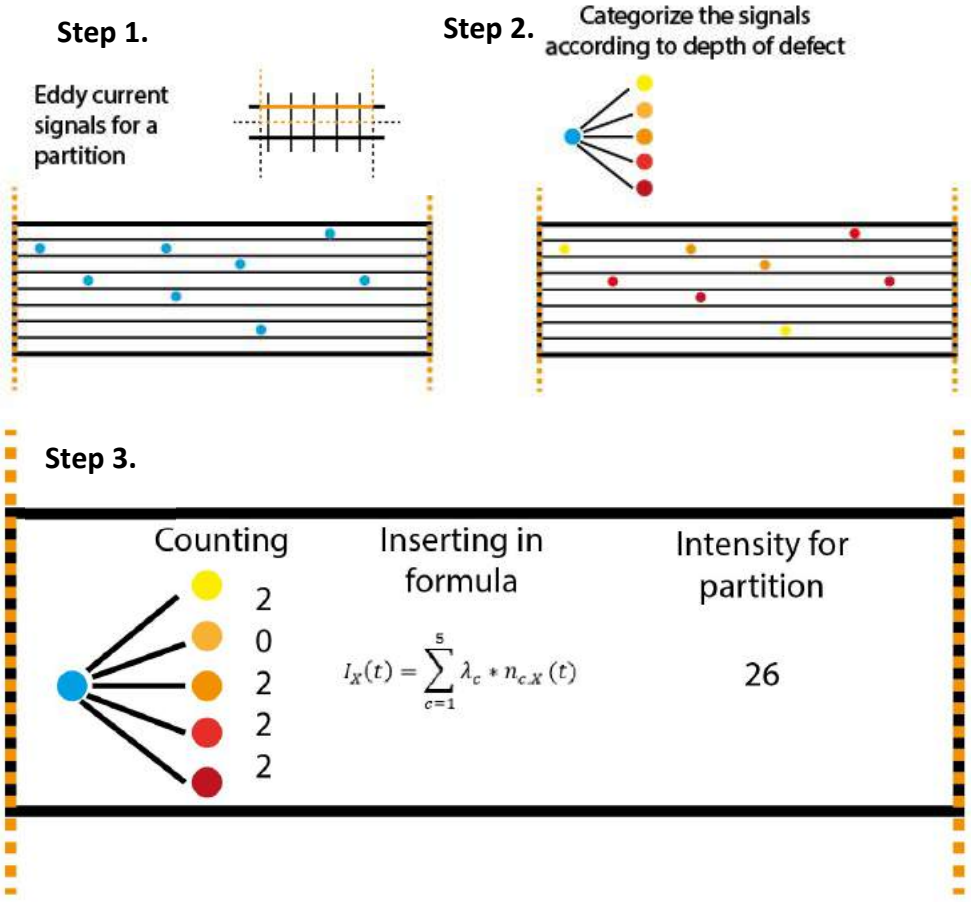

Figure 26: Overview of the steps taken to determine the intensity for a certain partition. The first step is the partitioning. The second step is measuring the partition. The third step is to determine in which category each signal from the measurement fits. The fourth step is counting how many signals there are for each category. The final step is using this input in the formula and determining the intensity for this partition.

3.2.1. Determining the intensities

The intensity excludes two defects at the same kilometre position and counts them as a single defect. Figure 27 shows an example of these double faults at the same km position, these are thus regarded as a single defect. As eddy current measuring occurs over several channels it is possible that in the case of a 'double fault' at the same km position different depths are being found. In this case the value of the deepest crack has been used at this position for safety reasons. Supplying this data leaving out the double faults has been done by the company Erdmann Software at the request of Infraspeed.

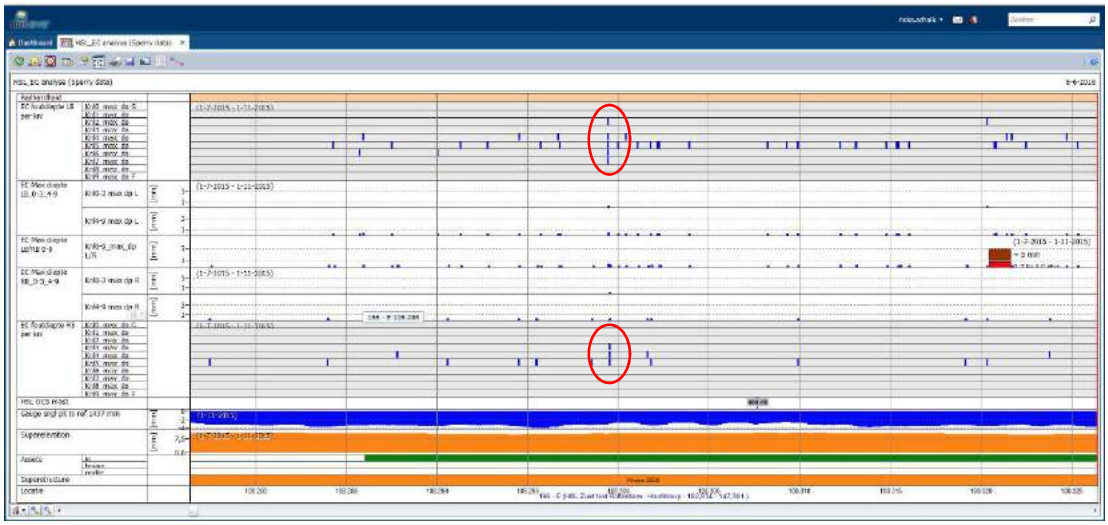

Figure 27: An example of an eddy current measurement in which more defects are found at the same kilometre position, these are highlighted by the red circles. These are thus counted as a single defect for the intensity calculation.

In order to compute the intensity values some different categories for the crack depth have been introduced the threshold values for crack depth are shown in Table 5. The cracks smaller than 0.10mm have been left out for the intensity calculation due to accuracy of the measurements between 0.01 and 0.10mm. Cracks larger than 5.00mm cannot be measured by eddy current as it doesn't exceed the penetration depth. These will show a 5.00mm result as a measurement value, this is therefore the upper limit for intensity category 5.

Table 5: Threshold values used in order to calculate the intensity values.

Intensity category c	Coefficient category λ_c	Lower threshold bound (mm)	Upper threshold bound (mm)
1	1	0.10	0.99
2	2	1.00	1.99
3	3	2.00	2.99
4	4	3.00	3.99
5	5	4.00	5.00

For the calculation of the intensity values the following formula has been introduced:

$$I_X(t) = \sum_{c=1}^{5} \lambda_c * n_{c,X}(t)$$

In which:

I_X= Intensity at rail partition X
X = Interval position; km x to x+500m
t= Time of measurement
c= Category

λ_c= Category coefficient
$n_{c,X}(t)$ = Number of defects in category c at partition X at time t

However, more intensity indexes have been introduced to analyse the partitions. This, in order to evaluate the intensity for defects larger than 1.00mm and defects larger than 3.00mm. This was found necessary as not all measurements proved to be very accurate in the 0.01-1.00mm zone. The reason for the evaluation for defects larger than 3.00mm was to confirm the initial selection of hotspots. These two additional intensity parameters have been calculated as follows:

$$I_x^1(t) = \sum_{c=2}^{5} \lambda_c * n_{c,X}(t)$$

$$I_x^3(t) = \sum_{c=4}^{5} \lambda_c * n_{c,X}(t)$$

In which I_X^1 is the intensity for defects larger than 1.00mm and I_x^3 is the intensity for defects larger than 3.00mm.

The output for the calculation of the intensity is a new parameter for all partitions. Using this parameter for track selections results in a distribution of intensity values for that track selection. This will show where the concentration of damages lie for this track selection.

3.3. The bottom-up approach

the bottom-up approach (B-U approach), is a parameter analysis which aims at finding the cause of the damages from the hotspots themselves. This process will be described according several steps which have been taken during the research. The first five steps of the B-U approach have been illustrated in Figure 28.

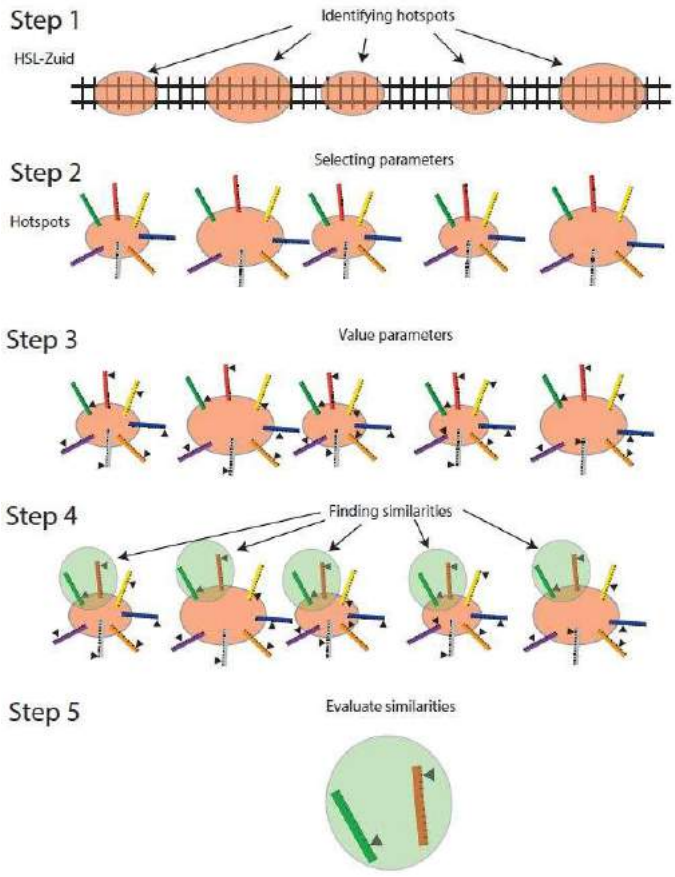

Figure 28: The first five steps which have been taken during the parameter analysis and how to identify the parameters on the hotspots which have similar values.

3.3.1. Identification of hotspots

One of the first steps which has been taken during the research was the identification of the hotspots. These are several zones among the track which are severely affected by RCF damages. The identification has been done for the whole track, including the turnouts around Breda with the exception for the rails along the maintenance yards.

The selection of the hotspots has been done according to four criteria which identify a hotspot, out of which 3 out of four should be met:

- Exceeding a set intensity threshold, dependent on the partition length.
- Visual evidence of the damages on the rail, by photo images.
- The severity of the damages caused the maintenance company to do corrective grinding.
- A total length of at least one whole partition, the measurements should point out the total length of the hotspot.

In (Jamshidi, Faghih-Roohi, et al., 2016a) and (Jamshidi, Faghih-Roohi, et al., 2016b) the categories proposed are more broad for crack, and also considers the visual length of the squat defects. In this thesis, the visual crack length was not accessible with the photos, so new categories were defined to better adapt to the reality of the HSL. The first criterion is related to the intensity parameter. Depending on the size for the partitioning a threshold value should be chosen which represents the worst affected areas by RCF. Another criterion is the visual evidence of the damages rail to verify the measurement. This visual evidence are pictures taken during visual inspections among the tracks. As this approach is more evaluative regarding previous actions, additional grinding is also one of the criteria. The minimum length of a hotspot should cover at least one partition in order to evaluate.

3.3.2. Selecting parameters

There has been a broad selection of parameters to evaluate these hotspots. This broad selection of parameters has been chosen in relation to parameters found in literature. For these parameters is evidence they can have an influence on track irregularities. The parameters where also chosen by expert judgement based on root cause analyses, which has been done the previous chapter. However the selection of parameters is limited by the data available for the rail infrastructure manager, but can also be expanded when more data is available.

3.3.3. Value parameters

During the valuing of the data, a lot of data should be gathered and processed among many different sources. During the processing of the data it will often occur that there will be two or more different signals for the parameter within the respective partition. For the nominal variables this will be processed as a mixed value; for instance there are two different rail grades used among the HSL-South, namely 350HT and 260. When both occurred within a partition and first the 260 and second the 350HT this can be processed as a mixed value mix. Another option regarding the processing of the data was using homogenous partitioning. Using this, no mixed values would have been processed, however because of the different partition sizes for each parameter this has not been done. It could have also affected the number of samples.

So, the mixed value occurs when there is a transition point present between both variables for the rail grade. This example is mathematically formulated as:

$$\delta_X^{rail}(k) = \begin{cases} 260 \text{ if } \delta^{rail}(x,k) = 260 \text{ for all } x \in X \\ 350HT \text{ if } \delta^{rail}(x,k) = 350HT \text{ for all } x \in X \\ mix \text{ if } \delta^{rail}(x_1,k) = 260, \delta^{rail}(x_2,k) = 350HT \end{cases}$$

For: $x_1 \neq x_2 \in X$

In which:

$\delta^{rail}(k)$: value of the parameter (δ) rail at moment of measurement k
X: partition
k: moment of the measuremet
x: location

For the quantitative variables (speed, radius, cant, etc.) the average value of the different signals within the 500m partition has been used. This is formulated with the example of the speed of the TRAXX as:

$$\delta_X^{VTRAXX}(k) = \frac{1}{N_X^{VTRAXX}(k)} \sum_{x \in X} \delta^{VTRAXX}(x,k)$$

For: $\delta^{VTRAXX}(x,k) \neq null$

In which:

$\delta^{VTRAXX}(k)$: Value of the parameter (δ) speed TRAXX at moment of measurement k
x: location
k: moment of measurement
X: Partition
$N_X(k)$: number of signals within partition X at moment of measurement k

3.3.4. Similarity

The fourth step of the process is to find similarities among the hotspots. These are parameters with the same values for the nominal parameters and closely lying values for the numerical ones. So here the parameter values among the different hotspots are compared to each other. This in order to be able to pinpoint the parameters which should be investigated more closely. The other argument would also to be able to exclude a number of parameters as the cause for the damages at the hotspots. Another opportunity arises when comparing the parameter values, is to see how they relate and be able to see numerical values which exceed for the parameters at the hotspots the values for the other non-affected areas.

The similarity function to describe the similarity of one parameter at two hotspots is:

$$V\left(\delta_{X_{h1}}(k), \delta_{X_{h2}}(k)\right) = \left\|\delta_{X_{h1}}(k) - \delta_{X_{h2}}(k)\right\|^2$$

In which:
V: similarity function
δ: parameter value
X_h: partition of hotspot
k: moment of measurement

The condition for similarity will be described according a similarity threshold ε_δ.

If: $V(\delta_{X_{h1}}(k), \delta_{X_{h2}}(k)) \leq \varepsilon_\delta$ we will say: $\delta_{X_{h1}}(k) \approx \delta_{X_{h2}}(k)$ thus similar.

3.3.5. Characterize hotspots using clustering

Regarding the similarities it can be that all hotspots share for instance the same value for one parameter. This will then be defined as a characteristic parameter value. However, it is not obvious that one set of characteristic parameter values will cover all hotspots as there can be different mechanisms causing RCF at a railway track. Therefore, the technique of clustering will be introduced, which aims at distinguishing types of hotspots. Clustering is a measure of classification, more specifically 'unsupervised classification' which aims at discovering groups in data (Govaert, 2009).

Regarding the clusters its required to be homogenous and well separated (Hansen & Jaumard, 1997). The sample for the clustering will be the set of hotspots which have been found earlier using the identification of the hotspots.

The clusters will consist of sets of characteristic similar parameters for a certain hotspot type according the formulas and Figure 29:

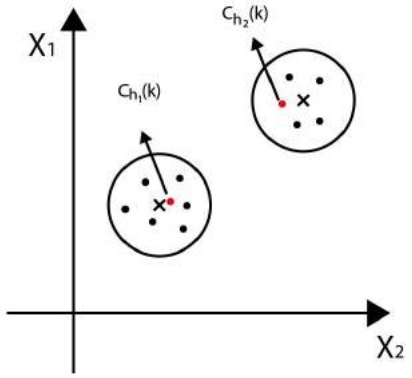

$$\overline{C_{h_1}}(k) = \begin{bmatrix} \delta_{h_1}^1 \\ . \\ . \\ . \\ \delta_{h_1}^m \end{bmatrix}$$

$$\overline{C_{h_2}}(k) = \begin{bmatrix} \delta_{h_2}^1 \\ . \\ . \\ . \\ \delta_{h_2}^m \end{bmatrix}$$

Figure 29: How the clustering works according two hotspot types.

$$C_i(k) \in C_{h_1} \text{if } \mathrm{V}(\overline{C_{h_1}}(k), C_i(k)) \leq \varepsilon_c$$

When there are five hotspots evaluated regarded clustering, the output can for instance be that two hotspots types are found which divide the five hotspots, which can be described mathematically as:

$$C_{h_1} = \{C_2(k), C_3(k)\}$$

$$C_{h_2} = \{C_1(k), C_4(k), C_5(k)\}$$

Where $C_{h_1}(k)$ is the selection of characteristic parameter values which are similar for a certain hotspot type h_1 at moment of measurement (k). The hotspot types are thus described as a vector which makes existing of a set of parameter values.

Note that according the clustering not every hotspot type will have an equal number of characteristic parameters. Also its possible that the clusters are not separated for every characteristic parameter, as some parameters can have an equal characteristic parameter.

3.3.6. Establish an hypothesis

The next step will be to evaluate the types of hotspots which have been identified using the clustering. Here the values for the characteristic parameters for the hotspot type should be evaluated. During this evaluation the parameter values will be linked to the literature regarding RCF. This in order to determine whether a single parameter or a set of parameters can be linked to causing RCF for these hotspot types.

According to this evaluation using a single parameter or set of parameters can be used to establish hypotheses for the types of hotspots. Looking at what can be the most probable cause for RCF. Thus the hypothesis results in a set of parameters which are conditional regarding the RCF to occur.

3.3.7. Checking the hypothesis

The last step will be checking the hypothesis. This will be the check among other parts of the track. The hypothesis establishes conditions for parts of the tracks to be vulnerable for damages. Now the whole track will be checked for other areas which share the same characteristics and if they are affected by (smaller) damages. There are different possible outcomes here:

- There are no other areas sharing the same characteristics (these are the only hotspots, probably a correct hypothesis), thus the following inequality is true:

$$C_{h_1}(k) \neq C_{nh}(k)$$

- There are other areas sharing the same characteristics but no damages according to eddy current measurements. Thus the following equality is true at least once:

  $$C_{h_1}(k) = C_{nh}(k)$$

  But when this condition arises the eddy current measurements show no damages. This can lead to the following situations. The eddy current measurement at these partitions is not correct which means the hypothesis can still be true, the partition(s) should be closely monitored. Or at least one of the parameters which make up the condition should be excluded. Another option is that the influencing parameter is not included.
- There are other areas sharing the same characteristics and similar damages according to eddy current measurements. Seems like the set of characteristic parameter values is correct regarding the hypothesis.
- There are other areas sharing the same characteristics, some got similar damages, others don't (possibly a partly correct hypothesis, awaiting new measurements for these areas to recheck them and recheck the hypothesis, evaluate how many share the similar damages and how many don't). Also the set of characteristic parameter values should be checked again for the areas which don't share the damages to see whether the set can be refined.

The steps regarding the hypothesis check can be represented by a flow chart as shown in Figure 30.

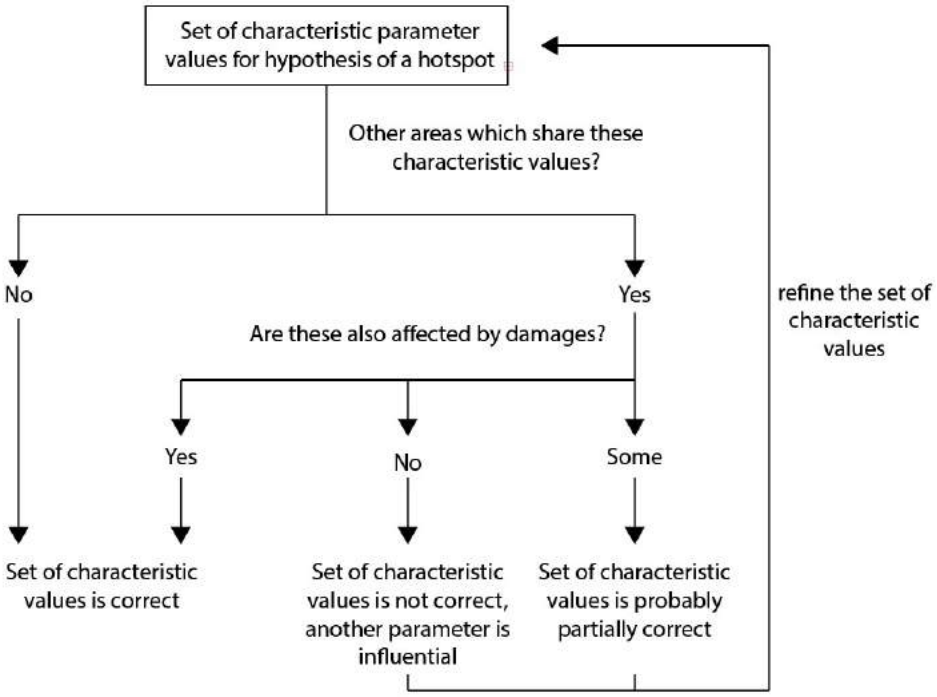

Figure 30: Flow chart regarding the hypothesis check.

According the results of the hypothesis check drawing conclusions regarding the cause of the damages should be done and the result will be that the influencing parameters regarding RCF for the railway track have been found. If there are no positive results from the hypothesis regarding the cause recommendations for future research should be given.

3.4. The top-down approach

The aim of the top down approach (T-D approach) is to link the whole track or selection of the track to the rail condition. The T-D approach is introduced in order to be able to rank the conditional parameters for the whole track. This can be done using the set of established parameters in a different way. This in order to see how each parameter relates to the condition of the rail. The intensity parameter is a performance indicator, the intensity will therefore be checked how it is influenced by certain other parameters. There are also different kinds of parameters which are being processed in the analysis, both quantitative and qualitative parameters have been processed. The qualitative parameters are nominal parameters, thus no ranking is involved. These will be processed differently than the quantitative parameters. The top-down approach evaluates each leg separately, which enables to characterise the legs being either the lower or upper leg in a curve.

3.4.1. Partitioning

The partitioning is illustrated in Figure 31. The number of samples will be important as the T-D approach consists partly of statistical methods. Also in this approach the same reasoning for partitioning applies: when choosing smaller partitions are chosen the results will become more accurate. To be able to gather more accurate with respect to the different behaviour of different vehicles the T-D approach uses partitions for each leg separately.

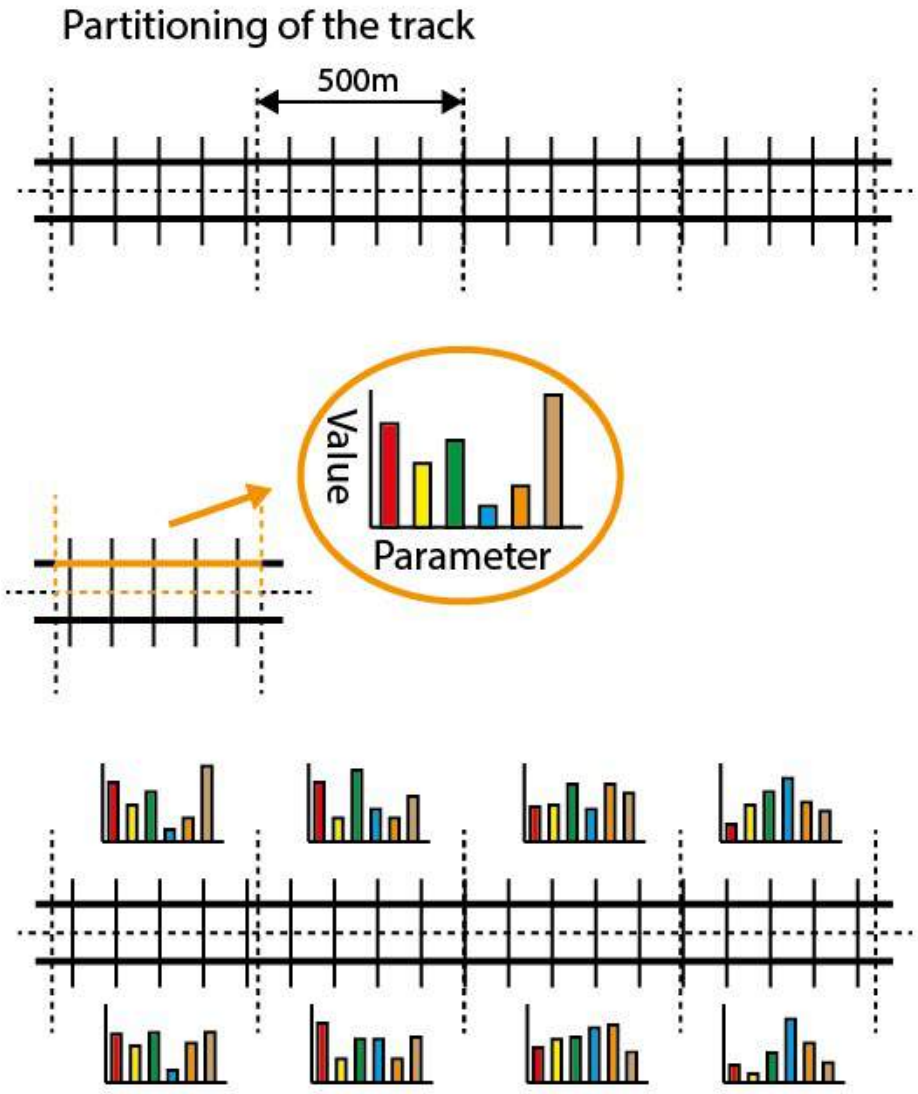

Figure 31: Partitioning in the T-D approach is done for each leg separately.

3.4.2. Numerical parameter evaluation

There are several data analysis techniques which can be used in order to evaluate numerical parameters. Using SPSS software enables to do simple statistical analysis among large data sets. Two considered options were:

- Linear regression analysis
- Correlation analysis

Both are much alike when it comes to identify a linear relation between two variables. The relationship between both can be formulated according (Lee Rodgers & Nicewander, 1988) as:

$$r = b_{Y \cdot X}\left(\frac{S_X}{S_Y}\right) = b_{X \cdot Y}\left(\frac{S_Y}{S_X}\right)$$

In this formula r is the Pearson's correlation coefficient and $b_{Y \cdot X}$ and $b_{X \cdot Y}$ are the slopes for the regression lines from Y to X and X to Y (Lee Rodgers & Nicewander, 1988). Regarding the computations, the parameters will be evaluated using Pearson's correlation. Doing this the relations can be viewed between all the parameters in a single table.

Pearson's correlation can also be used to measure relations on an interval or ratio scale (Egghe & Rousseau, 1990). The original mathematical formula for correlation by Pearson for two variables designed in 1895 is as follows:

$$r = \frac{\sum(X_i - \bar{X})(Y_i - \bar{Y})}{[\sum(X_i - \bar{X})^2(Y_i - \bar{Y})^2]^{\frac{1}{2}}}$$

Here the output will be a Pearson's correlation coefficient which is a standardized coefficient which resembles the strength of the relationship between two variables. This coefficient values range between -1 and 1.

Where -1means that when one variable changes the other changes in the opposite direction by the same amount. The value 1 means that when the first variable changes the other one changes by the same amount. The value 0 means the there is no relationship, when one variable changes the other doesn't change at all.

3.4.3. Looking for significant correlation

The other output value is the significance value, which is a p-value. The significance value gives a probability for getting the correlation value for this sample size if the null hypothesis were to be true (thus no relation between the parameters) (Field, 2009). Significance criterions handled are usually 0.05 or 0.01, thus the lower the significance value the less likely the null hypothesis is true. The significance values are related to the sample sizes being used for the analysis.

Using the output of the parameters, the significant parameters can be ranked. This can be done according to their p and r values, which tell which parameters influence the intensity most.

3.4.4. Nominal parameter evaluation

As correlation is not a suitable technique to evaluate the relation between the intensity and qualitative variables. Another technique should be used to evaluate these relationships. It is especially interesting to see how the values for the intensities are being distributed among the nominal variables and to compare these among the nominal variable values.

A suitable method for this is the use of comparative boxplots, which allows easy visual comparison between of the features of different sets (Navidi, 2010). The boxplot can show: the level, spread and symmetry of distribution of the data, using the median, first and third quartiles and the outliers in a sample (Williamson, Parker, & Kendrick, 1989). The anatomy of a boxplot is shown in Figure 32.

The interquartile range (IQR) represents the difference between the first and the third quartile and therefore 50% of the data lies within the interquartile range. The outliers for a boxplot are shown individually. The whiskers represent the values which are not considered as outliers but are values outside first and third quartile.

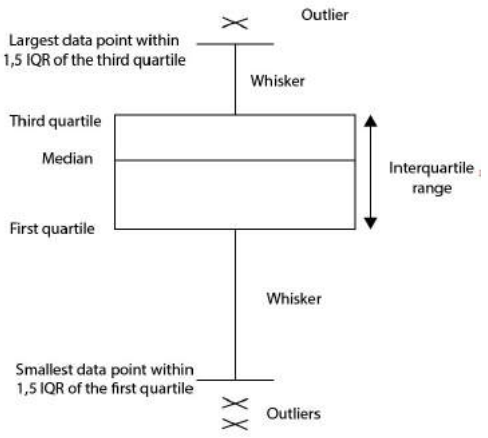

Figure 32: A boxplot and its anatomy, the 1,5 IQR is a common definition for an outlier but other thresholds like 3 IQR can also be used.

The quartiles are the basis for the whiskers to flag potential outliers and can be defined for the lower- and upper whisker as:

$$Q_1 - k(Q_3 - Q_1) \text{ and } Q_3 + k(Q_3 - Q_1)$$

Where k is the value to define the outliers. Different values for k are suggested in literature where (Frigge, Hoaglin, & Iglewicz, 1989) suggest that $k = 1$ is too small for evaluator purposes, as $k = 1{,}5$ is suggested being used standard.

Another method to process the data is looking for the averages of the nominal variable values and comparing them and the different intensities. This in order to see the relationships between this data. Here bar graphs will be used.

Each of the categorical parameters will be evaluated according the results regarding their assumed relation to the intensities. Remarkable results and trends will be studied more closely, to explain the relations.

3.5. Combined approach

Another possibility considering both approaches is using them both in a combined approach. This combined approach will use the results of the B-U approach for the T-D approach. As the bottom-up approach presents conditional parameter values for RCF in its hypothesis, this can be used in the T-D approach to do a correlation analysis for certain track selections. Doing this an additional check can be done regarding certain hotspot types. Hereby executing an additional check for both approaches and compare the results to refine the conclusions.

4. Case study: HSL-South

This chapter will demonstrate the use of the approaches to identify influencing parameters regarding RCF for the Dutch railway track HSL-South. Both approaches and a combined approach will be discussed stepwise. The size for the partitioning has been set on 500m pieces of track. This because of the size of the HSL being two parts of about 45km of double track, which results into about 700 data signals for a correlation analysis and 350 signals for the B-U approach. Also it is a size which can provide enough data signals regarding the assets and curve characteristics and provide enough detailed information regarding the characteristics.

4.1. Introduction to the case

The high-speed line in the Netherlands (HSL-South) is one of the more recent additions to the Dutch railway network and also copes with these RCF-related problems which are being discussed and investigated in this thesis. Also two different types of trains use the HSL tracks which makes this a suitable case for this study.

The high speed line south (HSL-South) is the first high speed line in the Netherlands. The track runs from Hoofddorp to Rotterdam and from Barendrecht to the Belgian border with switches halfway connecting to the ProRail tracks to Breda. The HSL-South has been designed for speeds up to 300km/h, connecting the Netherlands and in particular Amsterdam, Schiphol Airport and Rotterdam to the European high-speed rail network.

Since the completion of the HSL-South in the Netherlands, Infraspeed BV is responsible for the maintenance in a 25-year long concession agreement (2006-2031) procured by the Dutch government. The HSL-South has officially been opened in 2006. The first commercial trains started using the track in 2009. An overview of more important events can be found in Figure 33.

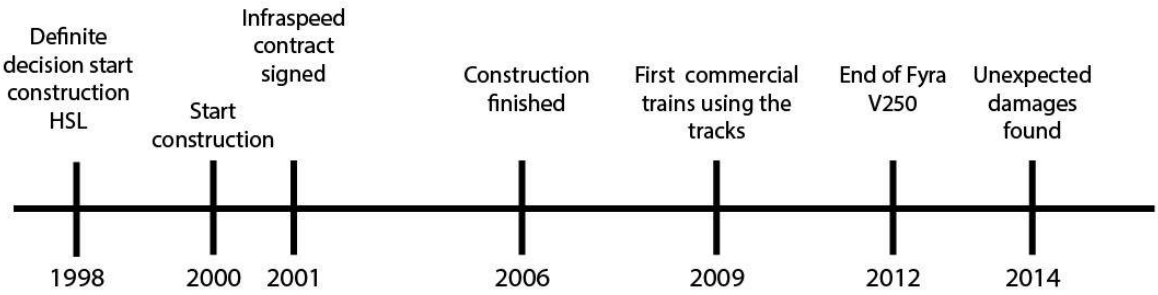

Figure 33: Timeline regarding HSL-South and the damages found.

In November 2014 during a visual inspection walk along the tracks, some unexpected severe damages were found. These severe damages were a surprise for the maintenance company Infraspeed as there were no indications of them being there during the regular ultrasonic-, eddy current measurements and visual inspections. These findings indicate the current monitoring program for the rails is not capable to detect defects in an early stage. The consequence is that the maintenance program is not yet tailored to the needs of the HSL. While the origin of the defects is not yet clear, an explanation could be the interaction between infrastructure and the trains using the track which are operating differently from the original design. The track has originally been designed for train speeds ranging between 220-300km/h. However, since the opening of the HSL also trains with maximum speeds of 160km/h are using the tracks of the HSL (van der Heide, 2009).

Following the findings of these damages, Infraspeed started investigating them. This investigation aimed at finding what these damages are, where they are located and what causes them. The first part of the Infraspeed investigation resulted in a new (visual) inspection procedure for the whole HSL track looking for similar damages. This procedure resulted in the detection of five other affected areas, so-called hotspots. Which will be explained in the bottom-up approach.

4.2. Damage specifications

Characteristic for the damages is their location on top of the railhead, therefore Infraspeed introduced a new eddy current measurement method. Using the Sperry eddy current walking stick, the whole HSL has been measured for cracks between July and October 2015. The Sperry eddy current walking stick is able to detect cracks up to 5 mm in the railhead where this was not possible in the past with existing measuring methods. As the old eddy current measurements by the fassetta only measured the gauge corners to detect head checks.

To know more about these damages, Infraspeed consulted DEKRA Rail to do a detailed material research on samples of pieces of affected rails from the Hoofddorp location. In October 2015 this resulted in a first report with first hypotheses of what kind of cracks they are, some characteristics and their possible causes (van der Stelt, 2015):

- Damages found have characteristics most similar to studs.
- White edging layer had been found at the surface of the rail with a maximum thickness of 30µm and an average thickness of 10µm.
- Damages are most likely caused by grinding as white edging layer has been found on both the running band of the rail and outside the running band.
- The used 350HT rail grade meets the material and chemical requirements according to the NEN-EN 13674-1 norms.
- According to the microscopically research among 8 rail pieces the maximum crack depth was 3-3.5mm.

Because this study was done for only one location, it is unclear whether the other hotspots show the same characteristics. It is important to know whether the damages at the other areas are caused by the same mechanism. This would also be essential information to customize the maintenance and monitoring program regarding the damages. Therefore further research is needed among the other hotspots.

Another investigation which has been done in the summer of 2016 where two pieces of affected track have been evaluated by the manufacturer Voestalpine. These pieces came from the hotspot Zoetermeer and had a 350HT rail grade. Here it was concluded that the material was 100% within specification and free of any irregularities (Künstner & Harrer, 2016). The defects found were not squats as they didn't meet the lung shape or depression at the surface characteristics, but were classified as spalling defects (studs), also thin layers of martensite had been found during the examinations. The examined damages are shown in Figure 34.

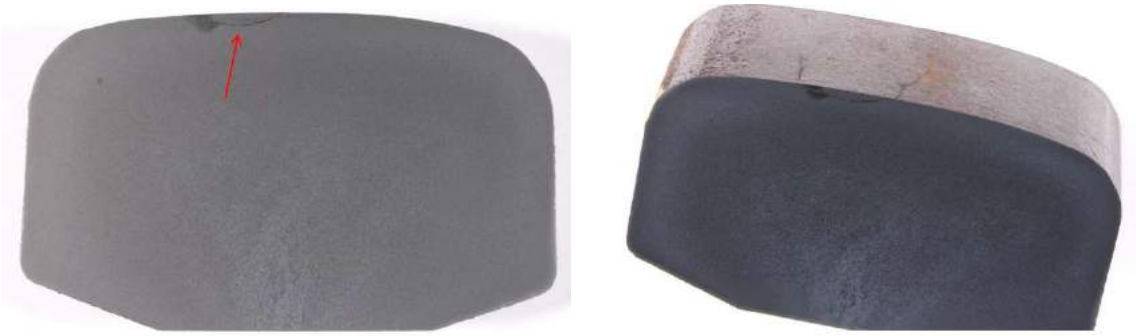

Figure 34: Pictures of the examined rails with damages. The cracks don't grow into the rails but stay relatively close to the surface. Source: (Künstner & Harrer, 2016)

Both studies showed that the 350HT rails which had been examined at the hotspots met the material specifications. They also showed the same results regarding the damages, both areas seem to be affected by spalling defects or studs. Also at both samples small layers of martensite had been found. According it seems likely that the same mechanism plays a role in the occurrence of these defects. That the damages were classified as studs seems plausible as the number of MGTs meet the characteristics of studs. Also the finding of white edging layer (martensite) is known to play a role in the occurrence of studs.

4.3. Bottom-up approach

4.3.1. Identification of the hotspots

The overview of the hotspots at the HSL-south is shown in Appendix B. hotspots HSL-South. Where the respective values are presented, the situation described and pictures of the damages are shown.

Figure 80 in Appendix C. Intensities related to the hotspots, shows the intensity distributions among the hotspots. The hotspots at Zoetermeer (km 120 NE), Hoofddorp (145 NW), and the hotspot around km 220 SW come out very clearly among all the intensity distributions as peaks. For the hotspots among Rijpwetering this is not the case, but they have been chosen as hotspots additionally because they met the grinding criterion very clearly as more than 3mm had been ground to remove RCF damages in November 2015. There are several other areas which show intensity peak areas but these didn't meet the criterion of grinding or the length criterion of a hotspot, for instance the peak around SE 230 was a small affected area at the ramp of bridge Holland Diep and the peak around SW 250 was also an area too small to consider a hotspot, both areas also didn't meet the grinding criterion.

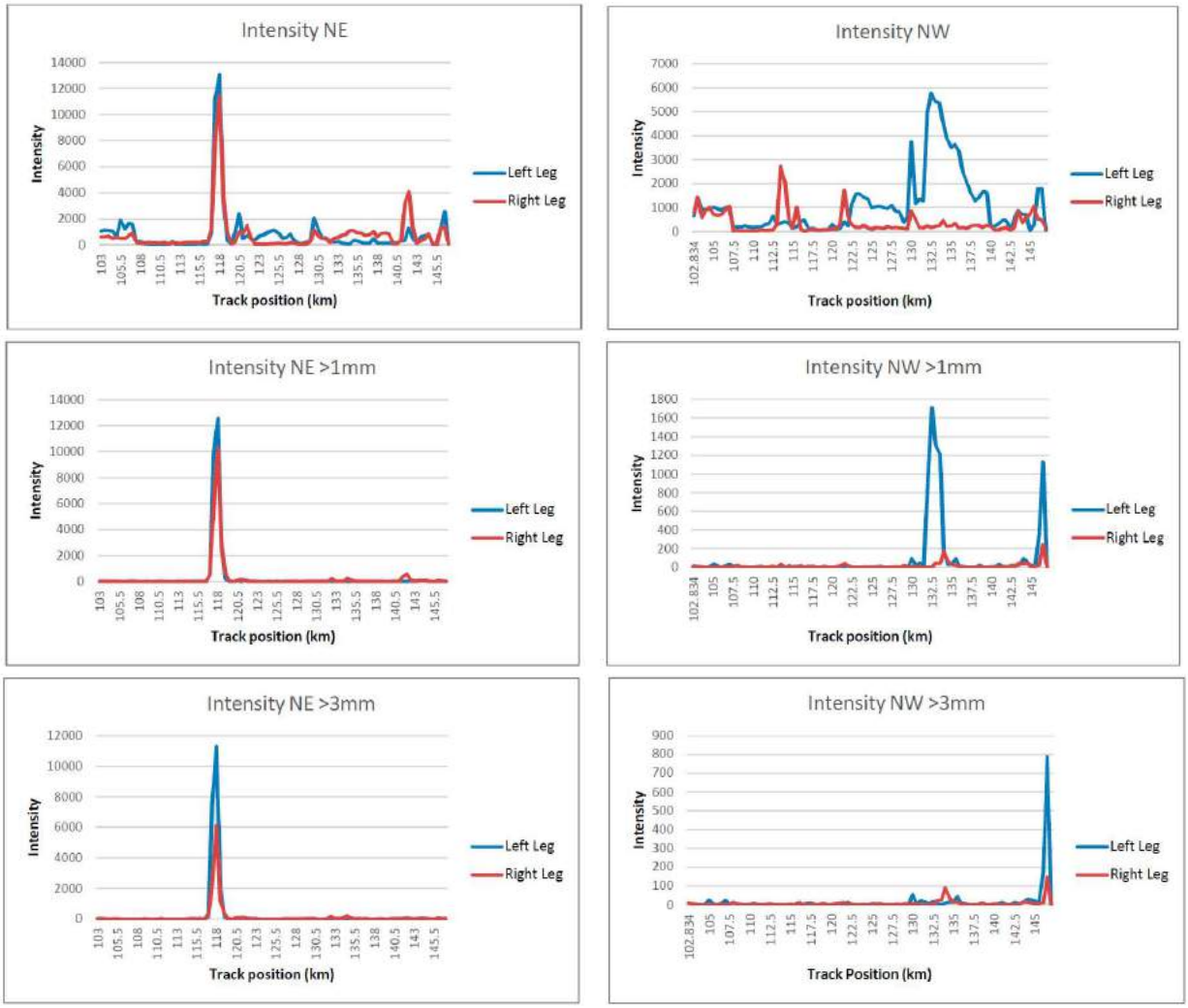

Figure 35: Intensities, all, >1mm and >3mm shown for the North tracks of the HSL-South. As can be seen here, km 118 NE is worst affected with cracks >3mm. Around km 132NW its clear that most cracks are not larger than 3mm.

An overview of the hotspots and how they meet the criteria is presented in Table 6. Clear from this table is that the hotspot at Zoetermeer is affected by a whole other magnitude of damage than the other hotspots based on the intensity for cracks larger than 3mm. The I^3 intensity threshold has been set at 50. Which corresponds to either 10 defects of 5mm on a leg in a partition or 17 3mm defects in a partition. Considering the intensity is

calculated for legs separately there are double those amounts of defects for a track partition which should be considered for a single corrective grinding action.

Table 6: Overview of how the hotspots meet the criteria.

	Zoetermeer NE 117.4-119.7	Hoofddorp NW 145.9-147	Turnout G 300.5-301.3	SE 218-221	Rijpwetering 1 NW 130-135	Rijpwetering 2 NE 132.5-134
Intensity^3 average	Yes 2418	Yes 189	Yes 60	Yes 321	No 17	No 38
Grinding	Yes 5,5mm	Yes 6,0mm	Yes 3,0mm	Yes 2,3mm	Yes 4,3mm	Yes 3,5mm
Visual evidence	Yes	Yes	No	Yes	Yes	Yes
length	Yes 1.3km	Yes 1.1km	Yes 0.8km	Yes 3.0km	Yes 5.0km	Yes 1.5

4.3.2. Similarities

The values of the hotspots are presented in Appendix B. hotspots HSL-South. A compact overview is shown in Table 7.The major similarity was the 350HT rail grade which is present among all hotspots.

Table 7: Overview of the parameter values in the hotspots.

	Zoetermeer NE 119.7-117.4	Hoofddorp NW 146.5-147.5	Turnout 300.5-301.3	SE 218-221	Rijpwetering NW 130-135	Rijpwetering NE 132.5-134
Superstructure	Rheda 2000	Ballast 160	Ballast 160	Rheda 2000	Rheda 2000	Rheda 2000
Rail grade	350HT	350HT	350HT	350HT	350HT	350HT
Assets	none	Voltage lock	Flyover, Voltage lock	none	Dam wall, tunnel entrance	none
Cant (mm)	110	105	75	140	160	175
Radius (m)	6000	1600	2200	4450	4495	4625
Height difference (m)	0	~0	9,5	~0	-21,5	-1
Design speed (km/h)	300	160	160	289-300	300	300
Speed TRAXX (km/h)	160	115-125	130-125	160	160	160
Speed Thalys (km/h)	300	150-125	n/a	240 -265	300	285-295
Traction TRAXX (%)	20	0	0	5	20	10
Traction Thalys (%)	70	0	0	75	70	60
Tonnage cum. (MGT)	29,9	30,1	17,5	25,7	30,1	29,9
Tonnage 2015 TRAXX/Thalys (MGT)	4,81/1,75	4,85/1,73	3,86/0	3,88/1,80	4,85/1,73	4,81/1,75
Cant deficiency TRAXX	-59	2	9	-92	-72	-104
Cant deficiency Thalys	67	40	16	40	77	50
Additional grinding (mm)	5,5	6,0	3,0	2,3	4,3	3,5
Upper/Lower/both legs	Both	Upper Leg	Lower Leg	Lower Leg	Lower Leg	Both

Based on this data, some general conclusions can still be made regarding the hotspots:

- All rails in the hotspots have a rail grade of 350HT.
- The hotspots are located among curves with a cant of at least 75mm.
- The anti-headcheck profile 60 E2 has been used in the upper leg of the curves (not clear yet whether the upper- or lower leg is more affected).
- The dominant load comes from the TRAXX. For the northern part it is roughly 3/4 TRAXX load, for the Southern part (damages km 218-221) this is roughly 2/3 TRAXX load, as for the turnout from Breda (turnout km 300-301) the only load comes from the TRAXX.
- On all investigated hotspots the average TRAXX speed is at least 30km/h lower than the prescribed speed of the track design.
- There are no damages in tunnels.
- Damages arise within 17,1MGT, this was the total load of the hotspot (300-301) until November 2015 which has been least loaded.
- All tracks of the HSL-South have been grinded by both Speno as the HSG-L grinder up to now.
- There are no similar damages at the tracks to Belgium which is only being used by the Thalys. Even though similar constructions for curves have been used there. But the total load up to November 2015 was only 9,1MGT.

Differences between hotspots, which should be taken into account when characterizing the hotspots using clustering:

- There are hotspots where the average train decelerates and accelerates.
- There are hotspots where both traction and no traction occurs.
- There are damages on both Ballast and Rheda superstructures.
- There are damages on tracks with both vertical curves and on flat tracks.
- Damages occur on different speed profiles, parts designed for 160km/h but also parts for 300km/h.

4.3.3. Characterizing hotspots

Looking more closely at the hotspots and their locations and cant deficiency/excess properties we can divide them in two types:

- Hotspots in open track zones: Zoetermeer, SE218-221, NW130-135, NE132.5-134
- Hotspots in entry zones: Hoofddorp, Split 300.5-301.3

The hotspots in the open track zones are considered to be different because they lie in curves in the zones where the designed speed is around 300km/h. Typically here is the TRAXX driving far slower than the designed speed for these curves resulting in driving with great cant excess. The open track hotspots have a Rheda Superstructure whereas the entry zone hotspots use Ballast 160. Also both trains here drive with traction which is absent due to the presence of voltage locks among the other two hotspots.

The other two lie in the entry zones of the HSL-South. Also the entry zone hotspots have in common that both the Thalys and TRAXX drive not as designed, although the design speed at these locations lie within their maximum speed range (with exception of the Thalys at Hoofddorp). The TRAXX here drives at a speed even resulting in driving within the theoretical cant leaving this type of train without a leading leg through the curves. Also they share a complex track geometry with height differences and S-curves. An overview of the characteristic parameter values of both types of hotspots can be seen in Table 8.

Table 8: Overview of the characteristic parameter values of both hotspot types.

Open track hotspots		Entry zone Hotspots	
Parameter	**Value**	**Parameter**	**Value**
Superstructure	Rheda 2000	Asset	Voltage lock
Rail grade	350HT	Superstructure	Ballast 160
Rail profile	60E2 upper leg	Rail grade	350HT
Design speed	300	Rail profile	60E2 upper leg
Speed Thalys	300	Vertical curves	yes
Speed TRAXX	160	Design speed	160 km/h
Cant excess TRAXX	>50	Cant Excess TRAXX	Theoretical canting
Dominant load	TRAXX	Dominant load	TRAXX
Traction TRAXX	Yes	Traction TRAXX	No
Traction Thalys	Yes	Traction Thalys	No

4.3.4. Hypothesis damages

Before establishing an actual hypothesis first the characteristic parameters will be discussed regarding how they can be related to the RCF at the hotspots.

Horizontal curves in hotspots

The curves in the hotspots have been evaluated by checking the cant deficiencies and the cant excesses which occur at maximum and minimum speeds in the hotspots. This check will be done because all the hotspots have in common that they lie in a curve and the dominant traffic load comes from the TRAXX. Another argument for running this check is the TRAXX having a maximum speed of 160km/h which is about 60km/h less than the tracks and therefore the curves have been designed for at the parts where trains travel at maximum speeds.

Comparison of the speed profiles

From the values retrieved for the (design) speeds major differences among the two types of trains and the design speed for the track have been found. A comparison of the different speed profiles can be seen in Figure 36. In this figure a clear deviation from the theoretical speed from both the Thalys and TRAXX trains can be seen. Though for the Thalys this mainly occurs at the end of both northern sections. For the TRAXX, it can be seen that it drives under the design speed at most parts of the HSL tracks. Which is actually quite logical because of its limited maximum speed, however the next paragraphs we show this will have an effect on its behaviour in the curves.

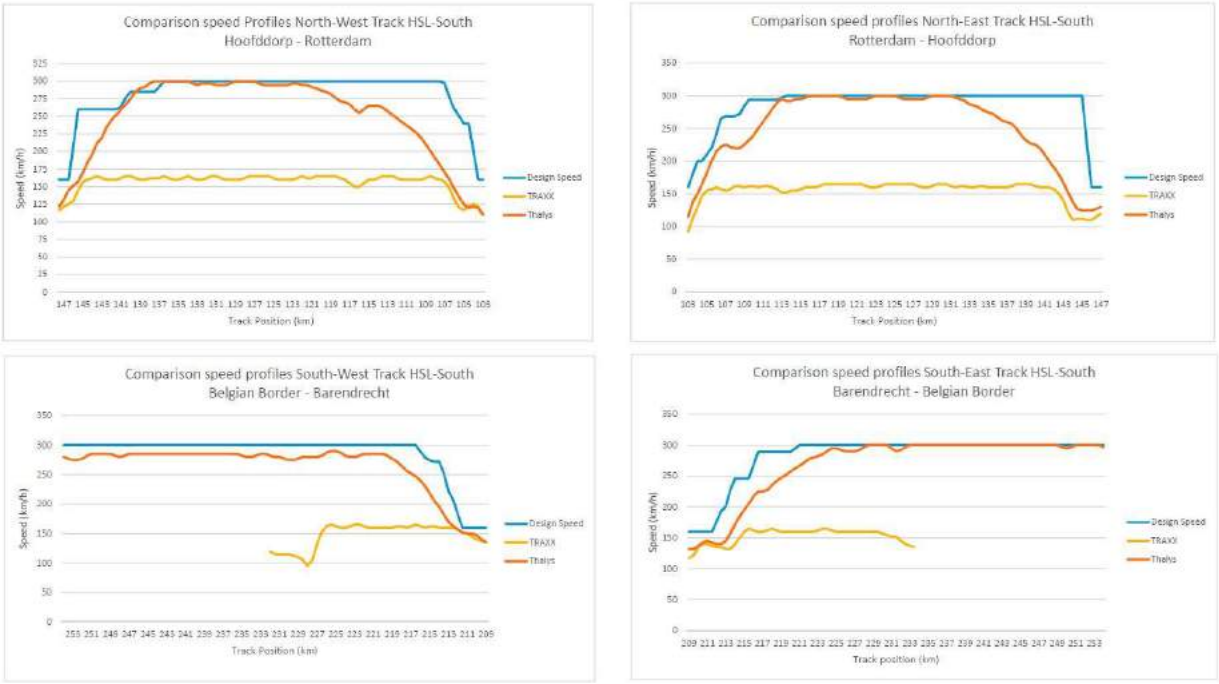

Figure 36: Comparison of the different speed profiles among the four major sections of the HSL. Note that there is only a speed profile for the TRAXX for half the southern section of the HSL this is because the TRAXX enters or comes from the turnout around kilometre 233.

Cant deficiency

For the theoretical- and actual speed profiles calculations have been done in order to evaluate the cant deficiencies regarding the hotspots in the HSL-South. The theoretical speed profile has been used in order to define the upper speed limit which is applicable for calculating the cant deficiency h_d. The results can be found in Table 9. As can be seen in Table 9 none of the hotspots have an ideal cant deficiency when the maximum design speed has been reached.

Table 9: Calculated cant deficiencies for the hotspots and the design speeds.

Properties of the curves for the theoretical speed profiles cant deficiency						
	NE 119.7-117.4 Zoetermeer	**NW 145.9-147.0 Hoofddorp**	**Turnout 300.5-301.3**	**SE 218-221**	**Rijpwetering NW 130-135**	**Rijpwetering NE 132.5-134**
Radius (m)	6000	1600	2200	4450	4495	4265
Cant (mm)	110	105	75	140	160	175
Vdesign max (km/h)	300	160	160	289	300	300
h_d Vmax design (mm)	67	84	63	82	77	75

Cant excess

The cant excess has been calculated for the hotspots and their theoretical speed profile, the results can be seen in Table 10. For the curves in the hotspots of Hoofddorp and Split 300.5-301.3 only the maximum values are known, the minimum values have been taken 20km/h less at 140km/h.

Table 10: Cant excess as calculated for the theoretical speed profiles in the Hotspots.

Properties of the curves for the theoretical speed profiles cant excess						
	NE 118.7-117.4 Zoetermeer	**NW 145.9-147.0 Hoofddorp**	**Turnout 300.5-301.3**	**SE 218-221**	**Rijpwetering NW 130-135**	**Rijpwetering NE 132.5-134**
Radius (m)	6000	1600	2200	4450	4495	4265
Cant (mm)	110	105	75	140	160	175
Vdesign min (km/h)	220	140	140	220	220	220
h_e Vmin design (mm)	14	-40	-31	11	32	41

A negative cant excess means the there is still a cant deficiency applicable for the minimum design speeds. This is the case in both the hotspots Zoetermeer and Hoofddorp. Cant excess is not a desired situation as it is most preferable in curves to guide trains by the outer rail thus a cant deficiency (AM Architectuur en Techniek, 2015). Taken this into account using the minimal design speeds, hotspots Hoofddorp and Split Zoetermeer seem to be within the ideal cant norms.

Cant excess results into some undesired effects, one being the different steering moment through the curve as shown in Figure 9. Where for cant deficiency a steering moment in the direction of the curve can be seen. For cant excess the steering moment is against the direction of the curve.

Comparison with the actual speed profiles

Here the actual cant deficiencies and cant excesses applicable for the hotspots are calculated. The cant deficiencies are not to be expected to change as much as the excesses because the deficiencies have been calculated during the design phase for speeds up to 300km/h. This speed is actually being reached by the Thalys. However, the cant excesses are thought to be different from the design as the TRAXX are driving slower than the originally planned V250 trains which had an operating speed up to 250km/h. The design for the largest parts of the tracks is 220-300km/h which has also been taken as boundary for the upper- and lower limits for the calculations of the curves, with exception for the hotspots Hoofddorp and Turnout 300.5-301.3 as these lie within the entry zones of the HSL-South, here trains are not yet running at full speed. The results of the calculations can be seen in Table 11.

From the results one can see that the cant deficiencies and cant excesses are not exceeding the applicable norms for the design speeds. Concluding there are no design flaws with regard to the curves and the theoretical speed profiles. That only in two occasions the ideal cant values are being reached is due to the fact that the HSL-South has not been designed for single speed traffic. It has been designed for both 220 km/h and 300km/h as outer speed boundaries, therefore both speeds must be designed with cant deficiencies and excesses within the applicable norms.

The cant deficiencies and cant excesses for the curves in combination with the actual speed profiles show worse results than the design, in some occasions even exceeding norms. The worst values are as expected to be found in the lower boundaries of the actual speed profile as the TRAXX speed profile deviates most from the design profile. The values for the TRAXX can be divided into two effects:

- Great cant excess.
- Within the theoretical cant deficiency.

Both are undesired effects, the first results in high loads on the inner rails of the curves. The second one causes the rail vehicle not having a leading leg through the curve. Both effects can be a possible cause for damages at the hotspots with as a cause the TRAXX using the tracks as there is not one hotspot the TRAXX drives through as desired. In Appendix E. Cant excess related to ground areas has been studied. Here can be seen that there seems

to be some correlation regarding exceeding cant excess values, theoretical canting and the hotspots and additionally corrective ground areas.

Table 11: Results of the calculations for the comparison of cant deficiencies and cant excess for the curves in the Hotspots at designed speed and actual speed. Green means within the ideal cant margins, yellow means not ideal but within applicable ProRail norm values, Orange means 10mm within the theoretical cant or between ProRail norm value and exceedance value, red means outside the ProRail exceedance value.

Properties of the curves						
	NE 119.7-117.4 Zoetermeer	**NW 145.9-147.0 Hoofddorp**	**Turnout 300.5-301.3**	**SE 218-221**	**Rijpwetering NW 130-135**	**Rijpwetering NE 132.5-134**
Radius (m)	6000	1600	2200	4450	4495	4265
Cant (mm)	110	105	75	140	160	175
Actual Speed						
Vmax (km/h)	300	140	130	260	300	285
Vmin (km/h)	160	120	125	160	160	160
h_d Vmax (mm) (Thalys)	67	40	16	40	77	50
h_e Vmin (mm) (TRAXX)	59	-2	-9	72	92	104
Design Speed						
Vdesign max (km/h)	300	160	160	289	300	300
Vdesign min (km/h)	220	140	140	220	220	220
h_d Vmax design (mm)	67	84	63	82	77	75
h_e Vmin design (mm)	14	-40	-31	11	32	41

Rail grade

Among all the hotspots a 350HT rail grade is present. This is due to the fact that this rail grade has been used because of its better features regarding wear prevention. This feature was thought to be advantageous regarding the life cycle costs of the rails. These have only been placed among the curves as they were expected to be more vulnerable to wear than straight tracks.

There are several scientific publications regarding RCF damages and head hardened rails. Several papers will be discussed in this section regarding the performance of heat-treated rails in relation to wear and rolling contact fatigue damages. This in order to see if the rail grade can be related to the damages which have been found at the HSL.

Investigation of rolling contact fatigue in a head hardened rail

The first paper (Dikshit, Clayton, & Christensen, 1991) focused on the performance of heat treated rails regarding the rolling contact fatigue and the formation of white edging layer among the rails. In this paper, metallurgical studies have been presented on parts of rails during several stages of life. This study has been done at the Northern Burlington heavy haul lines regarding curves among the tracks.

One of the most interesting findings was that the total number of cracks decreased as the tonnage increased (Dikshit et al., 1991). The number of short cracks (0-0,1mm) was greatest during the first MGT's after grinding. However as the total number of cracks decreased the amount of larger cracks increased during the rails service life. This suggests that some of the shorter cracks develop into larger cracks and some of the initial cracks were lost by wear (Dikshit et al., 1991).

Another finding in this study is the correlation found between the appearance of WEL and cracks among the surface. Here the researchers examined how much percentage of the rail surface has been affected by WEL. The results showed that this percentage decreased over the rail surface life. Also the depth of the WEL decreased when more MGT's had passed the rails.

The last check which has been done during this research was to find out what percentage of cracks are associated with the WEL. This percentage was very high at the lowest number of MGT's and decreases eventually. Furthermore a large number of observed larger damages at the higher MGT's had been associated with surface features that could have been sites of spalled WEL (Dikshit et al., 1991).

Concluding the authors suggested that these surface initiated defects arose very early in the service life of the rail. Almost certainly as a direct result of the formation of white edging layer (Dikshit et al., 1991). This article didn't focus on the cause of the WEL formation. But the authors suspect the cause is not the result of the wheel-rail contact.

The article is from 1991 and freight traffic has been examined instead of high-speed traffic. But suggests there are some relations with WEL formation, heat-treated rails and RCF damages which can be related to WEL formation. Which is very interesting as the study by DEKRA also shows clear evidence of the presence of WEL and also suggests that this presence might initiate the damages.

Testing of HSH (350HT) rails in high-speed tracks to minimise rail damage

Another article which will be discussed to get better insight of the performance of heat treated rail is a paper by Heyder and Girsch from 2003. This will give more insight in the performance of heat treated rails at high-speed tracks, also a comparison has been done by the authors among the performance of other rail grades (220 and 260).

The investigation has been done installing different rail grades in high- and medium speed curves and in tangents and wide curves at the German high-speed line Hannover-Würzburg (speed maximum 250km/h). The performance regarding wear, corrugation and head-checks among the different rail grades had been studied after 80MGT for the high-speed curves.

Results showed the 350HT rail grade had the lowest wear rate, about half compared to the 260 and two-thirds lower than the 220 rail grade (René Heyder & Girsch, 2005). The results regarding the damage depth showed that the 350HT rail grade also performed better here. The depths of the head checks were only one third of those of the 260 rail grade, the 220 rail grade showed the largest depths despite the higher wear rate. Also the results regarding corrugation proved advantageous for the 350HT profile. In the test sections on the high-speed line it is showed that the corrugation was a third less than for the 260 grade (René Heyder & Girsch, 2005). Also grinding tests have been done to look at how many grinding passes were needed among the different rail grades to remove the head checks. For 350HT this was only half compared to 260 and only about a quarter compared to 220, which is logical taking into the larger depths of the cracks.

The paper concludes that by applying an appropriate maintenance programme a significant increase of rail service life can be expected when using 350HT. Also the maintenance costs can be reduced because of the lower grinding efforts (René Heyder & Girsch, 2005).

This paper suggests the use of 350HT can prove very advantageous compared to softer rail grades. Though the damages among the tracks here were head checks whereas the HSL is affected by damages at the rail head. Also the performance of the rail grade has only been examined at one moment 2,5 years after placement.

Rolling contact fatigue in relation to rail grinding

The last paper regarding the rail grades which will be discussed is a paper from 2016 by Steenbergen. The author did research on the relation of spalling defects, grinding and different rail grades.

This paper discusses the RCF defects found specifically as spalling defects and notices they typically occur on heat treated rails. The defects occur in a track with a RCF maintenance regime and occur very early in the maintenance cycle <15MGT (Steenbergen, 2016).

The research was set-up for two different rail grades, namely 260Mn and 370crHT at a regular Dutch railway track with mixed traffic (passenger and freight). At this track, a cyclic grinding regime is being executed, removing 0.2mm of material by a rotating stone grinding machine. Directly after the grinding, a sample from the rail was taken off and after a few days another sample was taken. For the research, these samples were further examined.

Both rail grades showed different results. For the standard rail grade the friction-induced martensite by grinding delaminates after consecutive train passing. However, the applied grinding induces severe plastic deformation at the top layer of the rail. This coincides with the ''pre-fatigue'' of the rail by trains passing over. The heat-treated rail behaves different, here the friction-induced martensite by grinding accumulates at groove edges during the grinding process. By trains passing over, they are pressed deeper in the pearlite material of the rail in combination with severe plastic deformation. This is the result of tangential wheel contact stresses. This is thought to yield extensive crack initiation at the onset of the rail service life (Steenbergen, 2016).

The paper suggests, to avoid spalling defects, operational grinding specifications should be reconsidered to avoid WEL formation by grinding with special attention to the heat-treated rail grades (Steenbergen, 2016).

This paper discusses findings which could explain the first paper by Dikshit, where most damages had been found very early on in the service life of heat-treated rails. Although, there are also some remarks to be made regarding these findings. The figures which showed the grinding results didn't look like a very nice finishing of the grinding. Also one should be careful generalizing these results for all the grinding actions among heat-treated rails. The article very clearly shows grinding could be initiating more defects even though the 370crHT rail grade was examined instead of the 350HT at the HSL. Also the author doesn't seem to be taking into account the process of natural wear which will eliminate in most of the cases the grinding marks. As the samples had been taken out this process of natural wear which could have stabilized the rail more could not have occurred yet. However, the differences found between the two rail grades could be explained by the difference in grinding results. As according to (Lundén & Paulsson, 2009), higher carbon content causes better material strength but also reduces the material toughness and makes it more vulnerable to thermal loading.

TRAXX

Regarding the TRAXX' influence, it is striking when looking at where the hotspots are located, which can be seen in Table 12. The hotspots are only found at locations where the TRAXX is using the tracks. At the parts where only the Thalys is using the tracks there are no hotspots.

Table 12: The traffic type related to the number of hotspots.

Traffic	Location	Number of hotspots
Mixed (TRAXX and Thalys)	NW, NE, SW 208-233, SE 208-233	5
TRAXX only	G, H	1
Thalys only	SW 233-254, SE 233-254	0
No traffic	J, K	0

Traction by the TRAXX

Regarding the TRAXX it has to be taken into account that until the damages had been detected it only was used driving with a single locomotive thus having only four driven axles. In Appendix D. Traction and breaking forces per axle, are shown. Regarding the TRAXX it is shown that these are not constant. Which is due to the fact that

the TRAXX are locomotives with large tractive efforts, which are also being used for freight traffic. The maximum speed of 160km/h is relatively fast reached. Because of the gradients among the HSL the traction forces per axle differ greatly over the whole HSL.

Especially compared to the Thalys which has to give more constant traction because of the maximum speed of 300km/h which is being reached after more km's. The traction forces on the rail by the train increase the shear stresses, which occur at the wheel-rail interface which can cause problems. This effect is also unevenly distributed among the rails in curves.

Hypothesis

The maintenance regime for the HSL-South was not sufficient as the regular eddy current measurements only used channels for gauge corner measurements, thus not being able to measure the rail head. Most of the damages at the hotspots are being found on the rail head. Ultrasonic measurements are able to measure damages starting at 4mm, thus not sufficient for measuring early defects. This made early intervention based on measurements impossible.

As shown during the further analysis of the curves in the hotspots, it is known both the Thalys and the TRAXX are not driving ideally through the curves among the hotspots. When looking at where damages occur, one would expect damages on the lower legs where the TRAXX drives with great cant excess, thus in the open track hotspots. How the damaged legs have been determined among the hotspots can be seen in Appendix G. Determining where the damages occur. This can be seen to be correct when viewing Table 13. When taking a look at the hotspots where there is damage on the upper leg it can be seen in 2/3 hotspots that the trains are driving through the curves with great cant deficiencies, the other one is Hoofddorp where the Thalys is driving within the ideal canting zone but the TRAXX having no leading leg this causes unpredictable behaviour. Another case which needs more investigation is why the upper leg in NW130-135 remains rather unaffected, which is not as expected.

Table 13: Types of hotspots, their cant excess and deficiency and the damages at these hot spots.

Type	**Entry zone Hotspots**		**Open track hotspots**			
Location	**NW 145.9-147.0 Hoofddorp**	**Turnout 300.5-301.3**	**NE 119.7-117.4 Zoetermeer**	**SE 218-221**	**Rijpwetering NW 130-135**	**Rijpwetering NE 132.5-134**
h_d Vmax (mm)	40	16	67	40	77	50
h_e Vmin (mm)	-2	-9	59	72	92	104
Damage depth (mm)	6,0	3,0	5,5	2,3	4,3	3,5
Upper/Lower/both legs	Both	Lower Leg	Both	Lower Leg	Lower Leg	both

Taking all this into account it seems the damages of the HSL-South are the result of mismatched monitoring of the tracks which has been solely focussing on head-check formation leaving the rail head unmeasured by Eddy current. Eddy current is the measurement technique to detect early defects as it can measure from 0,1 up to 5mm's.

The TRAXX and the Thalys both driving at the hotspots in 10/12 situations not ideally with the TRAXX never driving ideally through these curves making these zones vulnerable to damages. The largest concentration of damages is also seem to occur at the beginning and endings of the curves which can be seen in Appendix G. Determining where the damages occur.

This indicates that the dynamical behaviour of one or both vehicles play a role here. As the damage concentrations seem to decrease when arriving further in a circular curve. This dynamical behaviour can result

in the train not being stable entering the curve and eventually reaches a stable condition. Which resembles the measurements.

For other possible factors which could have played a role upon why serious damages as these could arise within loads of only 30MGT's, we should take a closer look upon the other parameters which these spots have in common like grinding, profiles and rail grades.

For instance the grinding could have played a role. On several occasions by high-speed grinding 0,2mms of rail have been removed. This has also been done on the hotspots not knowing there were probably already minor damages. Not removing a crack completely still leaves the crack in the rail so it will still be able to grow into a larger crack.

Also during current practices both 350HT and 260 rail grade profiles are being ground using the same specifications, not taking into account they are different. According to experts from Speno (grinding company), the grinding process and removal rate conducted in the HSL have been the same in both cases. 350HT profiles are harder because of using a different processing operation resulting in finer grained material. Higher hardness results in less wear this is also why the head hardened rails have been chosen for the curves in the HSL but the additional hardness also results in additional carve sensitivity . Grinding marks are still clearly visible on the rails in the hotspots. This might indicate that the introduced roughness by grinding wears away much slower than in softener rails this effect lasts much longer due to fact the HSL is not a very congested. The different results regarding RCF for the two rail grades could be explained by different results after grinding.

Another closer look should be taken at the profiles, knowing that due to curves and the speeds in the curves great cant excesses and deficiencies occur but the question is how the real wheel-rail contact is in reality. The damages clearly occur on the rail head indicating there are some high stresses there. It might be that the profile is not fit for these situations and that there is no two point contact but maybe a single contact point on the rail head leading to both the normal and tangent forces transferred through the head of the profile. Also the presence of traction in the open track hotspot zones raises the stresses at the wheel-rail contact area which can cause the damages at the hotspots in combination with the other factors.

The influential parameters regarding the hypothesis are thus the cant excess regarding the TRAXX, theoretical cant for the TRAXX, tractive efforts by both vehicles at the open track hotspots, 350HT rail grade and grinding. Whereas the last two are the same among both hotspot types.

4.3.5. Hypothesis check open track hotspots

This paragraph will describe the check which has been done regarding the hypothesis. Firstly, the data has been checked regarding exceeding the cant excess norm of 50mm by the TRAXX among the other hotspots of the HSL which is being used as the main characteristic parameter value. From this check another total of thirteen curves have been found sharing a cant excess of 50mm or more and not being located in tunnels. These curves were located among the four main sections of the HSL.

These curves were accordingly evaluated among the other characteristic parameter value, which the open track hotspots share namely: rail grade of 350HT, Traction present by both TRAXX and Thalys and eddy current proof of damages >3mm. Also the damages have been checked upon their damage concentrations being >3mm damage per metre in order to be able to quantify the results. The intensity has not been used here as most curves are too small to cover a whole partition. Another check which has been added the curve being correctively ground during the latest corrective grinding action in December 2015. This provides evidence the cracks were actually present. This doesn't mean the other damages measured are not present on the rails but we only know they have not been ground. An overview of the hypothesis check can be found in Table 14.

What can be seen from this check is that there are five out of these thirteen curves which share all the characteristics of the open track hotspots. When we look at the damages from the eddy current measurements we can see the curves sharing all the characteristics have larger damage concentrations than the curves which share less characteristics. The exception for this is the curve located at NE 130.982-132.685. Though, when taking a closer look at this curve it can be seen that this curve has a small difference in radius and canting after

the previous curve which is also among this list and has larger damage concentrations. This can be seen in Appendix G. Eddy current measurements hypothesis check.

For the two curves which have a 260 rail grade its notable they share very low or no damages. Which supports the hypothesis. We also see that the traction from the TRAXX seems to be more dominant for damage concentration than the traction by the Thalys. Regarding the check which has been done this can be explained that all curves share large cant excess by the TRAXX. This effect can be seen in the curves located at NE 136.375-138.971 and NE 140.028-143.499.

4.3.6. Hypothesis check entry zone hotspots

Regarding the entry zones. There are no other areas which share the same characteristic parameter set. Two of the other entry zones are located in tunnels, respectively tunnel Rotterdam Noord and Roof Barendrecht. Another entry zone is located at the Belgian border, this entry zone is only being used by the Thalys and it drives at his maximum speed.

Table 14: Hypothesis check, list of curves with similar characteristics as the open track hotspots.

Km start	Km end	Track	Cant	Radius	Cant Excess	Rail grade	Traction TRAXX	Traction Thalys	Eddy Current	3mm damage/m	Corrective Grinding
110.781	113.485	NW	120	5999.5	68	350HT	Yes	No	2 damages>3mm	1/1352	No
113.485	115.945	NW	145	5100.5	85	350HT	No	No	No damages >3mm, though several areas with smaller damages	0/2460	1,80 mm
117.216	121.709	NW	120	5999.5	66	350HT	Yes	Yes	14 damages >3mm	1/320	3,00 mm
113.485	115.942	NE	135	5095	79	350HT	No	Yes	3 damages >3mm	1/819	No
130.399	130.982	NE	175	4325.5	100	350HT	Yes	Yes	3 damages >3mm	1/194	No
130.982	132.685	NE	165	4494.5	97	350HT	Yes	Yes	1 damage	1/1703	No
136.375	138.971	NE	140	5505	81	350HT	Yes	No	5 damages >3mm	1/519	No
140.028	143.499	NE	150	4495	85	350HT	Yes	No	7 damages >3mm and additional larger areas with smaller damages	1/495	3,30 mm
217.896	221.269	SW	165	4455	97	350HT	Yes	Yes	8 damages >3mm	1/421	No
228.817	229.788	SW	105	6000	82	260	Yes	Yes	1 damage	1/971	No
229.788	230.454	SW	70	8000	51	260	Yes	Yes	No damage	0/666	No
225.889	226.523	SE	125	5435	69	350HT	Yes	Yes	10 damages >3mm	1/63	1,57 mm
228.118	228.817	SE	110	5994.5	59	350HT	No	Yes	1 damage	1/699	No

4.4. Top-down approach

This check has been done using IBM's SPSS Statistics software. For the whole track the total available number of intensity values gathered from the Eddy current measurements was 740. Though both trains don't use the whole track the correlation regarding vehicle parameters was less but still more than 500 values have been gathered for both trains, thus the sample sizes are quite large.

The correlation analysis has been done for the three intensities as for five different situations, so providing the data for both the top-down and combined approach:

- The whole track.
- The whole track without tunnels.
- Open track (design speed=300km/h).
- Open track without tunnels.
- Entry zones.

The whole track will be examined to find out if there is a relation for the whole track regarding intensity and other parameters. Tunnels were seen as an important parameter which also should be examined differently because parameter values like cant excess and traction can also be present in tunnels but we see very low intensity values in tunnels and no significant reported damage in the past. The open track and entry zones have also been examined separately in order to see if the initial hypothesis regarding influencing parameters also proof to be influential by a correlation study.

For the correlation analysis Pearson's correlation has been executed resulting in a Pearson correlation coefficient r and a significance value.

4.4.1. Results of the correlation analysis for the whole track

The numerical parameters have been used in the correlation analysis thus not only the previously identified parameters which might have an influence on the presence of damages. This in order not to rule out any possible cause which could have been overseen in the application of the B-U approach.

The results for both whole track situations are presented in Table 15. It is notable that for the I_x value there are more correlating parameter than for the I_x^1 and I_x^3 values.

Table 15: Results of the correlation study for both whole track situations, showing the correlating parameters.

	Intensity	Correlating parameter	Pearson's correlation (r)	Significance value
Whole track	I_x	Traction TRAXX	0.183	0.000
		Theoretical cant TRAXX	0.167	0.000
		Speed TRAXX	0.126	0.001
		Cumulative tonnage	0.123	0.001
		Canting	0.099	0.007
	I_x^1	Traction TRAXX	0.183	0.000
		Traction Thalys	0.091	0.013
		Canting	0.087	0.018
		Speed TRAXX	0.083	0.024
		Cumulative tonnage	0.078	0.034
	I_x^3	Traction TRAXX	0.133	0.000
Whole track without tunnels	I_x	Traction TRAXX	0.204	0.000
		Theoretical cant TRAXX	0.186	0.000
		Speed TRAXX	0.141	0.001
		Canting	0.131	0.001
		Cumulative tonnage	0.129	0.001
		Theoretical cant Thalys	0.108	0.022
		Traction Thalys	0.099	0.015
	I_x^1	Traction TRAXX	0.184	0.000
		Traction Thalys	0.106	0.009
		Cumulative tonnage	0.101	0.013
		Canting	0.093	0.023
	I_x^3	Traction TRAXX	0.167	0.000
		Traction Thalys	0.080	0.049

However, when looking back at Figure 80 it is expected that the correlations found contributing most to the damages, are at the hotspots for the I_x^3 intensity values as these show clear peaks at the hotspots. Furthermore, it can be seen at both situations, the strongest correlations are found for the traction by the TRAXX, which shows correlation for all the intensities and in both situations. It was expected to see also more curve related parameters like cant deficiencies coming back in this study though this seems not the case but is probably due to the fact that in both situations still lots of curves are present which score rather low for the intensity parameters. Also the cumulative tonnage comes out in the I_x and I_x^1 in both situations.

4.4.2. Results for the correlation analysis for the open track

Also for the open track areas the same analysis has been done. This in order to look if there are any notable changes compared to the analysis of the whole track and to check the initial hypothesis for the hotspots regarding cant excess and traction by both vehicles. The open track area was defined as the area which is designed for a maximum speed of 300km/h. This check has also been done for open track without tunnels as we see no problems in the tunnels expecting to gather better indicators for parameters which have an effect on intensity.

Table 16: Results for the correlation analysis regarding the open track areas and the open track areas without tunnels.

	Intensity	Correlating parameter	Pearson's correlation (r)	Significance value
Open track	I_x	Traction TRAXX	0.259	0.000
		Theoretical cant TRAXX	0.184	0.000
		Theoretical cant Thalys	0.149	0.003
		Cumulative tonnage	0.148	0.001
		Traction Thalys	0.128	0.003
		Speed TRAXX	0.129	0.003
		Cant deficiency Thalys	0.116	0.021
		Canting	0.101	0.020
	I_x^1	Traction TRAXX	0.208	0.000
		Traction Thalys	0.105	0.015
		Cant deficiency Thalys	0.102	0.042
		Cumulative tonnage	0.096	0.027
		Speed TRAXX	0.091	0.037
	I_x^3	Traction TRAXX	0.183	0.000
		Traction Thalys	0.091	0.036
Open track without tunnels	I_x	Traction TRAXX	0.292	0.000
		Theoretical cant TRAXX	0.209	0.000
		Theoretical cant Thalys	0.177	0.001
		Cumulative tonnage	0.167	0.000
		Traction Thalys	0.158	0.001
		Speed TRAXX	0.150	0.002
		Cant deficiency Thalys	0.123	0.028
		Canting	0.117	0.013
	I_x^1	Traction TRAXX	0.254	0.000
		Traction Thalys	0.129	0.006
		Cumulative tonnage	0.121	0.011
		Cant deficiency Thalys	0.116	0.037
		Speed TRAXX	0.115	0.015
	I_x^3	Traction TRAXX	0.223	0.000
		Traction Thalys	0.110	0.020
		Cumulative tonnage	0.097	0.042

Looking at the results regarding correlating parameters. We see a partial confirmation of the initial hypothesis. Though it seems that the traction by the TRAXX is more dominant than expected. Were the first assumption had been made regarding the cant excess to be the dominant parameter regarding damages in the open area zones we now see that traction by the TRAXX is most dominant. The traction by the TRAXX is in all six simulations the most correlating parameter, followed by the traction of the Thalys. The traction by the Thalys has also been identified as a influencing parameter regarding the first hypothesis. Furthermore the cumulative tonnage also comes out as a significant correlating parameter in five out of six simulations.

4.4.3. Results for the correlation analysis for the entry zones

The last correlation analysis has been done for the entry zones. This in order to check the initial hypothesis regarding complex geometry being the cause of damages. The results are presented in Table 17

Table 17: Results of the correlation analysis for the entry zones.

	Intensity	Correlating parameter	Pearson's correlation (r)	Significance value
Entry zones	I_x	Cant deficiency Thalys	-0.312	0.001
		Cumulative tonnage	-0.305	0.000
		Canting	0.226	0.006
		Cant deficiency TRAXX	-0.211	0.023
	I_x^1	Cant deficiency TRAXX	-0.322	0.000
		Canting	0.307	0.000
	I_x^3	Canting	0.271	0.001
		Cant deficiency TRAXX	-0.223	0.016
		Theoretical cant TRAXX	0.188	0.043

From the correlating entry zone parameters we see indeed cant-related parameters correlating with the intensity parameters. We see a negative correlation with the cant deficiencies, meaning that negative cant deficiency is present regarding stronger intensity values. Negative cant deficiencies are cant excess. Also the constructed canting in the track comes back as a correlating parameter showing the intensities are highest in the curves of the entry zones.

4.4.4. Discussion regarding the correlation analysis for the whole track

In the last sections all parameters have been presented having a significance value under 0.05. Depending on the sample sizes having correlation values between 0.08 and 0.3 which are still not very strong correlation as being 0.00 value being no correlation at all and 1 perfect positive correlation.

We will now take a closer look at the correlating parameters regarding the I_x^3 correlating parameters of the previous section as being the best indicator for hotspots as shown in Figure 80.

For the whole track as significant correlating parameters regarding I_x^3 traction by the TRAXX came out. Figure 37 (A) shows how both parameters relate to each other. This figure show clear peak values at the 15 and 20 percent zones of maximum traction by the TRAXX. Though its notable that the peaks are not at the higher 25 and 30 percent of maximum traction zones.

For the whole track without tunnels this check has also been done and we get nearly the same figure from the results as can be seen in Figure 37 (B). Although the peaks are higher here suggesting that when we leave the tunnels out where also traction is being given the peaks become even clearer. Also the traction by the Thalys showed correlation with the intensity for cracks over 3mm. These results are shown in Figure 37 (C). In this figure we see clearer results that more traction is present at higher intensities.
The traction from both trains have also been related to the I_x^3 parameter which can be seen in Figure 38. Here we see one major peak which is the location of the hotspot Zoetermeer. The other peaks are the other hotspots which also score lower for intensities. We see that for the highest intensity scores traction is present.

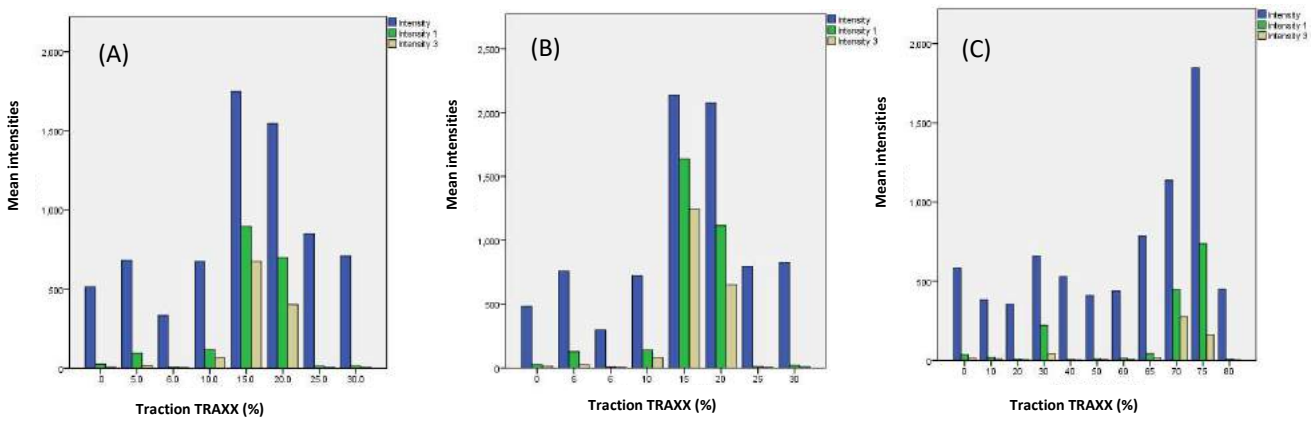

Figure 37: (A)Traction TRAXX related to the mean intensities for the whole track. (B) shows the intensity related to the traction by the TRAXX for the whole track without tunnels. (C) shows the results regarding the traction of the Thalys and the intensity parameters for the whole track without tunnels.

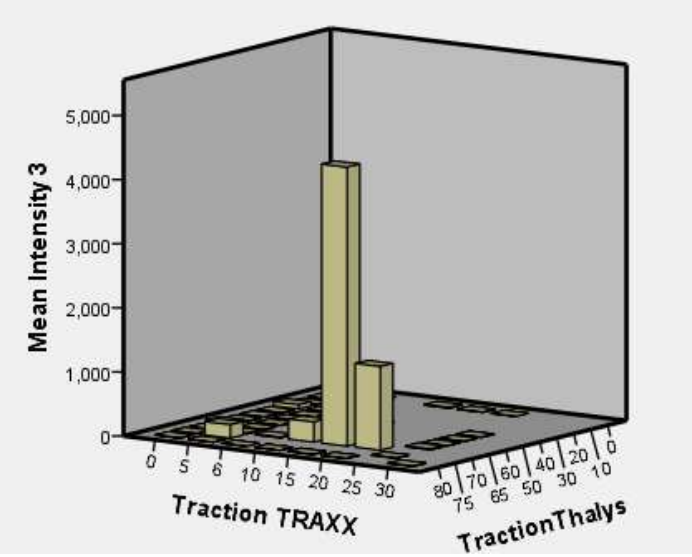

Figure 38: Traction by both vehicles related to the mean intensity I_x^3.

4.4.5. Discussion regarding the correlation analysis for the open track

The next check which has been done was to check the initial hypothesis regarding the open track hotspots. Influencing numerical parameters which had been identified initially were:

- Cant excess (negative cant deficiency).
- Traction TRAXX.
- Traction Thalys.

Considering the cant excess it is expected that for the open track correlation analysis this will result in negative correlation with cant deficiency and positive correlation with theoretical cant by the TRAXX and canting.

Looking at the results presented in Table 16 regarding the I_x^3 parameter we see the strongest correlation with the traction by the TRAXX. The relation between the I_x^3 intensity and the traction by the TRAXX is presented in Figure 39 (A). Comparing to the results for the whole track we now only see peaks for the traction, the little values for 10 and 0 have now disappeared. Which confirms the stronger correlation which have been found for this analysis. Looking at the traction by the Thalys we find a single large peak for the 70% maximum traction value Figure 39 (B). This shows that the presence of traction for the open track is indeed a necessary condition for the intensity I_x^3.

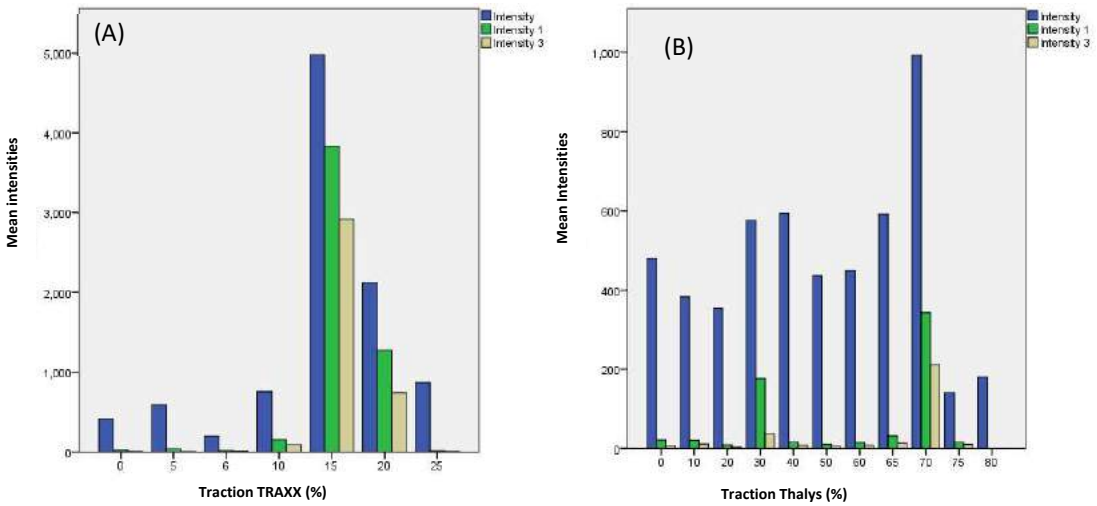

Figure 39: Traction TRAXX (A) and Thalys (B) for the open track.

The additional check had been done for the open track without tunnels though as additional correlating parameter only cumulative tonnage came out. The results are shown in Figure 40. The explanation is quite obvious we see the peaks lying around 30MGT which are the tonnages for the northern part of the HSL which is indeed the area where most hotspots are located. These results have been shown as an histogram to see the distribution. This gives some indication though that more tonnage is required for increased intensity.

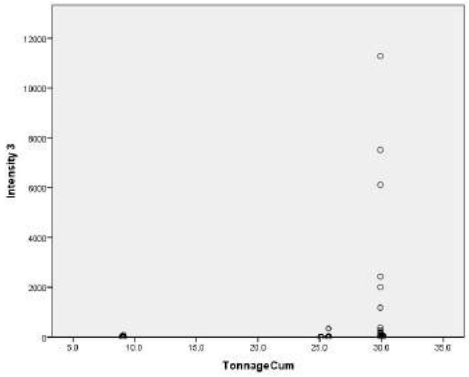

Figure 40: Cumulative tonnage compared to the intensity I_x^3 for the open track without tunnels.

So confirmation has been found regarding the presence of traction at the open track as a condition necessary for damages. Though for I_x^3 the confirmation regarding the curves is not present. It was expected to not show significant results for the open area, but therefore the open area without tunnels was introduced. Though not showing the numerical correlation the results are presented in Figure 41. This shows indeed that for three intensity parameters we see the distribution of intensity indeed in negative cant deficiency (excess). Though this logical as the open track was designed for speeds of 300km/h. Only conclusion being able to draw here is that more cant excess doesn't contribute to higher intensity scores. For the I_x^3 intensity we see the clear peak around 60 being the Zoetermeer hotspot.

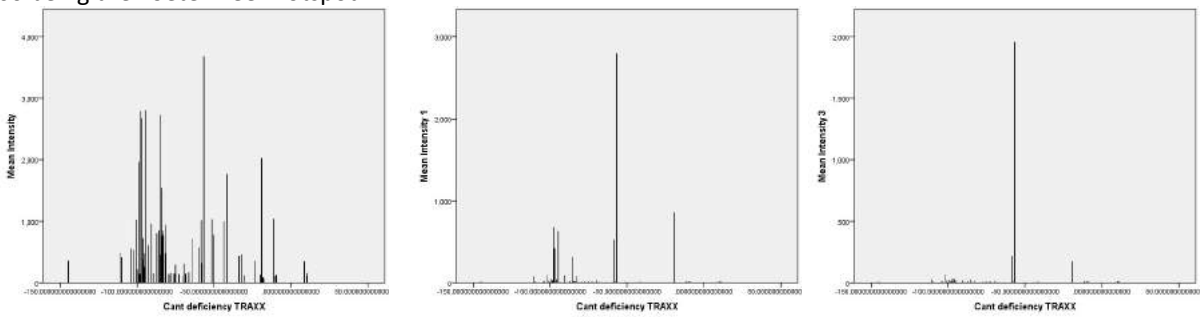

Figure 41: Intensities compared to the cant deficiencies of the TRAXX for the open areas without tunnels.

4.4.6. Discussion regarding the entry zone correlation analysis

For the entry zones the initial hypothesis was that there was no traction present at both hotspots located here. Traction was thus not expected to be a correlating parameter in these cases. This was confirmed as we look at the results which are presented in Table 17. For the entry zones the hotspots showed as a similar characteristic that there was complex geometry present being s-curves and vertical gradients. S-curves cannot be identified in these correlational analysis as there is no parameter for it. Though the presence of canting and related cant deficiencies can. Which can also give an identification which train shows correlation with the intensities.

Looking at the results we see as expected no correlation with traction which confirms the initial hypothesis regarding these hotspots. For I_x^3 we only see curve related correlations. The canting is being presented in Figure 42 (A), here we clearly see the mean intensity being largest as the curves having a bigger cant.

A negative relationship with the cant deficiency by the TRAXX had been identified, suggesting cant excess has an influence on the intensity parameter which was rather unexpected. This because previously the theoretical cant was of influence in these areas. The relationship between these parameters is presented in Figure 42 (B). Here we see two peak values, one indeed lying in the theoretical cant area being the hotspot Hoofddorp, the other one lying around -75 which is strong cant excess. Looking at the input data this turned out to be the hotspot

around km 220 SE. When we look at the definition of the entry zones being the area where trains enter the HSL until the design speed of 300km/h has been reached this area indeed lies just before the 300km/h area. In this area the TRAXX has already reached its maximum speed and the Thalys is still accelerating thus having more in common with an open track hotspot where traction and cant excess play a major role.
The last correlating parameter for the entry zones was theoretical cant by the TRAXX though here we see similar problems (see Figure 42 (C))as with the cant deficiency of the TRAXX. Knowing that the major peak at 80 is the hotspot at km 220 SE. Making this analysis for the entry zones rather disputable.

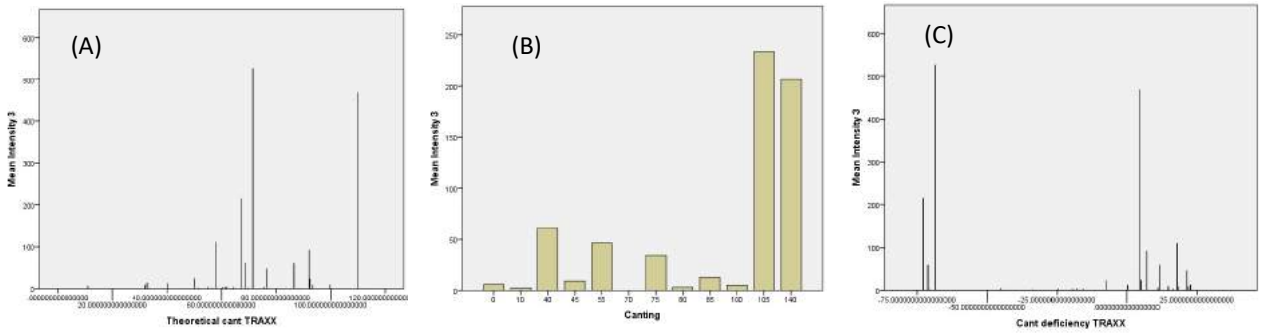

Figure 42: (A) Theoretical cant by the TRAXX related to the mean intensity I_x^3in the entry zones.(B) canting related to the mean intensity I_x^3 in the entry zones. (C) Cant deficiency TRAXX related to the intensity I_x^3in the entry zones.

4.5. Non-numerical parameters compared to intensity parameter

For the non-numerical parameters like superstructure, affected rail in the curve, rail grade and the assets a correlation analysis was not possible. Therefore an analysis for different situations has been done. This being the same situations which have been used for the correlation analysis to check the initial hypothesis using figures.

4.5.1. Assets related to intensity

In Figure 43 (A) is shown why the tunnels are discussed as a different situation for the correlation analysis. We actually see very low intensities there especially for I_x^1 and I_x^3. Because other factors like traction and cant excesses are present in the tunnels for the open track analysis also situations without the tunnels have been analysed.

Furthermore we see peak values for intensity at the damwall and flyover this is because at both areas hotspots are present and there is only one damwall and flyover among the track explaining the peak values. For I_x^3 the strongest values occur at the open track this because other hotspots are present here. The open track scores relatively low values because of the number of data points covered by the open track. This is presented in Figure 43 (B). Note that 'open track' as an asset is actually the absence of an actual asset, not to be confused with 'open track' used as a term in the previous section.

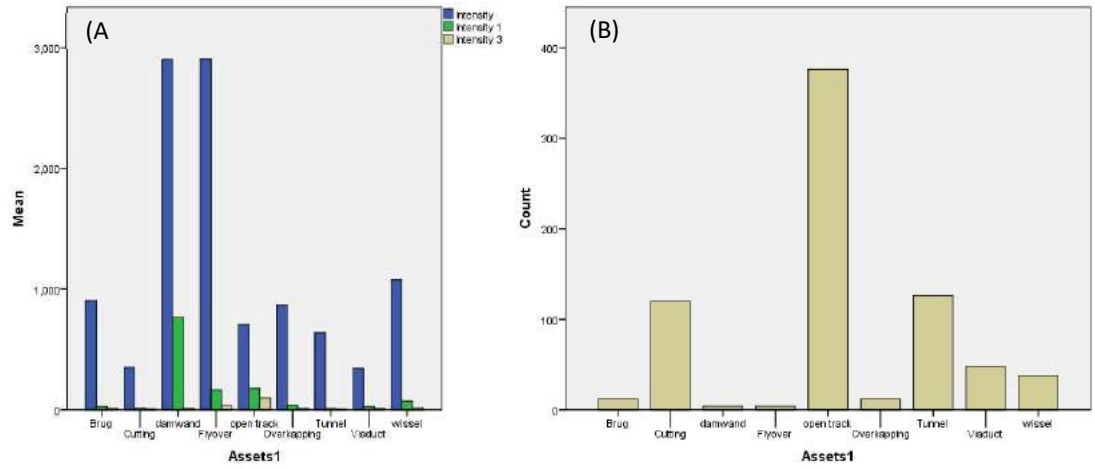

Figure 43: In (A) the assets regarding the whole track are related to the intensities. In (B) it is shown how many data points each asset is composed of.

Using boxplots additional information regarding the distribution of the data among the different variables and intensities can be evaluated. In Figure 44 two boxplots for the whole track are presented regarding I_x and I_x^3. Here can be seen that the distributions for I_x are very different from the distributions for I_x^3. Interesting are the large outliers which only occur at the open track for I_x^3, which represent the hotspots.

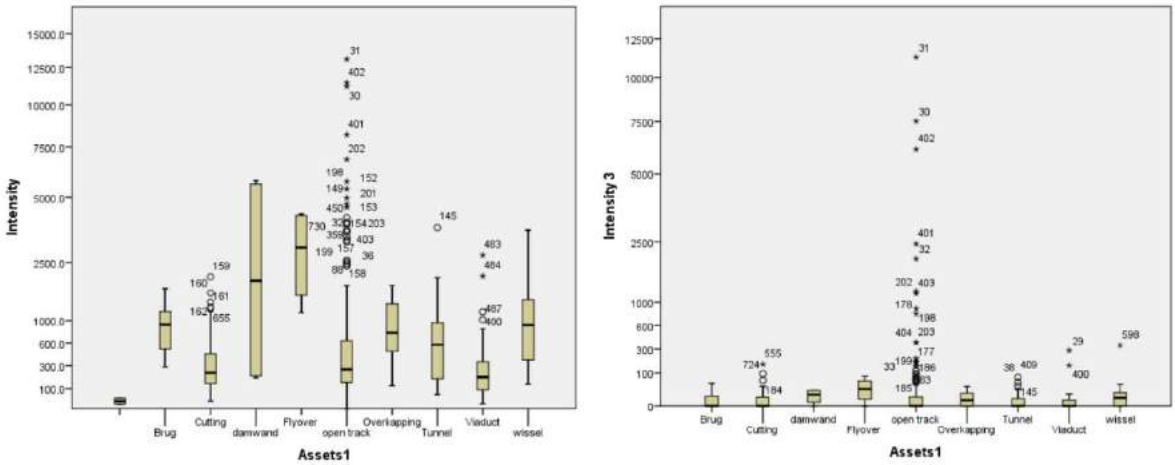

Figure 44: Boxplots for the whole track regarding the intensities or all cracks and cracks larger than 3mm.

4.5.2. Rail grade related to intensity

For the whole track the relation of the rail grade to intensity is presented in Figure 46(A). For the rail next to the two rail grades 260 and 350HT an additional category has been added, namely the 'mix' category. This because the whole track had been divided over 500m parts thus there are sections present where one rail grade is being connected to the other, these sections were classified as the mix category.

Regarding the hypothesis that the harder 350HT rail grade was more prone to be affected by cracks. We see this back in Figure 46(A) showing higher mean intensities than the 260 and mix rail grades. Especially for I_x^1 and I_x^3 significant differences can be seen. Supporting the hypothesis regarding the crack growth and wear rate differences in both rail grades. Another explanation can be that both rail grades behave differently regarding the grinding by rotating stones and that 350HT behaves differently under grinding.

The rail grades have also been evaluated by boxplots, the results are presented in Figure 45. Here can be seen that the outliers are to be found only at the 350HT rail grade.

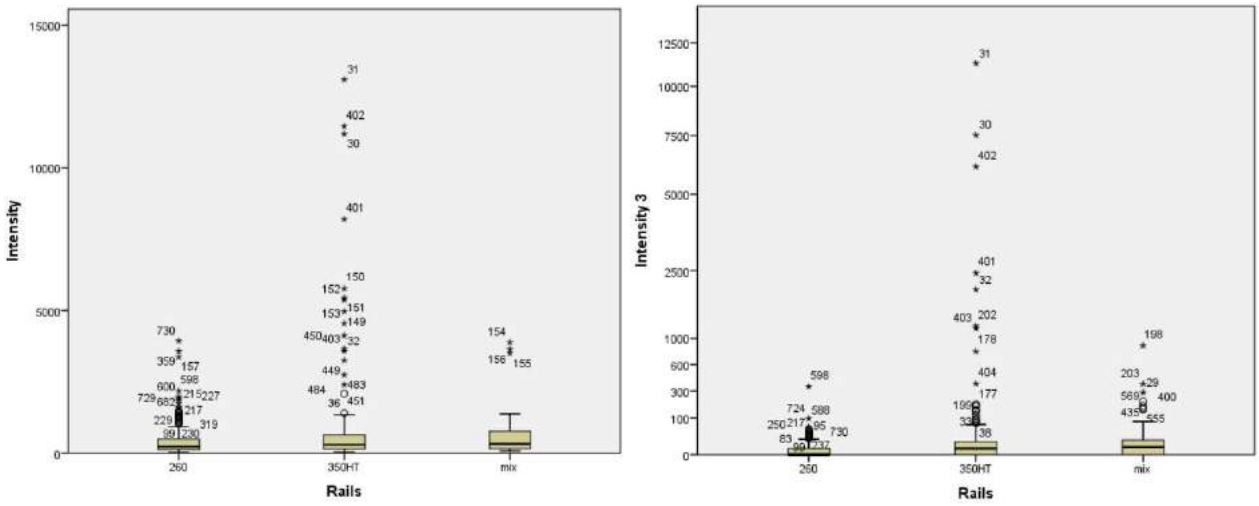

Figure 45: Boxplots for the rail grade and intensities for the whole track.

4.5.3. Superstructure related to intensity

Also a check has been done regarding the different superstructures among the HSL. Like in the rail grade parameter also a mix superstructure category has been introduced here to cover the shifts in the superstructures among the different 500m sections for the HSL.

For the whole track the results are presented in Figure 46 (B). Here we see clear peak values for the Ballast 160 parameter regarding the normal intensity but also significant scores for the other two intensities. This can be explained for the Ballast160 that this parameter consists of a low number of data points but having two (entry zone) hotspots located there.

The Ballast300 has the lowest scores this because there is only a small section covered by Ballast 300 and its only being used by the Thalys.

The Mix category scores relatively high for I_x^1 and I_x^3 because of its location in the beginnings and end of curves. Causing it to be present at least once in every open track hotspot.

The Rheda superstructure scores highest for I_x^1 and I_x^3 because the open track hotspots like Zoetermeer are located at Rheda superstructure.

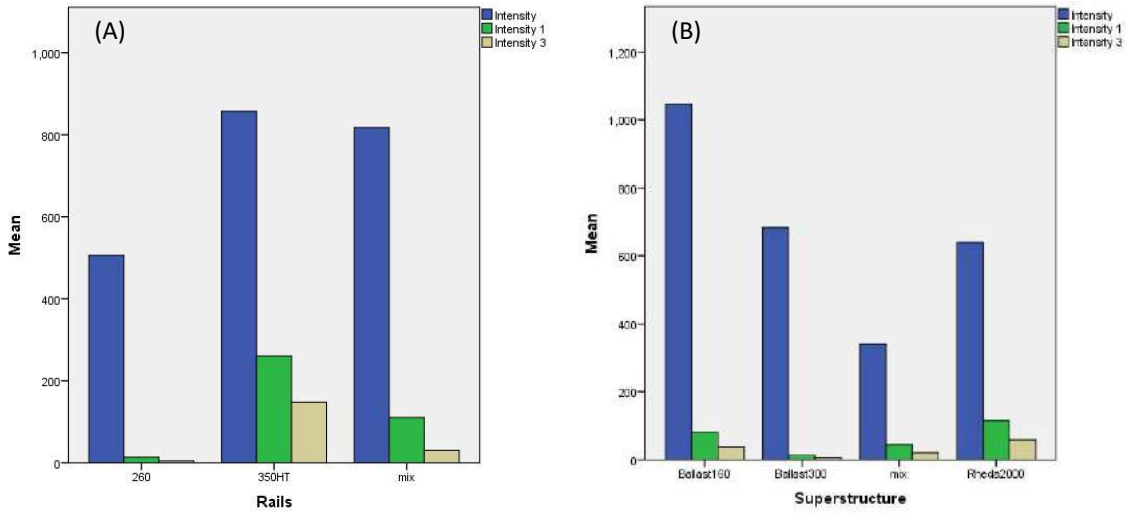

Figure 46: (A) shows the rail grades and (B) the superstructure related to the mean intensities for the whole track.

Though to the many data points we still see relatively low mean intensity values compared to for example the traction outcomes in the previous section. The boxplots (Figure 47) show the distributions of the intensities and the superstructure values. Here can be seen that the highest outliers are to be found among the Rheda2000

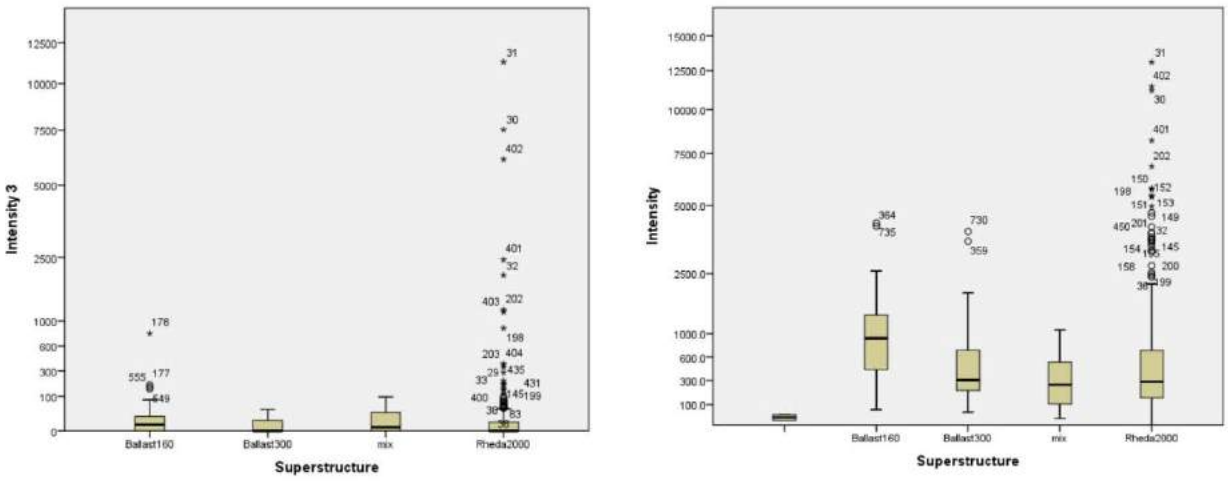

Figure 47: Boxplots regarding the intensities and superstructures for the whole track.

superstructures. For the Ballast160 sections the distribution for the intensity regarding all cracks show worse distribution than the Rheda2000.

4.5.4. Leg type related to intensity

For the whole track the leg types have been rated. These have been divided into four categories; two curve categories being upper- and lower leg and two categories for the straight track being right and left leg.

This has been done for two reason; firstly to be able to confirm whether we indeed see the higher intensities lying in the curves and secondly to see which leg in a curve is affected most. The last one to possibly be able to suggest which of the two trains affect the rails most, because they behave differently in the curves due to their different speed profiles.

Figure 48 (A) shows the mean intensities for the four leg types in the whole track. Showing that the higher intensities indeed are to be found in the curves. This is especially clear when we look at the average values found for I_x^1 and I_x^3. For the right and left leg we see for both I_x^1 and I_x^3 values of nearly zero showing that the serious cracks indeed occur in the curves. For the curves we see the lower leg being on average more affected by damages than the upper leg.

This check has accordingly also been done for the open track sections leaving the tunnels out in order to be able to obtain even more fixed results for these areas to support the hypothesis for this type of hotspot. Looking at Figure 48 (B)we see again the same pattern in the distribution of intensity values among the leg types. Though we see higher average results among the upper- and lower legs for both I_x^1 and I_x^3 as was expected. Though according to the initial hypothesis a stronger difference between lower- and upper leg was expected. As was thought that the lower leg would show clearer worse results compared to the upper leg in curves.

A similar check has been done for the entry zones which is presented in Figure 48 (C). Here was also expected to find damages in the curves but for both the upper- and lower leg the same distribution on average. This because trains driving within the theoretical cant was thought to be the problem.

We see the curve being confirmed in the results as the peak values for I_x^1 and I_x^3 are located here. Notable are the small differences for I_x^3 and the large differences for the I_x^1 scores. Though from section 4.4.6 the entry zone data is somewhat disturbed which could explain the differences.

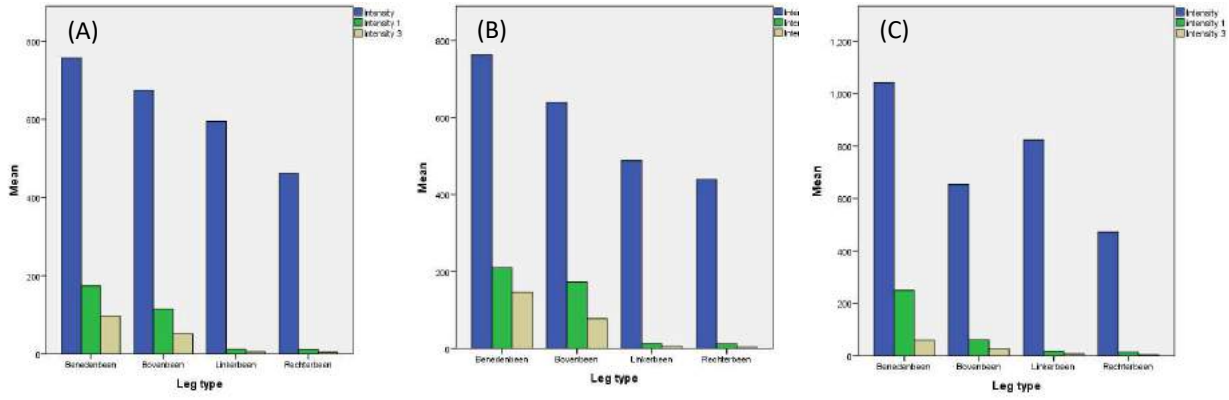

Figure 48: Relation between the leg types and intensities for:(A) the whole track, (B) open track and (C) the entry zones.

The results for the boxplots are shown in Figure 49. Her is shown that there is a broad distribution among the legs for all cracks when the normal intensity is represented and that the outliers are located at the lower and upper legs. Regarding the I_x^3 distribution is less spread and the outliers are now clearly located solely in the curves.

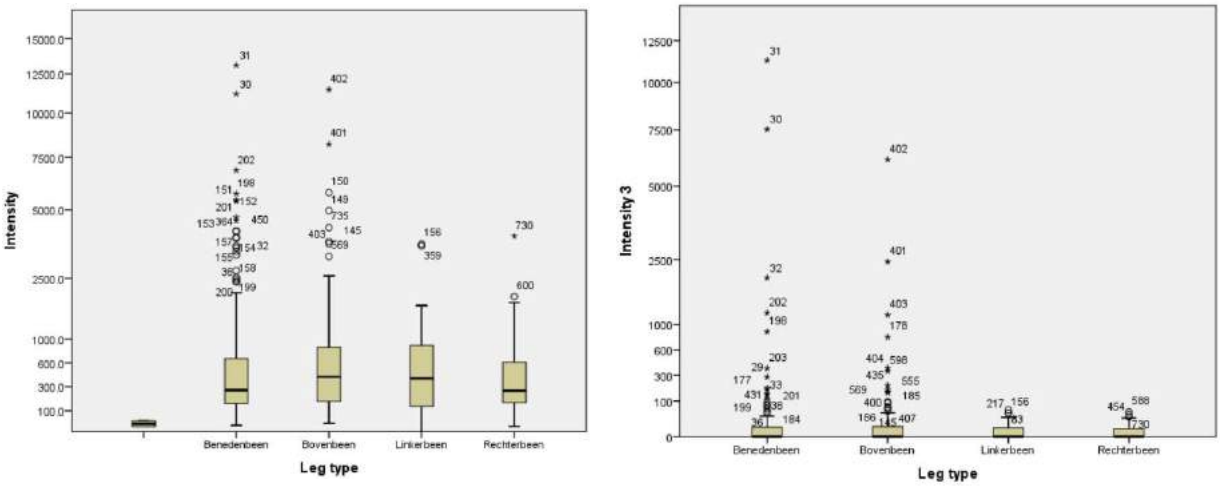

Figure 49: Boxplots for the open track and the distribution of intensities for the leg type variables.

4.6. Conclusions and recommendations HSL-South

4.6.1. Conclusions

Concluding from this study, the monitoring programme regarding the rails was not sufficient in the past. The measurement method to detect early damages was eddy current measurement in the gauge corner. But as the damages are concentrated on the rail head they could not have been detected in the early stages.

Regarding the cause of the damages the study was not able to establish one single cause for the damages. It seems that a combination of factors is causing the damages at the HSL. However the most striking results regard the presence of the TRAXX which at all hotpots showed undesired behaviour in the curve which either resulted in driving under high cant excess or within the theoretical cant. This study shows that it has all to do with the low driving speeds and high tractive efforts which are most likely causing problems regarding RCF at the HSL-South. The B-U approach enabled to differ the hotspots into two types, which have been named: the open track hotspot and the entry zone hotspot. Whereas the Top-Down approach was able to confirm most of the hypothesis regarding both types of hotspots and able to rank the quantitative parameters.

Types of hotspots

The damages for the open track hotspot are likely due to the low traffic speeds of the TRAXX over the HSL. The curves have not been designed for these low traffic speeds which causes the TRAXX driving with cant excess in the curves. The values of the cant excess even exceeds the original norms by ProRail. The cant excess in combination with traction result in different stresses at the rails which are likely to contribute to the crack initiation and rapid growth.

For the entry zone hotspots there is a different situation which causes other behaviour by the TRAXX. Also here low traffic speed seems to be the problem this time resulting in driving within the theoretical canting. This can cause very unpredictable and possibly unstable behaviour by the trains, as there is no resultant regarding the lateral acceleration in the curve. What also contributes here is the complex geometry of the hotspots with S-curves and gradients among them.

Rail grades and grinding

Another factor which can explain the fast growth of the cracks is the 350HT rail grade which has been used among the hotspots. It is supported by literature that in current practices the grinding process for heat-treated rail can act as an initiator for damages. It is rather unclear if this is actually the case at the HSL. But as there are some other curves which share the same characteristics as the curves at the hotspots with the exception of the

rail grade its very striking that the curves with the softer 260 rail grade seem to be much less affected by damages. Though further research upon this subject is needed to confirm these measurements. Infraspeed recently did a renewal to the softer 260 rail grade at one hotspot and it would be interesting to monitor whether new damages arise here.

The (rotating stone) grinding also seems to be a factor reckoned with. The heat input by grinding can cause white edging layer at the rail surface, cracks can arise at this white edging layer which can grow into the rail surface. At the rails at Hoofddorp the white edging layer had been found at both the running band and outside the running band, which is likely to be caused by grinding. Grinding using different grinding stones should be tested, to see whether new specifications can be set to get better rail surface results regarded grinding.

One of the crucial things which was not available was the growth rate of the cracks. As the study was based on one eddy current measurement set only. Now there are more measurements but in between the first measurements with the cracks and the second measurements the hotspots had been ground. Knowing the growth and wear-rate would help to see if there is actually a problem regarding the rail grade. For future monitoring its recommended to track the growth rate of cracks closely. One thing that is known about the growth rate is that should be fluid driven as there are no problems in tunnels. The difference among the results for both rail grades is thus likely to be caused by either the grinding results or the difference between crack growth/wear ratio.

Traction

The last factor which could have contributed to the damages is the traction by the TRAXX which is larger than the traction by the Thalys. For the open track hotspots we see indications that curves with exceeding cant excess and traction by the TRAXX are more vulnerable to damages than curves where only traction by the Thalys is present. Also the correlation analysis showed the traction by the TRAXX is the most dominant parameter.

To be able to confirm these findings its recommended to do simulations for curves at the hotspots of the HSL. Doing this we could really be able to see how the trains behave in the curves and what stresses arise in the rail. These simulations could also be used to look for a rail profile which performs better under the current circumstances and could distribute the stresses better.

Maintenance

Regarding the maintenance there seems to be a structural problem as being a mismatch between the design of the tracks and the actual usage of the tracks. The HSL has not been designed for this relatively low speed traffic. For the open track hotspots there are very limited possibilities to change the track geometry to better fit the TRAXX. We should also be aware geometry changes would also affect the performance of the Thalys.

Infraspeed is now monitoring the rails for damages four times a year. Though the hotspots have all been ground after the first measurement. We are thus not yet able to monitor their growth but it is expected to be possible within short notice as the TRAXX will still be using the tracks. It is essential to know the growth rate of the cracks to be able to design a tailored maintenance program. This will enable Infraspeed to control the damages

To solve the problem of cant excesses and deficiencies in the hotspots we should again handle them in two categories namely the entry zones and open track zones.

4.6.2. Recommendations

For the entry zones we know both the Thalys and TRAXX are currently driving slower than designed. One solution could be looking if it is possible for them to drive through these hotspots at the desired speeds. Another more expensive one is to look whether it is possible to change the cant in these hotspots this would be theoretically possible as these tracks have a Ballast superstructure which could be adapted. Calculations should be made how much cant is needed to change the situation to ideal driving for both Thalys and TRAXX.

For the open track areas these solutions are much harder to implement as the TRAXX already drives at its speed limit. Also the Rheda superstructure makes it much harder to make major adjustment to the canting. It might even be impossible to create good driving conditions for both trains as their speed levels differ so much. Another (costly) long-term option would be replacing the TRAXX for high-speed trains, the major advantage would being

able to optimize all the curves for high-speed trains instead of dual traffic. But as Infraspeed is the contractor regarding the maintenance they have no control over which trains use the tracks.

Also we could take a look at optimizing the rail profile to be able to withstand the current stress levels in their most affected zones, but more insight in this is needed first. Simulations with both trains and different rail profiles should be done to investigate if better conditions could be created by grinding in a different rail profile. The rail grade also seems to be an important factor, as lately the softer 260 rail grade has been placed at Zoetermeer it should be closely monitored whether it behaves different regarding crack growth and wear rates.

One possible option would be changing the driving speed of the Thalys more towards the TRAXX, at for instance 220 km/h and make some adjustments to the cant. Though this would also result in economical disadvantages towards other parties as this results in additional traveling times. Changes in the cant are also very expensive investments.

Another option could be for the whole HSL driving with the sandwich configuration regarding the TRAXX. This results in double the driving axles, reducing the tractive efforts per axle. Also tests with limited traction at certain parts in combination with monitoring of the rails can provide interesting results.

However, as the most probable cause is the presence of the TRAXX, preferably adaptions to this vehicle should be implemented, like considering improvements to the wheel profile to distribute stresses better and introducing traction limitation among certain areas. But this is not in control of Infraspeed. An overview of the recommendations for Infraspeed regarding their rail maintenance is shown in Table 18.

Table 18: Overview of the influencing factors regarding the damages at the HSL and the recommended actions and feasibility.

factor	Recommendation	feasibility
Rail grade	Close monitoring the renewed tracks at the hotspots Hoofddorp and Zoetermeer. This to see whether new cracks arise and if so what their growth rate is, a desired outcome would be a wear rate equal or greater than the crack growth so wear-based maintenance in combination with periodic grinding could be introduced instead of a RCF rail maintenance regime. If this is the case, phased replacement of other hotspots should also be considered.	Already started at two hotspots. Its costly for the rail infra manager, but in these cases it was necessary because of the large number of severe cracks.
White edging layer	It is very much likely the WEL at Hoofddorp was introduced by grinding operations. Tests should be done using different grinding stones and finishing techniques to achieve better results regarding WEL formation and rail roughness results. Also tests should be done to reduce the heat input by grinding under the transformation temperature from pearlite to martensite. This in order to formulate desired results which can be used in grinding specifications.	Can be done during next grinding actions in co-operation with the grinding company.
Traction	There are now some areas where peaks in the tractive efforts by the TRAXX occur. In co-operation with the train operators it should be examined whether these tractive efforts should be limited in these areas and to investigate what its effects are on the rails. Also the new composition of the TRAXX using two locomotives is supposed to lower its tractive efforts per axle.	The sandwich composition has already been introduced between Rotterdam and Hoofddorp. Looking whether peaks in tractive efforts could be reduced should be done in co-operation with the train operators.
Canting	Canting can be re-examined for the areas constructed with a ballast superstructure. As both trains are driving below design speed, more optimal canting conditions for both trains can be achieved. For the Rheda superstructure changing the canting is only very limited possible. Also the speeds of both types of trains differ too much to achieve optimal conditions for both trains. Changing the canting towards a more optimal condition for the TRAXX will result in worse conditions regarding the Thalys.	Changing the canting in the Ballast tracks is possible, but will be very costly but when done it can create better conditions for both trains.
Profile	By doing simulations for the curves in the hotspots one can examine what the wheel-rail positions are at these areas. Also the stress levels can be measured here. By doing this for different rail profiles one can choose a rail profile which best distributes the stresses for both vehicles. This profile can be eventually be grinded at these areas.	The simulations for two hotspots are currently being done by Ricardo rail. An eventual change of the profile will take longer to implement because the specifications for the rail profiles at the HSL should be changed then.
Train speeds	One of the main problems is the speed differs a lot between both trains. The speed limit of the TRAXX is 160km/h, the trains should be replaced if one wants to increase the lower speed for the HSL. The speed of the Thalys can be reduced in order to have closer lying speed ranges for both vehicles making it possible to optimise track conditions.	Replacing the TRAXX will be very costly and the costs will not be paid by the maintenance company. However faster trains will also result in lower traveling times which creates other profits. Reducing the speed of the Thalys will increase the traveling times.

5. Conclusions and recommendations

In this thesis two approach have been proposed to evaluate rail conditions and to find influencing parameters regarding RCF on a track, using data analytics techniques. The use of the approaches have been demonstrated at the Dutch HSL-South track. Both approaches were able to identify influential parameters in their own respective way.

Intensity

Both approaches use the intensity parameter as a KPI, which proved its value as a performance indicator as it was able to detect most of the hotspots. But, is also vulnerable when only one measurement is available. As the measurements have been done using an eddy current walking stick both methods depend greatly on the experience of the measuring personnel and the accuracy of the walking stick. However, it is a relatively new measuring method and will be improved in the future. The advantage of using intensity as an KPI is that it is relatively quick to process when a measurement has been done, and is powerful when it comes to identifying where the worst affected areas for a track are located.

Dependency

The first approach (B-U) was designed to look at the worst affected areas, so called hotspots. It has been designed as an evaluative method as one of the criterions is the corrective grinding, together with the visual evidence it confirms there are actually problems around these areas, thus not solely depending on the eddy current measurements. Whereas, the T-D approach depends solely on the eddy current data as this is the KPI set for rail condition and is used for correlation. Both methods are also heavily dependent on the available data for a railway track. When an infrastructure manager doesn't use eddy current measurements the methods cannot be used like this. However, ultrasonic measurements could be considered for being used, but as it detects only cracks larger than 4mm, less signals are generated and the use of threshold values will be difficult regarding intensity. Regarding the data available, introducing more relevant parameters, like for instance the actual forces being transferred at the wheel-rail interface could improve the results greatly.

Types of data

One of the difficulties regarding both approaches is that lots of different types of data are being processed into one model, both numerical and nominal data. Which can cause problems regarding the partitioning. Choosing a good partitioning value is crucial for the accuracy of both models. In general, the smaller the partitioning, the more data signals will be created and more accurate results can be gathered. Also, the length of the variables differ a lot, for instance the speed profile or eddy current measurements generate data signals every few cm's but a superstructure can be present for several km's. The gathering and initial processing of the data for this study have all been done manually, theoretically when all data is already available, automatic processing could be done. However, regarding the types of data processed, each of the methods is able to cope with them up to a certain level. The nominal influential parameters, had been found using both methods. However, both methods were not able to rank them among the numerical parameters. Regarding the numerical parameters, large sets of different data had been used, with different standard deviations and means. However, the data set was very large, more accurate results regarding the correlation can be achieved normalizing the data before analysing it by the T-D approach. For the B-U approach this is not necessary, as the establishing of an hypothesis is greatly based on expert judgement of the values for the set of characteristic parameters. An overview of the influential parameters for the open track hotspots using either one of the methods is shown in Table 19. The bottom-up approach identified more, but was not able to rank them.

Table 19: The influential parameters regarding the open track hotspots, showing which ones have been identified using which approach.

	Bottom-Up	Top-Down
Traction TRAXX	Yes	Yes
Traction Thalys	Yes	Yes
Cant deficiency TRAXX	Yes	No
Rail grade	Yes	Yes

Processing

Regarding the processing the bottom-up approach is much more complex than the top-down approach. Whereas the top-down approach is using the intensity, it can theoretically be processed automatically when developing new software. For the bottom-up approach, the identification of the hotspots is based greatly on expert judgement. Only the clustering of hotspot types and hypothesis check is also theoretically possible automated. However, both methods regarding their results and setting up an hypothesis is still greatly dependent on expert judgement, as lots of knowledge regarding the parameters and RCF root causes are needed.

Recommendations

The use of only one eddy current is somewhat vulnerable regarding strong conclusions. The main advantage of using these methods periodically processing measurements, is that trends can studied. One would for example be able to see whether a track was ground if its intensity increases faster than other track parts. Also regarding the data analysis improvements are possible. For instance cant excess didn't result in a dominant parameter from the correlation analysis, but was one of the dominant parameters in the B-U approach. This highlighted one of the shortcomings from the T-D approach. As cant excess is present over more partitions in a curve but if the damage concentrates only in the beginnings and endings of curves it will not correlate significantly with the intensity. Normalizing data will also result in better results regarding the correlation.

Also one can consider using homogeneous partitioning, this can for instance improve modelling the full curves and especially the qualitative parameters. As the qualitative parameters now use a mix variable for transitional partitions, using homogeneous partitioning these can all be removed. However, it will reduce the number of samples for the correlation analysis and evaluation. But as the number of samples for this study was already large, more accurate results are expected. Using smaller partitions also more accurate results can be accumulated, however processing and gathering data will be intensive.

Using both methods to evaluate rail conditions whereas the set of characteristic parameters of a certain hotspot is being used to evaluate in the T-D approach has proved useful. As RCF can have different root causes one type of hotspot can be evaluated more accurately.

Further research should be considering dealing with nonlinearity regarding the T-D approach. As only Pearson's correlation has been used to link the intensity to other parameters. Nonlinear relations are hard to trace down, another method dealing with this issue should be considered here to identify these relations.

Another issue regarding both approaches is that there was no parameter able to study the influence of grinding and relate it to the affected areas. Several parameters had initially been used like the mm's of grinding and number of grinding actions by each type grinding. None of them proved to be useful. Introducing rail roughness measurements and compare them to the hotspots might help to introduce a parameter which can evaluate rail conditions after grinding.

As both approaches were able to identify influencing parameters for rail conditions it can also be used to evaluate other issues regarding a railway track. This because for both methods use various sets of parameters which are coupled to the locations at a railway track. These can be used to identify other defects, for instance other performance indicators can be used to evaluate another condition. As an example for instance the conditions of fishplates or railroad ties, can be used as a parameter to evaluate.

To be able to couple the damages at the hotspots to one type of train its recommended that the T-D approach is expanded. On one side a supplemented simulation of a hotspot should be done where the wheel-rail contact positions of the locomotives and rail units are calculated. These contact positions could be coupled to eddy current data. Hereby again intensity can be used but then distributed as intensity for the rail head and gauge corner, or even for all the 10 eddy current channels. When trains behave very differently it could be fruitful to test this approach.

Bibliography

Åhrén, T., & Parida, A. (2009). Maintenance performance indicators (MPIs) for benchmarking the railway infrastructure: a case study. *Benchmarking: An International Journal, 16*(2), 247-258.

AM Architectuur en Techniek. (2015). Ontwerpvoorschrift Baan en Bovenbouw Deel 4.1 Alignement (pp. 16, 31): ProRail.

Bogdanski, S. (2002). A rolling contact fatigue crack driven by squeeze fluid film. *Fatigue & Fracture of Engineering Materials & Structures, 25*(11), 1061-1071.

Cannon, D. F., Edel, K., -O., Grassie, S. L., & Sawley, K. (2003). Rail defects: an overview. *Fatigue & Fracture of Engineering Materials & Structures, 26*(10), 865-886.

Carroll, R., & Beynon, J. (2007a). Rolling contact fatigue of white etching layer: Part 1: Crack morphology. *Wear, 262*(9), 1253-1266.

Carroll, R., & Beynon, J. (2007b). Rolling contact fatigue of white etching layer: Part 2. Numerical results. *Wear, 262*(9), 1267-1273.

Clark, R. (2004). Rail flaw detection: overview and needs for future developments. *NDT & E International, 37*(2), 111-118.

Dikshit, V., Clayton, P., & Christensen, D. (1991). Investigation of rolling contact fatigue in a head-hardened rail. *Wear, 144*(1-2), 89-102.

Dollevoet, R. P. B. J. (2010). *Design of an Anti Head Check profile based on stress relief*: University of Twente.

Egghe, L., & Rousseau, R. (1990). Introduction to informetrics: Quantitative methods in library, documentation and information science. 63-64.

Esveld, C. (2001). *Modern railway track* (2 ed.). Zaltbommel: MRT-Productions.

Evans, G. (2013). Managing rail profile. *Ironmaking & Steelmaking, 40*(2), 115-119.

Evans, J., & Iwnicki, S. D. (2002). *Vehicle dynamics and the wheel/rail interface.* Paper presented at the Proceedings of the IMechE Seminar on Wheels on rails–an update, London, UK.

Faghih-Roohi, S., Hajizadeh, S., Núñez, A., Babuska, R., & de Schutter, B. (2016). *A deep learning approach for detection of rail defects*. Paper presented at the IEEE WCCI 2016, Vancouver, Canada.

Feller, H., & Walf, K. (1991). Surface analysis of corrugated rail treads. *Wear, 144*(1), 153-161.

Field, A. (2009). Discovering statistics using SPSS:(and sex and drugs and rock 'n'roll). Introducing statistical methods (pp. 177-179): London: Sage.

Frigge, M., Hoaglin, D. C., & Iglewicz, B. (1989). Some implementations of the boxplot. *The American Statistician, 43*(1), 50-54.

Govaert, G. (2009). *Data analysis*. London: ISTE.

Grassie, S. L. (1996). Short wavelength rail corrugation: field trials and measuring technology. *Wear, 191*(1), 149-160.

Grassie, S. L. (2012). Squats and squat-type defects in rails: the understanding to date. *Proceedings of the Institution of Mechanical Engineers, Part F: Journal of Rail and Rapid Transit, 226*(3), 235-242.

Grassie, S. L. (2015). *Studs and Squats: the evolving story*. Paper presented at the 10th International Conference on Contact Mechanics, Colorado Springs, Colorado, USA.

Grassie, S. L., Fletcher, D. I., Hernandez, E. G., & Summers, P. (2011). Studs: a squat-type defect in rails. *Proceedings of the Institution of Mechanical Engineers, Part F: Journal of Rail and Rapid Transit*, 0954409711421462.

Grassie, S. L., & Kalousek, J. (1993). Rail corrugation: characteristics, causes and treatments. *Proceedings of the Institution of Mechanical Engineers, Part F: Journal of Rail and Rapid Transit, 207*(1), 57-68.

Hansen, P., & Jaumard, B. (1997). Cluster analysis and mathematical programming. *Mathematical programming, 79*(1-3), 191-215.

Hartleben, D. (2009). *Task for mobile railway machining and Predestined machining methods.* Paper presented at the 8th International Conference on Contact Mechanics and Wear of Rail/Wheel Systems (CM 2009), Firenze, Italy.

Heyder, R., & Girsch, G. (2005). Testing of HSH® rails in high-speed tracks to minimise rail damage. *Wear, 258*(7), 1014-1021.

Heyder, R., & Hempe, T. (2009). *Maintenance strategies and material concepts to control rolling contact fatigue of rails.* Paper presented at the Proceedings of the 8th International Conference on Contact Mechanics and Wear of Rail/Wheel Systems (CM2009), Firenze, Italy.

INF - TSI 1299/2014/EU, 4.2.4.3. C.F.R. (2014).

Infrastructuur en Milieu. (2015a). *Voortgangsrapportage 36 Hogesnelheidslijn Zuid*. (36).

Infrastructuur en Milieu. (2015b). *Voortgangsrapportage 37 Hogesnelheidslijn Zuid*. Retrieved from https://www.rijksoverheid.nl/binaries/rijksoverheid/documenten/rapporten/2015/10/01/37e-voortgangsrapportage-hsl-zuid/37e-voortgangsrapportage-hsl-zuid.pdf.

Jamshidi, A., Faghih-Roohi, S., Núñez, A., Babuska, R., de Schutter, B., Dollevoet, R., & Li, Z. (2016a). A big data analysis approach for rail failure risk assessment. *Under review*.

Jamshidi, A., Faghih-Roohi, S., Núñez, A., Babuska, R., de Schutter, B., Dollevoet, R., & Li, Z. (2016b). *Probabilistic defect-based risk assessment approach for rail failures in railway infrastructure*. Paper presented at the CTS 2016, Istanbul, Turkey.

Jamshidi, A., Núñez, A., Dollevoet, R., & Li, Z. (2016). Robust and predictive fuzzy performance indicators for condition monitoring of squats in railway infrastructures. *Journal of Infrastructure Systems*.

Jamshidi, A., Nunez, A., & Li, Z. (2015). *Maintenance decision indicators for treating squats in railway infrastructures.* Paper presented at the 94th Annual Meeting Transportation Research Board, Washington, USA, 11-15 January 2015; Authors version.

Jamshidi, A., Núñez, A., Li, Z., & Dollevoet, R. (2015). *Fuzzy Maintenance Decision Support for Treating Squats in Railway Infrastructures.* Paper presented at the 2015 Joint Rail Conference.

Jun, H.-K., Lee, D.-H., & Kim, D.-S. (2015). Calculation of minimum crack size for growth under rolling contact between wheel and rail. *Wear, 344*, 46-57.

Kapoor, A., Fletcher, D., & Franklin, F. J. (2003). The role of wear in enhancing rail life. *Tribology Series, 41*, 331-340.

Künstner, D., & Harrer, J. (2016). *Laboratory Examination on R350HT – Infraspeed*. Voestalpine Schienen GmbH.

Larsson-Kråik, P.-O. (2009). Managing the wheel-rail interface Railway infrastructure maintenance in a severe environment: The Swedish experience. *Wheel—rail interface handbook*.

Lee Rodgers, J., & Nicewander, W. A. (1988). Thirteen ways to look at the correlation coefficient. *The American Statistician, 42*(1), 59-66.

Lewis, R., & Olofsson, U. (2009). Basic tribology of the wheel-rail contact. *Wheel-Rail Interface Handbook*, 34-57.

Li, S., Wu, J., Petrov, R., Li, Z., Dollevoet, R., & Sietsma, J. (2016). "Brown etching layer": A possible new insight into the crack initiation of rolling contact fatigue in rail steels? *Engineering Failure Analysis, 66*, 8-18.

Li, Z. (2009). Squats on railway rails. *Wheel/Rail Interface Handbook," In: R. Lewis and O. Olofsson, Eds., Woodhead Publishing Ltd, Oxford*, 409-436.
Li, Z., Molodova, M., Núñez, A., & Dollevoet, R. (2015). Improvements in axle box acceleration measurements for the detection of light squats in railway infrastructure. *IEEE Transactions on Industrial Electronics, 62*(7), 4385-4397.
Li, Z., Zhao, X., Dollevoet, R., & Molodova, M. (2008). Differential wear and plastic deformation as causes of squat at track local stiffness change combined with other track short defects. *Vehicle System Dynamics, 46*(S1), 237-246.
Li, Z., Zhao, X., Esveld, C., Dollevoet, R., & Molodova, M. (2008). An investigation into the causes of squats—Correlation analysis and numerical modeling. *Wear, 265*(9), 1349-1355.
Lichtberger, B. (2005). Track compendium. *Eurailpress Tetzlaff-Hestra GmbH & Co. KG, Hamburg, 634*.
Lundén, R., & Paulsson, B. (2009). Introduction to wheel-rail interface research. *Wheel/Rail Interface Handbook (editors R Lewis and U Olofsson), Woodhead Publishing, Cambridge (UK)*.
Magel, E. E. (2011). *Rolling contact fatigue: a comprehensive review*. Retrieved from http://ntl.bts.gov/lib/43000/43400/43400/TR_Rolling_Contact_Fatigue_Comprehensive_Review_final.pdf
Magel, E. E., & Kalousek, J. (2002). The application of contact mechanics to rail profile design and rail grinding. *Wear, 253*(1), 308-316.
Regeling hoofdspoorweginfrastructuur, art 8. 1.e C.F.R. (2005).
Molodova, M., Li, Z., & Dollevoet, R. (2011). Axle box acceleration: Measurement and simulation for detection of short track defects. *Wear, 271*(1), 349-356.
Molodova, M., Li, Z., Núñez, A., & Dollevoet, R. (2014a). Automatic detection of squats in railway infrastructure. *IEEE Transactions on Intelligent Transportation Systems, 15*(5), 1980-1990.
Molodova, M., Li, Z., Núñez, A., & Dollevoet, R. (2014b). Validation of a finite element model for axle box acceleration at squats in the high frequency range. *Computers & Structures, 141*, 84-93.
Navidi, W. (2010). *Principles of statistics for engineers and scientists*: McGraw-Hill New York.
Nieuwenhuis, M. (2016, 16-2-2016). HSL vaker stilgelegd uit angst voor harde wind. *Algemeen Dagblad*. Retrieved from http://www.ad.nl/ad/nl/37141/Fyra-debacle/article/detail/4246018/2016/02/16/HSL-vaker-stilgelegd-uit-angst-voor-harde-wind.dhtml
Olofsson, U. (2009). Adhesion and friction modification.
Parida, A., & Chattopadhyay, G. (2007). Development of a multi-criteria hierarchical framework for maintenance performance measurement (MPM). *Journal of Quality in Maintenance Engineering, 13*(3), 241-258.
Pohl, R., Erhard, A., Montag, H.-J., Thomas, H.-M., & Wüstenberg, H. (2004). NDT techniques for railroad wheel and gauge corner inspection. *NDT & E International, 37*(2), 89-94.
Popović, Z., Lazarević, L., Brajović, L., & Vilotijević, M. (2015). The Importance of Rail Inspections in the Urban Area-Aspect of Head Checking Rail Defects. *Procedia Engineering, 117*, 601-613.
Pyzalla, A., Wang, L., Wild, E., & Wroblewski, T. (2001). Changes in microstructure, texture and residual stresses on the surface of a rail resulting from friction and wear. *Wear, 251*(1), 901-907.
Rajamäki, J., Vippola, M., Nurmikolu, A., & Viitala, T. (2016). Limitations of eddy current inspection in railway rail evaluation. *Proceedings of the Institution of Mechanical Engineers, Part F: Journal of Rail and Rapid Transit*, 0954409716657848.
Schultz van Haegen-Maas Geesteranus, M. H. (2012). *Regeling van de Minister van Infrastructuur en Milieu, van 5 maart 2012, nr. IENM/BSK-2012/23596, tot wijziging van de Regeling hoofdspoorweginfrastructuur in verband met de implementatie van de interoperabiliteitsrichtlijn* Retrieved from https://zoek.officielebekendmakingen.nl/stcrt-2012-4831.html.
Scott, D., Fletcher, D., & Cardwell, B. (2014). Simulation study of thermally initiated rail defects. *Proceedings of the Institution of Mechanical Engineers, Part F: Journal of Rail and Rapid Transit, 228*(2), 113-127.
Sectie Weg- en Railbouwkunde. (2014). *Deel 4. Constructief ontwerp van spoorwegen*. CTB3320 Weg- en Railbouwkunde. Reader. Faculty of Civil Engineering and Geosciences. Delft University of Technology. Delft.
Steenbergen, M. (2016). Rolling contact fatigue in relation to rail grinding. *Wear, 356*, 110-121.
Stenström, C., Norrbin, P., Parida, A., & Kumar, U. (2016). Preventive and corrective maintenance–cost comparison and cost–benefit analysis. *Structure and Infrastructure Engineering, 12*(5), 603-617.
Stenström, C., Parida, A., Lundberg, J., & Kumar, U. (2015). Development of an integrity index for benchmarking and monitoring rail infrastructure: application of composite indicators. *International Journal of Rail Transportation, 3*(2), 61-80.
Tanvir, M. (1980). Temperature rise due to slip between wheel and rail—an analytical solution for Hertzian contact. *Wear, 61*(2), 295-308.
Thompson, D., & Jones, C. (2009). Noise and vibration from the wheel-rail interface.
Torstensson, P., & Nielsen, J. C. (2009). Monitoring of rail corrugation growth due to irregular wear on a railway metro curve. *Wear, 267*(1), 556-561.
van der Heide, L. (2009, 10-7-2009). Trage tweedehands treinen rijden op hsl-zuid. *NRC Handelsblad*. Retrieved from http://www.nrc.nl/handelsblad/2009/07/10/trage-tweedehands-treinen-rijden-op-hsl-zuid-11753121
van der Stelt, J. (2015). *Materiaalkundig onderzoek spoorstaafschades*. Utrecht: DEKRA Rail.
Vossloh. High speed grinding. Retrieved from http://www.vossloh-rail-services.com/en/products_services/high_speed_grinding/high_speed_grinding.html
Wild, E., & Reimers, W. (2004). White Etching Layer on Contact Surface on a Worn Railway Wheel. Retrieved from http://hasyweb.desy.de/science/annual_reports/2004_report/part1/contrib/41/12348.pdf
Williamson, D. F., Parker, R. A., & Kendrick, J. S. (1989). The box plot: a simple visual method to interpret data. *Annals of internal medicine, 110*(11), 916-921.
Wilson, A., Kerr, M., Marich, S., & Kaewunruen, S. (2012). *Wheel/rail conditions and squat development on moderately curved tracks.* Paper presented at the CORE 2012: Global Perspectives; Conference on railway engineering, 10-12 September 2012, Brisbane, Australia.

Appendix

Appendix A. Parameter overview

This appendix will provide an overview of all the parameters used for the analysis. Also a description of the parameter will be given, source of the data and how the parameters will be valued during the analysis.

For the parameter analysis, an excel sheet has been used. On the vertical axis the location of partitioned areas of 500m and for the horizontal axis all the different parameters. The 500m long partitions were chosen because it can provide a detailed overview of the whole track which consists of roughly 2 times a 50km double track. The 500m partitions will provide enough data points to do a statistical analysis, will also provide enough detailed information regarding the characteristics at local areas and was also manageable regarding the processing and gathering the data. If more details are needed one can zoom in on the data of each partition to look for more information.

A.1. Track description HSL-South

The track has been divided into two parts, the northern-(46km) and the southern part (50km). The first one running from Hoofddorp to Rotterdam and the second one from Rotterdam to the Belgian border and a split to Breda. Between these two parts there is a transition zone to the regular railway tracks in Rotterdam. Another transition zone is located around the connection to Breda, though here only the connection Rotterdam-Breda is currently being used; no commercial trains are currently using the Breda-Antwerp connection. An overview of the connections and number of kilometres can be viewed in Figure 50.

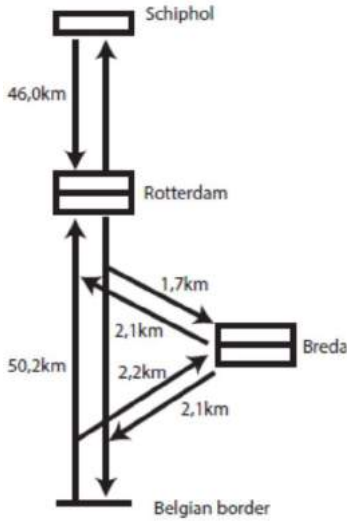

Figure 50: Schematic overview of the HSL-South, its connections and number of kilometres track for each part.

Typical for the HSL track are the long curves used in the open track most have radii between 4500 and 6000m. Among the tracks several large civil works have been built, such as the Tunnel Groene Hart, Bridge Hollands Diep and several other tunnels and viaducts. Among these civil structures of the substructure the HSL-South has also been divided by 5 civil clusters. The superstructures used among the tracks are Rheda2000, Ballast300, Ballast160 and Ballast40. Whereas the Rheda2000 is used among most parts of the track and the Ballast superstructures are used among the transitions to the maintenance area (Ballast40), Belgian HSL track (Ballast300) and the regular ProRail tracks (Ballast160). More detailed track specifications will be provided in this chapter.

A.2. Track geometry

Track geometry is essential in the dynamic behaviour between track and vehicles. The most common track characteristics to describe geometry are:

- Track gauge.
- Inclination.
- Canting.
- Horizontal curve radius.
- Transition curves.

Track gauge

The definition of track gauge or track width is the length between the two rails in the track. The standard track gauge is 1435mm. In Figure 51 an example of track gauge is shown. The track gauge for the HSL-South is 1437mm.

Figure 51: Example of track gauge. Source: http://www.gvgrc.ca/aboutgscale.html

Inclination

Rails are always placed with an inward inclination. In the Netherlands, two inclination standards are being used namely 1:40 and 1:20. The HSL-South uses the 1:20 inclination.

Canting

The height difference between two rails in a curve is called the cant *h* (or superelevation) as show in Figure 52. The cant is designed in curves to compensate lateral accelerations.

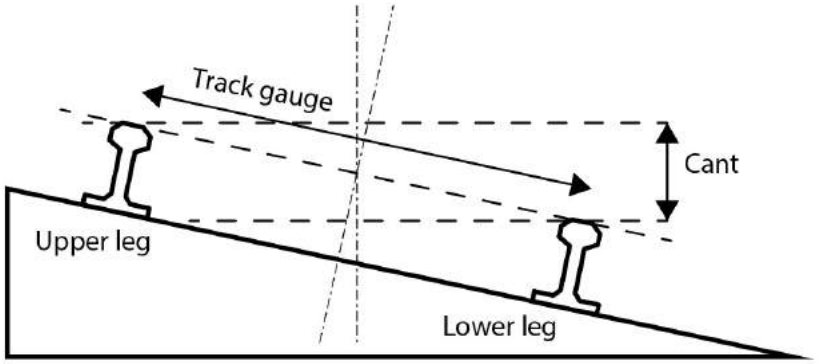

Figure 52: Illustration for cant.

There is a maximum cant value in order to preserve safe conditions for trains standing still and slow running traffic. Also maximum cant values are defined in order to prevent the following situations (Esveld, 2001):

- Passenger discomfort at lower speeds or standstill.
- Derailment of freight trains due to the combined effect of high lateral and vertical forces at the upper leg in the curve.
- Displacement of wagon loads.

Horizontal curve radius

Another parameter for a curve in the track is its radius *R*. Straight track can also be seen as a curve with infinite radius. A smaller curve radius results in a sharper curve.

Transition curves

The transition curves are the curves between the straight track and circular curve. When canting is present at the circular curve, then among the transition curve also a super elevation ramp will be present. This, in order to provide a smooth transition to the maximum used cant among the curve. Transition curves with linear increasing curvature are generally used (clothoid) (Lichtberger, 2005). The transition from straight track to a circular (full) curve regarding curve radius and cant is shown in Figure 53.

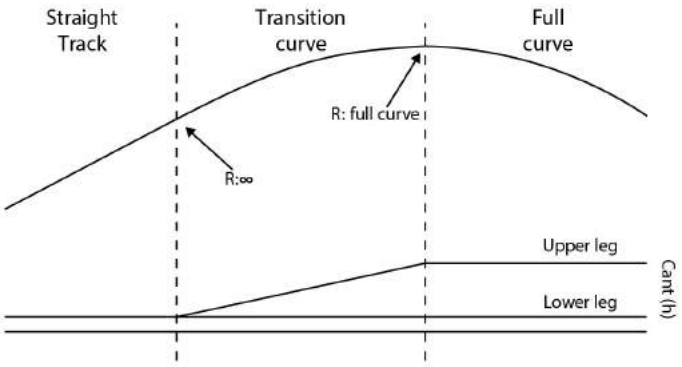

Figure 53: Transition of the canting and radius from straight track to a circular curve.

A.3. Rolling Material

The high-speed line HSL-South is currently being used by two types of trains for commercial exploitation. The Nederlandse Spoorwegen (NS) uses TRAXX locomotives and the Thalys uses its PBA and PBKA locomotives. For the parameter analysis only the current services have been taken into account. So only the influence of the TRAXX and Thalys have been taken considered. No additional split will be made between the PBA and PBKA Thalys as they have the same properties. There is no direct input from the rolling material but derivatives are used. The properties of both trains are taken into account in the parameter study resulting in: tonnage, traction, speed and cant deficiencies.

TRAXX

NS uses the TRAXX F140 MS2 (Figure 55) locomotives for their intercity Direct trains on the Breda-Amsterdam service. As of 2011 these trains travel 32x a day between Rotterdam and Breda. Since 2013 there are additional services between Rotterdam-Amsterdam which will be expanded to 33x services a day in the first quarter 2016. They have been manufactured by Bombardier.

Since April 2015 tests started in the northern part of the HSL-South with TRAXX driving with a so-called ''sandwich configuration''. This means driving with two locomotives, one in the front pulling- and one in the back pushing the train. The reason for this is to increase the reliability of the Intercity Direct services (Infrastructuur en Milieu, 2015b). The major advantage is that when the trains reach the endpoints of the service in Breda and Amsterdam they don't have to be disconnected to turn. In December 2015 this new configuration has been officially implemented for all the TRAXX driving in the northern part of the HSL-South. In the southern part of the HSL-South the TRAXX is still traveling with the normal configuration. The TRAXX drives with 6 wagons on both the northern and southern part of HSL-South. The wagons used are the ICRm vehicles. A TRAXX locomotive has four axles which are all powered, the sandwich formation thus has eight powered axles. The operating speed of the TRAXX is at 160km/h.

Thalys

Also the TGV Thalys PBKA and PBA (Figure 55) are using the tracks they serve the international services from Amsterdam to Belgium and France. Currently, they are being used on a service between Amsterdam and Brussels 3 times a day, Amsterdam and Lille 2 times a day and Amsterdam to Paris 9 times a day. The manufacturer of the train is GEC Alstom. The trains have been manufactured between 1995 and 1997. The main difference between the two types is the shape of the head of the locomotive, the newer PBKA type has a rounder shaped head than the PBA. The Thalys carries 8 wagons and has two locomotives. The four axles of both locomotives are powered, the total number of powered axles is thus eight. The operating speed for the Thalys is 300km/h.

Fyra

Figure 55: A TRAXX F140MS2 in service, carrying also one Fyra wagon. Source: http://www.martijnvanvulpen.nl/materieel/elektrische-locomotieven/254-traxx-f140-ms2

Figure 55: A Thalys PBA in Rotterdam Central Station. Source: http://www.treinenweb.nl/materieel/THALYS

In 2004 NS and NMBS/SNCF ordered the Fyra V250 (Figure 56) trains to provide the service over the HSL-South and HSL-4 in the Netherlands and Belgium. The initial delivery was planned for 2007. But this was delayed several times due to problems with ETCS specifications.

In 2012 the trains have been provisionally certified to be used over the HSL tracks. As from September 2012 a limited service was provided by the Fyra between Rotterdam and Amsterdam and as of December 9th 2012 these trains were being used permanently for the Amsterdam-Brussels service. But this was only short-lived, due to technical complications the service was suspended on January 13th 2013. During this short period there have been safety and reliability problems regarding snowy weather and a floor plate has fallen off one of the trains, which has been the reason for the Belgian rail operator to revoke the provisional certification for the Fyra. In May and June 2013 the NMBS and NS decided to definitely stop the Fyra project due to these issues.

The TRAXX F140 MS2 are replacing the V250 but were already using the tracks during the time the Fyra was still being tested. The Fyras' operating speed was at 250km/h.

Figure 56: Fyra V250 in Rotterdam Central Station. Source: http://www.treinenweb.nl/materieel/V250

Future services

Currently there are also plans to start from December 2016 with additional services using the TRAXX locomotives. A new service between The Hague and Eindhoven, using the Southern part of the HSL tracks from

Rotterdam to Breda this new service is planned for 32x a day. Another planned service scheduled for December 2016 using the TRAXX locomotives will be traveling from Amsterdam to Breda and then continuing to Brussels, this one is scheduled 16 times a day. Though the latter one is more uncertain as research is being done how it fits the train table (Infrastructuur en Milieu, 2015a). An overview of the current and planned services using the HSL-South tracks is shown in Figure 57.

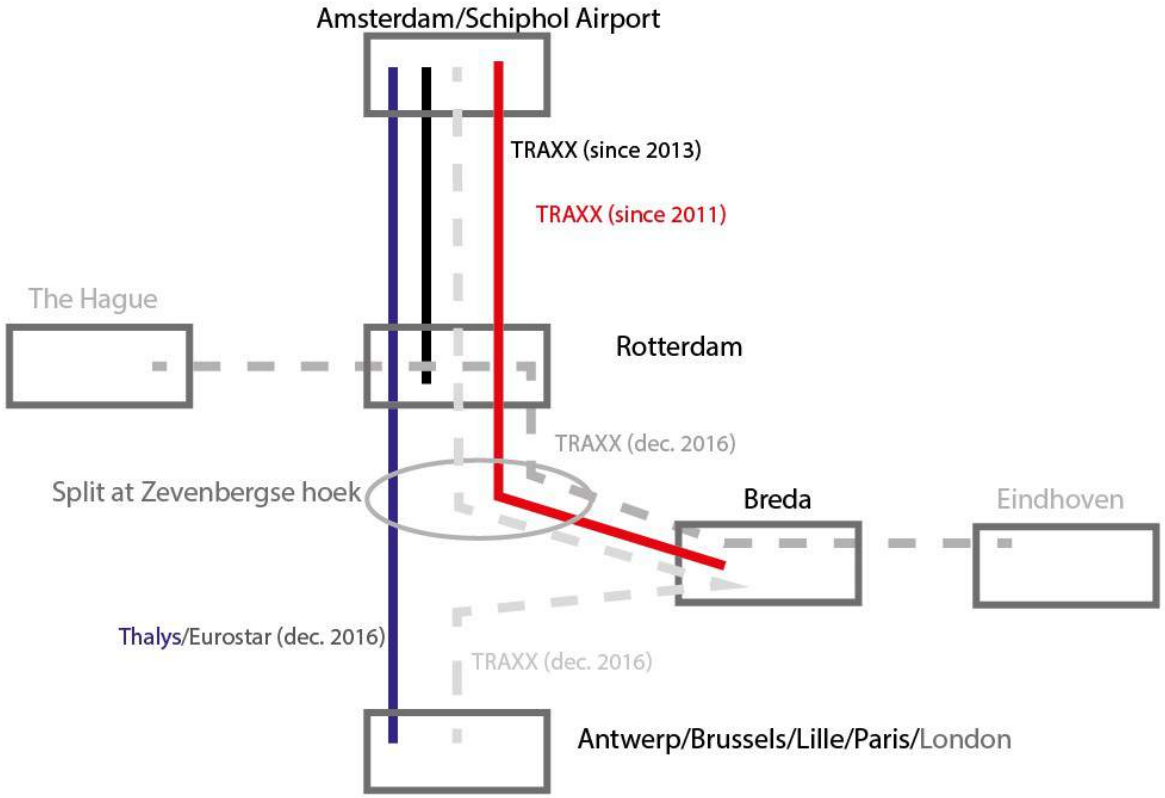

Figure 57: Overview of the current and future services using the HSL-South tracks.

There are also plans for a new service by Eurostar starting from December 2016 using the Siemens Velaro e320 trains, these will travel two times a day between London and Amsterdam. The operating speed of the Velaro e320 is like the Thalys at 300km/h.

A.4. Tonnages

It was expected before construction that the tracks would carry 750MGT during 25 years but as the first trains only started using the tracks 3 years after construction between Rotterdam, Amsterdam and Belgium. The split to Breda followed two years later. As of January 2016, 10 years after construction was finished only 30 MGT have been carried over the tracks which is much less than expected. Currently the usage of the track is estimated at 6MGT a year but will be increased in 2017 as new services will be introduced on the HSL-South tracks (0). An

overview of the cumulative tonnages from 2006 until November 2015 by parts of the track is shown in Figure 58.

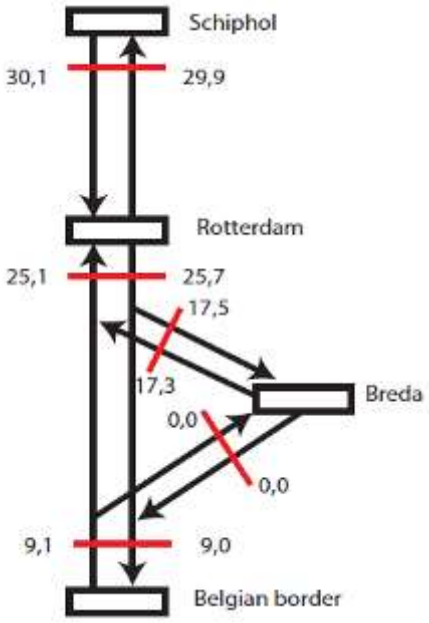

Figure 58: Overview of the cumulative MGTs from 2006 to November 2015.

The input for this data has been gathered using the Infraspeed assurance database which collects data from the trains and systems among the tracks. Using this, Infraspeed knows which trains drive over the HSL-South at which time. Infraspeed uses Atlas FO (Gotcha) systems to measure the tonnage per train and the static and dynamic forces on the rails. This because there are certain allowable standards for both the maximum axle loads and maximum static and dynamic forces. They have installed this system at two points of their tracks, one at kilometre 117.3 and the other one at 244, both have been installed on both the tracks to measure the trains in both two driving directions.

As both train types have different average weights, for the Thalys locomotive with 8 wagons this is on average 410 Tons and for the TRAXX carrying 6 wagons this is 355 Tons. For the parameter analysis the cumulative loads per section until November 2015 has been taken, as these were the most recent numbers when working on it. This means adding all the tonnages of all the trains since the line went operational. Also for the whole year 2015 the tonnages have been calculated and split up between Thalys and TRAXX for all the sections. Incidental testing with for example the ICE train has been left out, the same goes for runs with the maintenance vehicles. This because the main goal was to know more about the Thalys/TRAXX ratios on the different sections of the HSL-South.

A.5. Traffic speed and cant deficiencies

Traffic speed has been taken as an additional parameter to check whether the design speed for the tracks meets the actual speed. Also interesting is to see how both the TRAXX and the Thalys behave on the tracks and differ in speed.

Theoretical speed profile

The theoretical speed profile had been implemented in the IRISsys database of Infraspeed and can basically be divided in three different zones:

- Accelerating zone: starts at the entrances of the HSL-South and ends when the trains reach full speed.
- Open Track zone: starts when the trains reach full speed and ends when the trains lower their speed .
- Rolling out zone: starts at the end of the open track zone and ends at the ends of the HSL-South.

In the theoretical speed profile the upper speed limit is 300km/h, which was designed for high-speed trains like the Thalys. An example of a theoretical speed profile can be seen in Figure 59 where also the different zones have been marked. Interesting to see is the different lengths of the zones the accelerating zone is always between 9-11 km's long and the rolling out is always shorter in our example only 2,5kms long but one has to take into account that there is never directly a station after the ending of the HSL but one transfers first to the regular ProRail tracks.

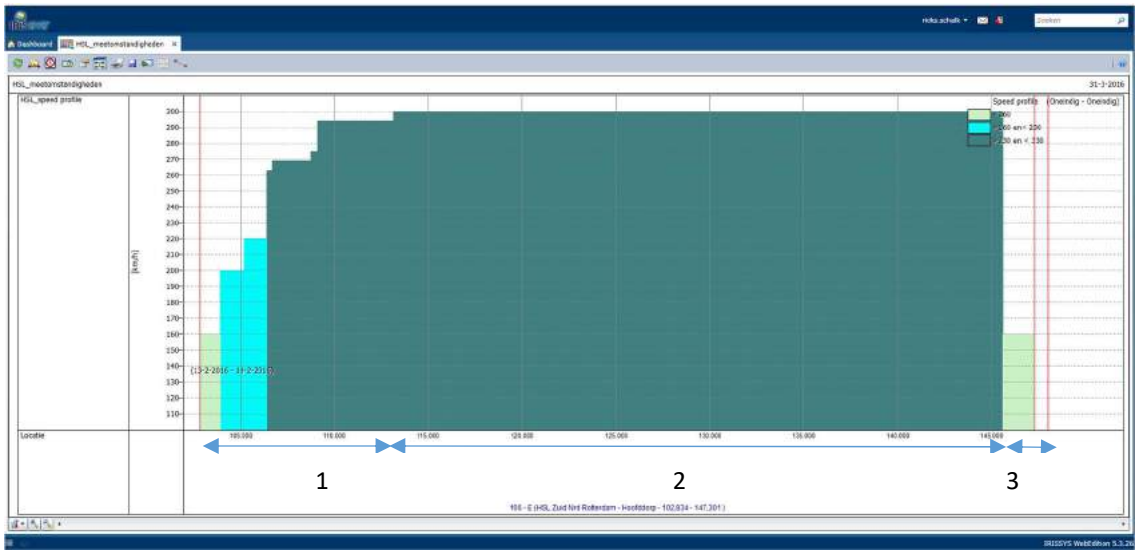

Figure 59: Theoretical speed profile in the IRISSys database for the NE section from Rotterdam to Hoofddorp with the three different zones, 1: accelerating zone, 2: Open Track, 3: Rolling out.

Determining the actual speed profiles

The actual speeds have been determined using the assurance database of Infraspeed. In this database the position reports of all the trains using the tracks are gathered. Once the trains enter the HSL-South every 6 seconds they send a position report. This position report contains data of the trains speed and position on the track. Using this, an actual speed profile for the two types of trains can be determined.

However the data can be somewhat disturbed by certain circumstances:

- Unforeseen stops can occur by for instance halting signs among the tracks, this causes the train to stop. Though the train will still be sending its position report every 6 seconds.
- Trains can be send to the other track in special circumstances.
- Due to special circumstances trains have to drive slower than normal, this is for instance often the case at bridge Hollands Diep when there are heavy winds (Nieuwenhuis, 2016).

The speeds used in the parameter analysis are the speeds when trains travel according schedule during normal circumstances. Gathered from the Assurance database these are more or less the median speeds for the trains. Also a check has been done to ascertain these profiles, using a GPS tracker during several rides by both intercity direct and Thalys.

Speeds have been determined for the 500m partitions of the track and taking the average from both rounding up from 0,5km/h to obtain whole numbers.

Speed TRAXX

The speed profile for the TRAXX is shown in Figure 60. In this figure also the distribution is shown between the different zones. For the main course of the HSL most of the tracks are covered by the open track zone for the TRAXX this is because its maximum speed doesn't greatly differ from its entrance/exit speed at the HSL which lies roughly around 100km/h. The maximum speed for the TRAXX is 165km/h. Notice that the TRAXX uses a

smaller part of the Southern track, this is because it doesn't drive towards the Belgian border but uses the connection to and from Breda at Zevenbergschen Hoek.

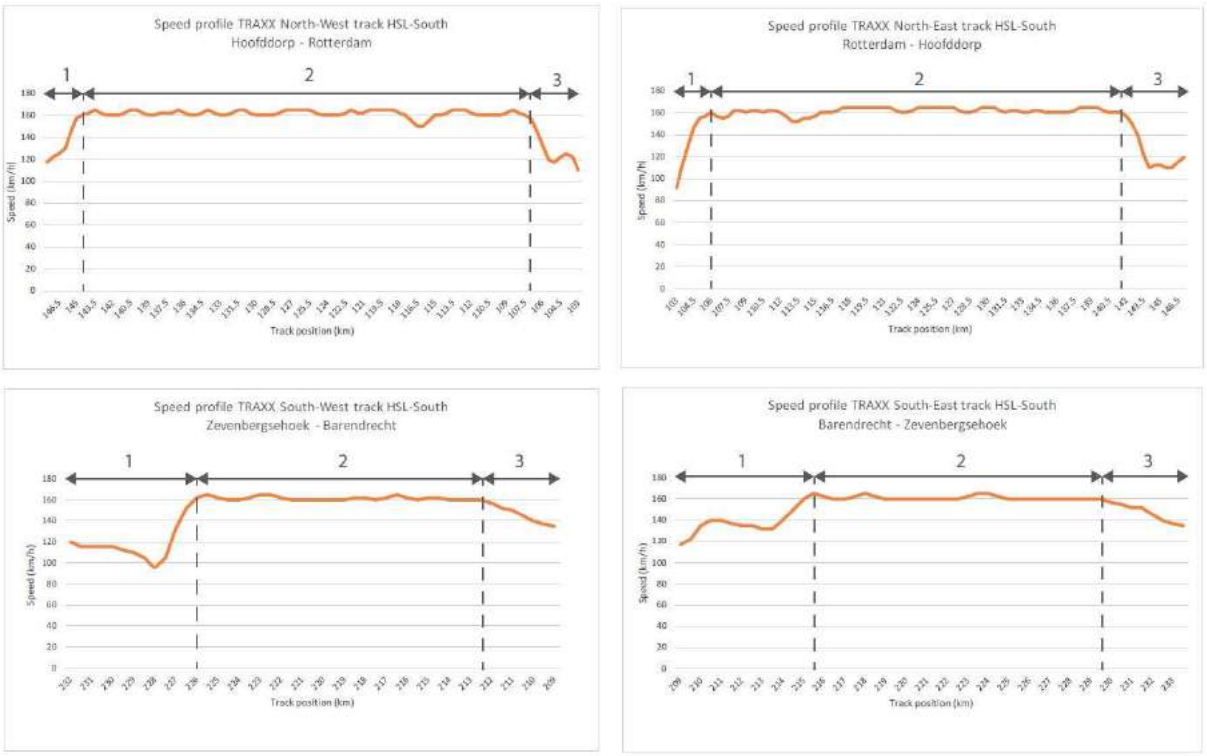

Figure 60: The speed profile for the TRAXX on the main tracks of the HSL-South. Also the different zones are shown; 1: Accelerating zone, 2: Open Track, 3: Rolling out.

Speed Thalys

The speed of the Thalys can be found in Figure 61. In this figure also the distribution of the different zones can be seen. For both the northern and southern parts of the HSL the maximum speed is 300km/h. The open track zone in the northern part in these actual profiles is about 16-18km long which is about 35-40% of the 44km track. For the southern part this is much larger which is due to the fact that the tracks are connected to the Belgian high speed network where the trains enter and leave the HSL with roughly 300km/h. The Thalys doesn't use the connection to Breda.

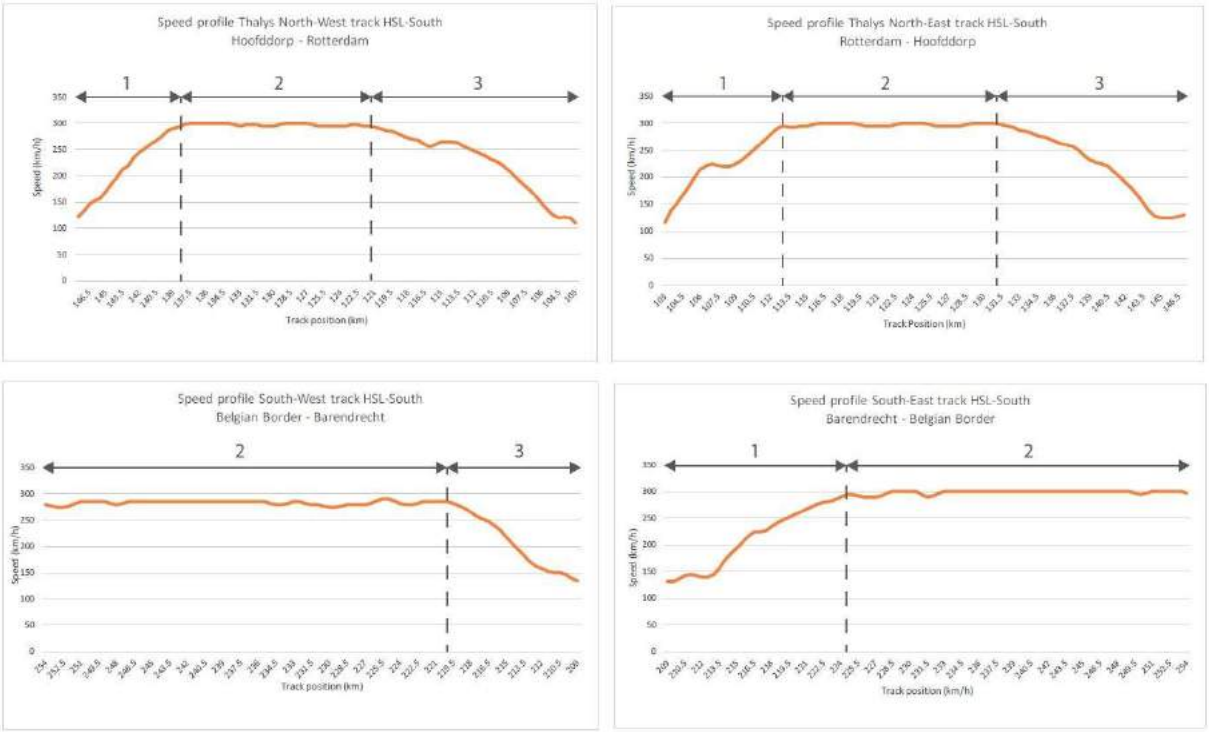

Figure 61: Speed profile of the Thalys for the main HSL-South tracks. Also the different zones are shown; 1: Accelerating zone 2: Open Track 3: Rolling out zone.

Cant deficiencies

The cant deficiencies for both types of trains have been calculated for all the curves of the HSL. Using the formula's presented in section 2.1.5, hereby using as input the following values for each curve: traffic speed, canting and curve radius. Cant excess can also occur, using the formulas this will result in a negative value for cant deficiency.

A.6. Traction

Traction TRAXX

The TRAXX at the northern part of the HSL currently drives in a sandwich formation. This means it drives with two locomotives pulling and pushing the train. However this sandwich has only been introduced in 2015. Before 2015 it was driving in pulling formation with only one locomotive. Regarding the analysis and the finding of the damages in 2014 only the pulling formation will be used. Each locomotive has four driving axis, meaning for the sandwich formation having eight driving axles in total. At the southern part the TRAXX drives with only one locomotive thus having four driving axles. A single TRAXX locomotive has a total power of 5600kW and a total tractive effort of 300kN at the HSL.

In Appendix D. Traction and breaking forces per axle, are shown for the TRAXX over the HSL track. The TRAXX is equipped with a diagnosis tool so that during driving time, location, traction and breaking forces are being recorded. This information has been used to determine the traction and breaking forces over the HSL by the TRAXX. In total 1600 measuring files have been used with data from 33 different TRAXX locomotives during the period of July 2015 until January 2016. This information has been used to determine the traction and breaking behaviour of about 8000 rides by the TRAXX on the HSL. This data has been gathered by Ricardo Rail commissioned by Infraspeed.

In Appendix B can be seen that traction by the TRAXX varies continuously over the track. This can be explained while the TRAXX is relatively quick at its maximum speed of 160km/h. This speed is kept constant by speed control. There are many gradients among the HSL which causes the TRAXX to shift a lot in traction to keep the speed constant at 160km/h.

Traction Thalys

The Thalys drives with two locomotives at the HSL with in between 8 wagons. Each locomotive has four driving axles, making a total of eight driving axles. The total power of the Thalys at the 25kV overhead line power used at the HSL tracks is 8800kW. The total tractive effort of the Thalys is 450kN.

For the Thalys there was no data available from the trains. Therefore the traction forces have been calculated using different sources:

- Acceleration measurements by Ricardo Rail from August 2014.
- Data from the traction forces and train resistance gathered from video recording within the driving cabin.

The acceleration measurements have been executed in the passenger wagons. During the measurements the accelerations have been measured in the longitudinal direction of the train. The accelerations were the effect of the traction by the train and the gravitation at driving at slopes. Using the traction characteristics of the Thalys and driving speed, the traction needed to attain a certain acceleration can be determined. This resulted in the traction which can be viewed in Appendix D. Traction and breaking forces per axle.

This calculation is based on evenly distributed traction forces on each axle. The Thalys has compared to the TRAXX a relatively constant traction distribution. This can be explained due to the fact that the Thalys needs more time and distance to attain its maximum speed of 300km/h. This can be seen in Figure 61 where the speed profile of the Thalys is shown. To keep its maximum speed a lot of traction needed, the Thalys also doesn't have the speed regulation which the TRAXX has. The maximum tractive force of the TRAXX is also about twice as high compared to the Thalys.

A.7. Assets

Among the HSL tracks there are some very special structures. We call these the assets among the tracks. The location of each asset has been retrieved from the track overview drawings. The special features will be described for each asset in this paragraph.

Tunnels

There are several tunnels among the tracks an overview of the locations and the lengths of the tunnels can be seen in Table 20. For this overview the lengths of the covered areas have been taken into account so the open tunnel entrances have not been taken into account. Also the type of tunnel is shown in the table, among the northern part of the HSL there are two land tunnels. Among the southern part there are two water tunnels crossing the Rivers Oude Maas and Dordtsche Kil.

Table 20: Location and lengths of the tunnels among the HSL.

Name	type	Km start	Km end	Total length (Km)
Tunnel Rotterdam	Land tunnel	103.200	105.150	1.950
Tunnel Groene Hart	Land tunnel	122.541	129.907	7.366
Tunnel Oude Maas	Water tunnel	215.506	216.891	1.385
Tunnel Dordtsche Kil	Water Tunnel	224.373	225.860	1.487

Roof Barendrecht

Roof Barendrecht is also an asset among the HSL. It has some similar characteristics to tunnels while it is also a covered structure. Though it differs from a tunnel as it is not going underground, thus tracks are relatively flat. It is located at the beginning/end of the HSL southern part around the Barendrecht station. It starts at kilometre 209.160 and ends at 211.002 thus having a total length of 1.842 meters.

Cuttings

A cutting can be characterised being an open tunnel. Usually build for other for road crossing over the tracks. In Table 21 a list can be found with the locations of the cutting among the HSL.

Table 21: Overview of the cuttings among the HSL.

Name	Km start	Km end	Total length (km)
Cutting Bergschenhoek	108.286	111.188	2.902
Cutting Mookhoek	221..947	222.881	0.934
Cutting Prinsenbeek	241.067	242.170	1.103
Cuting Galder	248.675	250.121	1.446

Viaducts

There is one major viaduct among the HSL-South. The viaduct is called viaduct Bleiswijk and is located at the northern part of the HSL. The total length of this viaduct is 5898m. The viaduct starts at kilometre 111.349 and ends at 117.247. Viaduct Bleiswijk is raised a few meters above ground level and can be seen in Figure 62.

Figure 62: Two pictures of viaduct Bleiswijk, taken by the author during a site visit in March 2016.

Bridge

There is one major bridge among the HSL. This is bridge Hollands Diep and is located at the southern part of the HSL. The bridge has a length of 1189 metres and has two ramps on each side of 359 and 426 metres. At its highest point the bridge reaches 24 metres above the water level. Though this has caused trouble making it vulnerable for the trains passing over the bridge when strong winds occur. These high winds cause the trains to driver slower over the bridge.

Flyover

There is one flyover among the Track this is located at the Turnout from Breda to the main HSL track at the southern part near Zevenbergschen Hoek. At the flyover the track goes over the HSL and then connecting to it again.

Switches

There are several switches among the HSL. These are switches between the east- and westtracks, switches to the two maintenance yards and the turnouts connected to the ProRail tracks around Breda. An overview of the switches among the HSL can be seen in Table 22. Regarding the analysis of the damages the switches are left out of scope.

Table 22: Overview of the switches among the HSL.

Location (km)	Track	Type	Angle of intersection
135.482	North-East	Between tracks	1:34.7
135.685	North-East	Between tracks	1:34.7
143.891	North-East	Maintenance yard	1:34.7
144.700	North-East	Maintenance yard	1:34.7
135.282	North-West	Between tracks	1:34.7
135.693	North-West	Between tracks	1:34.7
144.010	North-West	Between tracks	1:34.7
144.263	North-West	Maintenance yard	1:12
144.485	North-West	Between tracks	1:34.7
209.618	South-West	Between tracks	1:15
209.701	South-West	Between tracks	1:15
233.069	South-West	Between tracks	1:34.7
233.189	South-West	Maintenance yard	1:12
233.398	South-West	Turnout	1:39.173
233.708	South-West	Between tracks	1:34.7
243.753	South-West	Turnout	1:34.7
252.930	South-West	Between tracks	1:34.7
253.556	South-West	Between tracks	1:34.7
209.493	South-East	Between tracks	1:15
209.715	South-East	Between tracks	1:15
232.894	South-East	Between tracks	1:34.7
233.874	South-East	Between tracks	1:34.7
234.064	South-East	Turnout	1:34.7
243.741	South-East	Turnout	1:34.7
252.990	South-East	Between tracks	1:34.7
253.464	South-East	Between tracks	1:34.7

Voltage- and phase locks

There are several voltage and phase locks among the track. The voltage locks have been placed to switch from 1.5kV DC power to the 25kV AC powered tracks at the HSL. Therefore these are to be found at the beginnings and endings of the HSL track. The only exception here is the ending of the southern part, here a phase lock is used because the Belgian tracks also use the 25kV AC powered system. The phase locks are placed among the track. One of the important issues regarding these locks is that around a voltage lock the traction and power is switched off temporarily. Around the phase locks it is also prohibited to use the traction for the trains passing through. In Table 23 the location of the locks can be seen.

Table 23: Location of the Phase and Voltage locks among the HSL.

Voltage locks		
Km start	**Km end**	**Track**
103	104	North
145.5	146.5	South
211	212	South
300	301	G
300	301	H
400	401	J
400	401	K
Phase Locks		
Km start	**Km end**	**Track**
114.5	115.5	North
230.5	231.5	South
254	254.5	South

A.8. Superstructure

The superstructure used among the HSL-South can be divided in four sub-subsystems:

- Rheda 2000 track sub-subsystem.
- Ballast 300 track sub-subsystem.
- Ballast 160 track sub-subsystems.
- Ballast 40 track sub-subsystem.

These are discussed in the next two subsections.

Slab track

Rheda 2000 is a type of slab track which has been used in most parts for the HSL-South with exception of the transitional zones to the ProRail-, Belgian- and maintenance yard tracks. In total about 88km's of track has been constructed using the Rheda2000 superstructure. Figure 63, shows the Rheda 2000 superstructure at the HSL.

The Rheda 2000 system has been installed first in the German high-speed line between Leipzig and Halle. Characteristic for the Rheda tracks is that the sleepers are cast into the concrete. For the HSL instead of a single sleeper, a variant with two blocks has been used. The advantages of Rheda track compared to conventional ballast track are that it needs less maintenance, is relatively light, smaller construction height and larger lateral stiffness. Disadvantages compared to ballast track are: larger temperature effects, longer construction time, limited adjusting possibilities and measures required in relation to noise and vibrations (Sectie Weg- en Railbouwkunde, 2014).

Figure 63: Rheda 2000 superstructure at a curve in the HSL-South. Source: http://www.rgprojecten.nl/images/projecten/rheda2000/HSL-002.jpg

Ballast track

Ballast track also known as the 'classical track' or 'conventional track' basically consists of a flat framework which is made up of rails and sleepers which are supported by ballast. This ballast bed rests on a sub-ballast layer which forms the transition layer to the formation, the rails and sleepers are connected by fastenings (Esveld, 2001). An overview of the principle of Ballast track is shown in Figure 64. The Ballast track sub-system for can be divided in three categories which have been used among the HSL. These will be individually discussed in this section.

Ballast 300

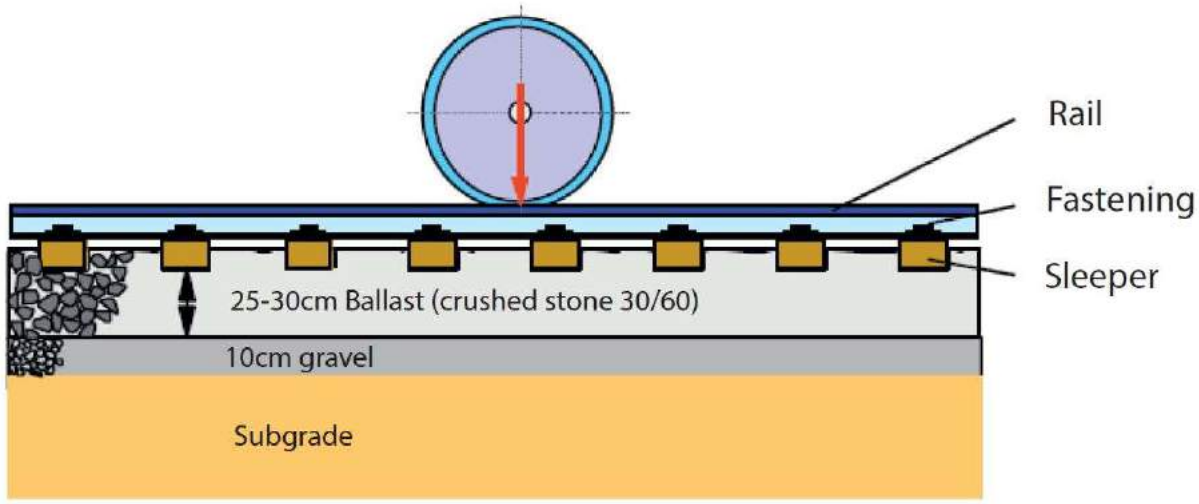

Figure 64: Longitudinal section of the ballast track principle. Source: (Esveld, 2001)

Ballast 300 is constructed at only one part of the line, being the connection between the Belgian part of the HSL and the Rheda2000 part at the south entrance of the cutting Galder. The lengths of the sections for the Ballast300 superstructure are given by Table 24.

Table 24: Lengths of the Ballast 300 sections.

	Km start	Km end	Length (m)
Galder – Belgian border SW track	250.082	254.503	4.421
Belgian border – Galder SE track	250.086	254.503	4.417

Ballast 160

The Ballast 160 sub-subsystems are the connections from and to the conventional Dutch railway networks. These have been installed at the start and the endings of the HSL for both the main tracks and the turnouts. In total about 14.8kms of Ballast 160 has been installed throughout the HSL. Table 25 gives an overview of the locations and track lengths of the Ballast 160 superstructure.

Table 25: Lengths and locations of Ballast 160 track sections.

Section	Km start	Km end	Length (m)
Hoofddorp NW track	145.881	147.151	1.270
Hoofddorp NE track	145.886	147.297	1.411
Barendrecht SW track	209.160	211.637	2.477
Barendrecht SE track	209.158	211.635	2.477
Zevenbergschen Hoek G	300.227	302.159	1.932
Zevenbergschen Hoek H	300.351	301.681	1.330
Breda West J	400.222	402.174	1.952
Breda East K	400.232	402.146	1.914

Ballast 40

The Ballast 40 superstructure has not been installed on the main tacks but only on the tracks at the maintenance yards. Among the HSL there are two maintenance yards, one on the Northern part at Hoofddorp and another one at the Southern part near Zevenbergschen Hoek. In total about 850m of Ballast 40 has been installed among the HSL. The Ballast 40 superstructure doesn't come forward in the parameter study as the tracks among the maintenance yards have not been studied for this thesis.

A.9. Track geometry

Horizontal curves

There are several curves among the HSL on both the southern and northern parts as on the turnouts. Characteristic for the HSL curves is that they have different properties as they become sharper, thus having a smaller radius. For the curves with a radius up to 6050m a rail grade of 350HT has been used instead of the 260 rail grade used among the rest of the tracks. In the upper leg of the curves also another profile has been shaped in the upper leg, the 60 E2 profile instead of the 60 E1. The sharpest curve among the tracks is the curve near Rijpwetering around kilometre 133 with a radius of 4260m and canting of 170mm. The characteristics of the curves have been retrieved from the design drawings.

Vertical curves

The HSL also got some vertical curves among the tracks. These are mainly structured among the assets. Assets like bridges, flyovers and tunnels got different vertical curves among them. Each of these got a slope in the front and the back. These vertical curves have been processed as the difference in height at the top of the rail between the 500m sections for the parameter analysis. This data has been retrieved from the design drawings of the HSL. The largest difference we between height for 500m sections were at the tunnel exits and entrances of the Tunnel Groene hart at 12 metres. At the bridge Hollands Diep we see the largest rise in levels among several 500 meter sections where the tracks rise over 1500m a total of 35metres. The maximum slope at the HSL is 25 promille.

A.10. Rail profile

For all sections on the HSL-South the rail type 60 E1 is used with a rail inclination of 1:20. The only exception is the use of rail type 54E1 with a rail inclination of 1:40 at the maintenance yards. Two rail steel grades have been used with different material properties and service performance:

- Rail grade R260.
- Rail grade R350HT.

The R350HT is used at the high-speed section (300km/h) in the curves (upper and lower leg) with radius <6050m and at the 160km/h sections in curves (upper and lower leg) with radius <3000m. Also anti head check profiles have been used at the high-speed sections where curves have a radius <6050m (including transition curves) an profile (60 E2) is ground in the outer rail (high leg), simulations during the design phase showed this would behave as an anti-head check profile. Furthermore these have also been used for curves at the 160km/h sections with a radius <3000m. These profiles have been applied to cope with the higher impact loading of a wheel on the rail in curves reducing the shear stresses, which leads to a longer lifetime of the rail.

A.11 Grinding

The purpose of grinding is to maintain a proper cross section of the rail head, levelling out irregularities and to reduce rolling (wheel-rail) noise emission of the rail. For the parameter analysis the mms of rail removal, technique (rolling stone or high-speed grinding) and date of grinding have been used. This in order to be able to check what the total removal has been at the parts of the HSL-South and which parts have been ground by which company.

The technique prescribed in the maintenance manual by Infraspeed is the rotating stone technique. The frequency in which it should be carried out based on the condition of the tracks which are monitored by regular measurements. There are two types of classification in grinding operations:

- the preventive actions which cover the planned grinding intervention, undertaken during scheduled maintenance windows and carried out in order to optimize asset life. Initial grinding (025-0.3mm), load based/cyclic grinding (0.15-0.3mm) and acoustic grinding are parts of the preventive grinding actions.
- Corrective actions are undertaken when the rail is in a bad shape and a critical value is reached. The rail will be reprofiled and cracks and corrugation will be removed. Corrective actions require intensive grinding, 0.5-3mm will be removed.

There have been several grinding operations since the completion of the HSL-South. Two companies have been grinding the tracks of the HSL-South since the completion in 2005; Speno and Vossloh.

Speno grinding

Speno ground the track on several occasions:

- initial grinding 2005/2006: shaping the 60 E2 profiles in the upper legs of the large curves. The exact grinding details are unknown, estimated 0.35-0.5mm of grinding of the whole track.

- Grinding 2009/2010: exact grinding details are unknown, but the grinding was due to the start of the operation of the HSL-South.

- Grinding December 2011 & December 2012: 0.3mm grinding on km's 250-251 of the South-West and South East tracks because of sound measurements tests for the Fyra V250.

- Grinding November 2013: two corrective grinding actions at 121.5-122.5 for both the North-West and East track, this was at the entrance of the tunnel Groene Hart due to slipping damages. The mm's of grinding is unknown.

- Grinding Dec. 2015: because of the damages found earlier that year several affected parts have been ground up to 5.5mm.

Vossloh grinding

Vossloh has ground the tracks of the HSL-South, using both the High-Speed grinder and High-Speed Light grinder.

- Grinding 2009: both the North-West and North East tracks have been ground using the HSG-L grinder, because of rust about 0.25mm had been removed.

- Grinding 2011, 2012, 2013: several parts of the northern track have been ground by the HSG-L due to exceeding acoustic norms, about 0,1mm has been grinded.

- Grinding 2012: parts J and K from and to the Belgium border from Breda had been ground because of the Olympic train using the track (otherwise unused), it is unknown how much had been ground.

- Grinding 2014: the whole HSL-South had been ground using the HSG grinder, removing about 0,2mm. This has been a preventive grinding action and because of noise reduction.

Appendix B. hotspots HSL-South

Zoetermeer, North-east Km. 117.4-119.7

The hotspot is located on the east track, trains here come from a viaduct and heading towards the tunnel Groene Hart (Figure 65). The damages are halfway a large curve (6005m radius) with a cant of 110mm. These curves have the 350HT rail grade and an 60 E2 anti head check profile in the upper leg. There is no height difference here. Both the Thalys and the TRAXX trains here travel at full speed, with traction and reach speeds of respectively 300 and 165km/h.

The cracks have been removed by grinding in December 2015 and were up to 5,5mm of depth. The damages are shown in Figure 66 and Figure 67. In these pictures we see a clear running band next to the middle of the rail. Within this running band the cracks appear around the dark spots around the middle of this running band.

At the end of February 2016 the tracks at this location have been replaced by softer rails with a 260 rail grade, the upper legs also have been ground reinstalling the 60 E2 anti-headcheck profile.

Figure 65: Aerial view of the damages near Zoetermeer (Google Maps)

Figure 66: Close-up of the damages with size measurements at the hotspot Zoetermeer

Figure 67: Close-up of the damages at Zoetermeer, we see the cracks here at the rail head.

Partition		Parameter														
Km start	Km end	Superstructure	Rail grade	Cant	Radius	Height difference	Design speed	Speed TRAXX	Speed Thalys	Traction TRAXX	Traction Thalys	Tonnage Cum	Tonnage ratio TRAXX/Thalys	Assets	Damage depth	Damage median
117.0	117.5	Rheda	Mix	35	6005	-1.46	300	162	300	20	70	29,9	48/17	viaduct	3	1
117.5	118.0	Rheda	350HT	90	6005	0	300	165	300	20	70	29,9	48/17	Open track	3	3
118.0	118.5	Rheda	350HT	110	6005	0	300	165	300	15	70	29,9	48/17	Open track	3	3
118.5	119.0	Rheda	350HT	110	6005	0	300	165	300	10	70	29,9	48/17	Open track	3	3
119.0	119.5	Rheda	350HT	110	6005	0	300	165	300	10	70	29,9	48/17	Open track	3	2
119.5	120.0	Rheda	350HT	110	6005	0	300	165	297	5	70	29,9	48/17	Open track	3	1
Assembled value		Rheda	350HT	110	6005	0	300	165	300	13	70	29,9	48/17	Open track	3	2

Hoofddorp, North-west Km. 145.9-147.0

This hotspot is located on the west track at the beginning of the HSL-South trains traveling here are heading towards a voltage lock (Figure 68).

The superstructure used here is still Ballast 160. There are also two curves among this hotspot with radiuses of 1600m and 2000m and cant of 105 and 90. Head hardened 350HT rails have been used with in the curve a anti head check profile grinded in the upper leg. In this 500m part the tracks are descending 5m in height.

Trains traveling here are generally speeding up, the average TRAXX starts here around 120km/h ending at 125km/h while the Thalys starts at 125 km/h ending at 140km/h. This part of the track had been designed for trains traveling at 160km/h.

At these parts an earlier corrective grinding action in 2013 has taken place by Speno to remove corrugation. While the latest corrective action took place in July 2015 where up to 6mm had been removed by Speno. This is one of the worst affected parts of the HSL-South. Pictures of the damages are shown in Figure 69 and Figure 70, characteristic for the damages here is that they lie on the field side of the rail head and come with repeating pattern.

This is the only part which has been investigated by DEKRA rail for its damages resulting in a material research report in October 2015. Conclusions were:

- Damages found have characteristics most similar to studs
- White edging layer had been found at the surface of the rail with a maximum thickness of 30µm and an average thickness of 10µm.
- White edging layer has been found on both the running band of the rail and outside the running band.
- The used 350HT rail grade meets the material and chemical requirements according to the NEN-EN 13674-1 norms.
- According to the microscopically research among 8 sections the maximum crack depth was 3-3.5mm.

Figure 68: Aerial overview of the hotspot Hoofddorp (Google Maps).

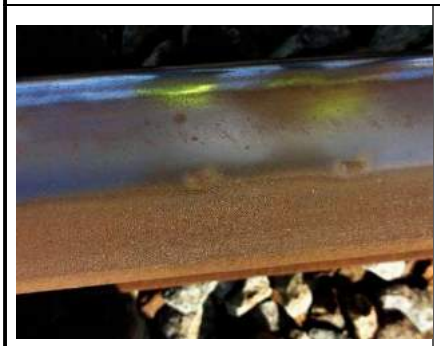

Figure 69: Close-up of the damages, the damages are lying at the border of the running band at the field side of the rail head.

Figure 70: The damages at Hoofddorp, with a repeating pattern between the distance.

Partition		Parameter														
Km start	Km end	Superstructure	Rail grade	Cant	Radius	Height difference	Design speed	Speed TRAXX	Speed Thalys	Traction TRAXX	Traction Thalys	Tonnage Cum	Tonnage ratio TRAXX/Thalys	Assets	Damage depth	Damage median
145.5	146.0	Mix	350HT	40	2000	4,43	210	130	152	0	0	30,1	48/17	Voltage lock	3	1
146.0	146.5	Ballast 160	350HT	90	1800	-5.07	160	125	145	0	0	30,1	48/17	Voltage lock	3	1
146.5	147.0	Ballast 160	350HT	110	1600	5.44	160	122	132	0	0	30,1	48/17	Open track	3	3
Assembled value		Ballast 160	350HT	80	1800	4,60	175	125	142	0	0	30,1	48/17	Voltage lock	3	2

Turnout Breda to Zevenbergschen hoek, South G Km. 300.5-301.3

This hotspot is located on the flyover coming from Breda entering the HSL-South in the direction of Rotterdam. Trains traveling here are entering the voltage lock located at 300.423-301.036 (Figure 71).

The superstructure used is Ballast 160 with both the 350HT 60 E2 in the curve and 260 60 E1 outside the curve. The curve has a maximum cant of 75mm in both directions. Which means at for this hotspots there is a s-curve present. There are also vertical curves among this hotspot, trains coming in are first descending up to 9m then entering the flyover, rising up to 9m.

Only the TRAXX are using these tracks which have been designed for 160km/h. The tracks are entering this hotspot at average around 140km/h slowing down to 125, then speeding up to 130 km/h again. In December 2015 up to 3mm has been ground.

In the Infraspeed databases there were no pictures regarding the damages at this hotspot. Therefore the eddy current data is being presented in Figure 72.

Figure 71: Satellite image of the location of the hotspot (Google Maps).

Partition		Parameter														
Km start	Km end	Superstructure	Rail grade	Cant	Radius	Height difference	Design speed	Speed TRAXX	Speed Thalys	Traction TRAXX	Traction Thalys	Tonnage Cum	Tonnage ratio TRAXX/Thalys	Assets	Damage depth	Damage median
300.5	301.0	Ballast 160	Mix	36	2200	9,57	160	130	-	0	-	17,5	1/0	Voltage lock	3	2
301.0	301.5	Ballast 160	350HT	75	1600	-9,18	160	132	-	0	-	17,5	1/0	Voltage lock	3	1
Assembled value		Ballast 160	350HT	60	1900	0,2	160	131	-	0	-	17,5	1/0	Voltage lock	3	2

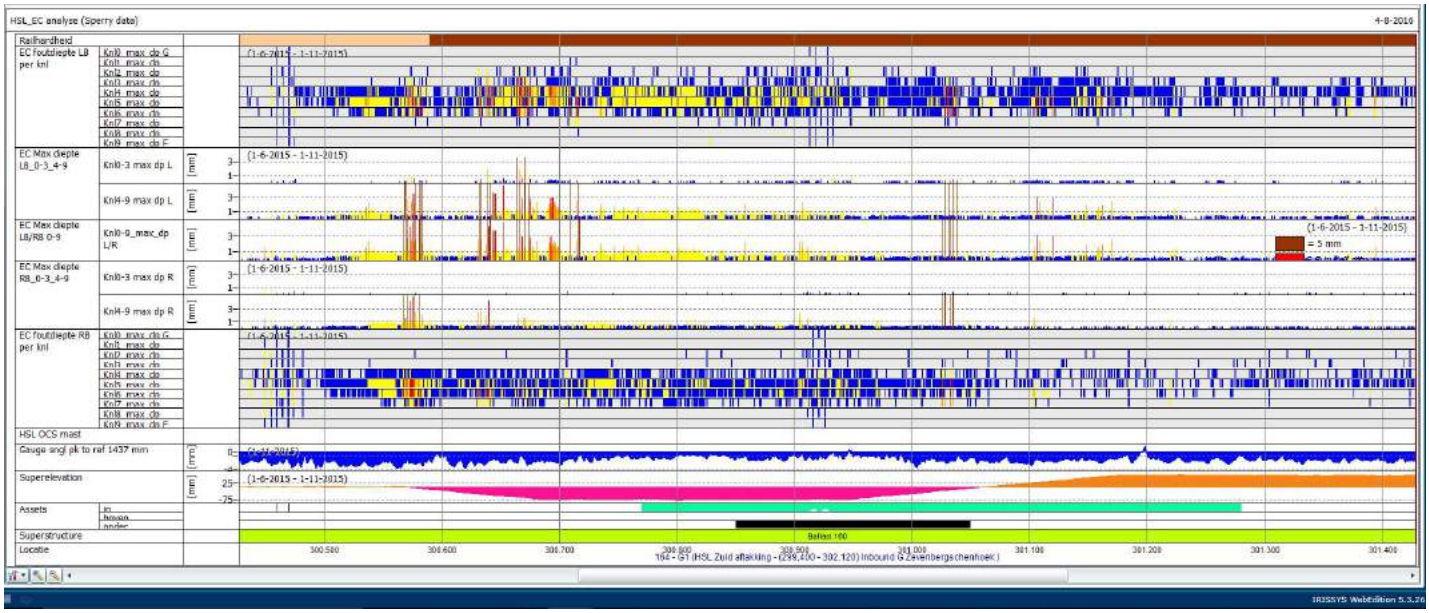

Figure 72: Eddy current measurements in IRISSys for the hotspot at the flyover. On the horizontal axis the location position is shown. At the vertical axis some track characteristics are shown. The most important ones are the measurements for the 10 different channels for each leg. The upper shows the measurements for the right leg and the lower one for the right leg. The different colors show the depth: blue:0,1-1,0mm. yellow 1,0-3,0 mm and red 3,0-5,0mm.

‘s-Gravendeel, South-east, km 218.0-221.0

This hotspot is located at the east track of the southern part of the HSL-South. The hotspot is located after a cutting, the Thalys traveling here heads towards the Belgian border, the TRAXX are heading towards Breda (Figure 73).

The superstructure used is Rheda 2000 with a 350HT rail grade in the curve which expands from 217.902 to 222.351 with a radius of 4449.5m and cant of 140mm, the anti-head check profile has been grinded in the upper leg of the curve . There is no vertical curve among this hot-spot. The Thalys traveling here is speeding up from 230km/h towards 260km/h while the TRAXX is already at full speed. The designed speed is 289km/h at the beginning of the hotspot and 300km/h at the end.

In December 2015 km’s 218.000-218.800 have been ground up to 2,3mm. Which is interesting as the measurements show deeper cracks, there is a good chance that not all cracks had been removed. Pictures of the damages at this location can be seen in Figure 74 and Figure 75. Interesting here is that we see wide running band and dual contact marks. Which shows that at least one of the trains has a dual contact position at this part of the track.

Figure 73: Satellite image of the location of the hotspot (Google Maps).

Figure 74: Close-up of the damages at this hotspot at the southern HSL-tracks. Notice that there seems to be two-point contract as both a running band at the rail-head can be seen as a contact area around the flange of the rail.

Figure 75: Close-up of a single crack at the gauge-side of the rail head.

Partition		Parameter														
Km start	Km end	Superstructure	Rail grade	Cant	Radius	Height difference	Design speed	Speed TRAXX	Speed Thalys	Traction TRAXX	Traction Thalys	Tonnage Cum	Tonnage ratio TRAXX/Thalys	Assets	Damage depth	Damage median
218.0	218.5	Rheda	Mix	100	4449.5	0	289	165	235	5	75	25,7	13/6	Open track	3	2
218.5	219.0	Rheda	350HT	140	4449.5	0.01	289	162	242	5	75	25,7	13/6	Open track	3	1
219.0	219.5	Rheda	350HT	140	4449.5	-0.19	289	160	247	5	75	25,7	13/6	Open track	3	2
219.5	220.0	Rheda	350HT	140	4449.5	0	289	160	252	5	75	25,7	13/6	Open track	3	2
220.0	220.5	Rheda	350HT	140	4449.5	0	289	160	257	5	75	25,7	13/6	Open track	3	2
220.5	221.0	Rheda	Mix	100	4449.5	0	294	160	262	5	75	25,7	13/6	Open track	3	2
Assembled value		Rheda	350HT	140	4449.5	0	289	160	250	5	75	25,7	13/6	Open track	3	2

Rijpwetering 1, North-west 130.0-135.0

The hotspot is located on the west track, trains come from a cutting 1km before the hotspot the hotspot ends at the entrance of the tunnel Groene Hart (Figure 77).

There are two large curves in both directions located among this spot, the radiuses are 4495m and 4260m with canting 160mm and 170mm. The 170mm cant is among largest cants used among the HSL-South. The used rail grade is 350HT and the 60 E2 anti head check profile has been used in the upper leg of the tracks. The track here is mostly flat until km 130-131.5 the level declines about 24m when entering the tunnel. Both the Thalys and TRAXX travel at full speed over this hotspot, using traction.

In july 2015 the first cracks have been removed by Speno between km 130.5-131.0 and were up to 3.0mm. This is also the reason why we see lower damage values for this partition, as it has been ground before the measurements. In December the remaining cracks have been removed by Speno and up to 4.3mm had been ground.

Figure 76: Aerial overview of the first hotspot around Rijpwetering (GoogleMaps).

Partition		Parameter														
Km start	Km end	Superstructure	Rail grade	Cant	Radius	Height difference	Design speed	Speed TRAXX	Speed Thalys	Traction TRAXX	Traction Thalys	Tonnage Cum	Tonnage ratio TRAXX/Thalys	Assets	Damage depth	Damage median
130.0	130.5	Rheda	350HT	165	4295	8.72	300	162	295	15	0	30,1	48/17	Tunnel entrance	3	1
130.5	131.0	Rheda	350HT	165	4740	2.89	300	165	295	10	0	30,1	48/17	Open track	2	1
131.0	131.5	Rheda	350HT	165	4740	-2.65	300	165	297	5	70	30,1	48/17	Open track	2	1
131.5	132.0	Rheda	350HT	165	4449.5	-0.69	300	162	297	5	70	30,1	48/17	Open track	3	2
132.0	132.5	Rheda	350HT	110	4449.5	0.22	300	160	297	5	70	30,1	48/17	Open track	3	2
132.5	133.0	Rheda	350HT	20	4449.5	3.51	300	160	295	5	70	30,1	48/17	Damwall	3	2
133.0	133.5	Rheda	350HT	132	4260	-0.59	300	162	297	5	70	30,1	48/17	Damwall	3	2
133.5	134.0	Rheda	350HT	170	4260	-3.65	300	165	300	20	70	30,1	48/17	Open track	3	2
134.0	134.5	Rheda	350HT	170	4260	-1.74	300	162	300	5	70	30,1	48/17	Open track	3	2
134.5	135.0	Rheda	Mix	120	4260	1.6	300	160	300	5	70	30,1	48/17	Open track	3	2
Assembled value		Rheda	350HT	160	4450	2	289	160	297	10	70	30,1	48/17	Open track	3	2

Rijpwetering 2, North-east 132.5-134.0

The hotspot is located on the east tracks, trains traveling here came out the tunnel Groene Hart 2 km's earlier. The spot is located where two large curves transfer to another.

The rail grade used is 350HT with and an anti-head check profile had been installed in the upper legs in the curves. The canting in the second curve is 175 which is the largest cant being used for the HSL. While the curve radius has a value of 4265. In the first 500m there is a small rise in height of 3m while in the last 500m's the tracks decline about 4,5m's. The TRAXX using this part of the tracks is still at full speed. The average Thalys is slowing down starting at 295 ending at 285. And its traction is also being decreased while still present.

In December 2015 the tracks have been ground at this hotspot and up to 3,5mms have been removed by Speno. Pictures of the damages can be seen in Figure 78 and Figure 79. In these pictures clear grinding marks can be seen among the rails. Also two very different running band widths can be seen. The damage looks however the same, a crack in the middle of the running band at the gauge side of the rail head.

Figure 77: Aerial overview of the hotspot (GoogleMaps).

Figure 78: Close-up of a crack, a running band can be seen at the gauge side of the rail head with cracks in the middle. Also the grinding marks are clearly visible here.

Figure 79: Picture of the damages at Rijpwetering. Here we see a wider running band with the same grinding marks and a crack in the middle of this running band.

Partition		Parameter														
Km start	Km end	Superstructure	Rail grade	Cant	Radius	Height difference	Design speed	Speed TRAXX	Speed Thalys	Traction TRAXX	Traction Thalys	Tonnage Cum	Tonnage ratio TRAXX/Thalys	Assets	Damage depth	Damage median
132.5	133.0	Rheda	350HT	165	4495	3,51	300	162	292	10	60	29,9	48/17	Open track	3	1
133.0	133.5	Rheda	350HT	10	4265	-0,59	300	160	287	10	40	29,9	48/17	Open track	3	1
133.5	134.0	Rheda	350HT	175	4265	-4,87	300	160	285	5	20	29,9	48/17	Open track	3	1
Assembled value		Rheda	350HT	170	4350	1,0	300	160	287	8	40	29,9	48/17	Open track	3	1

Appendix C. Intensities related to the hotspots

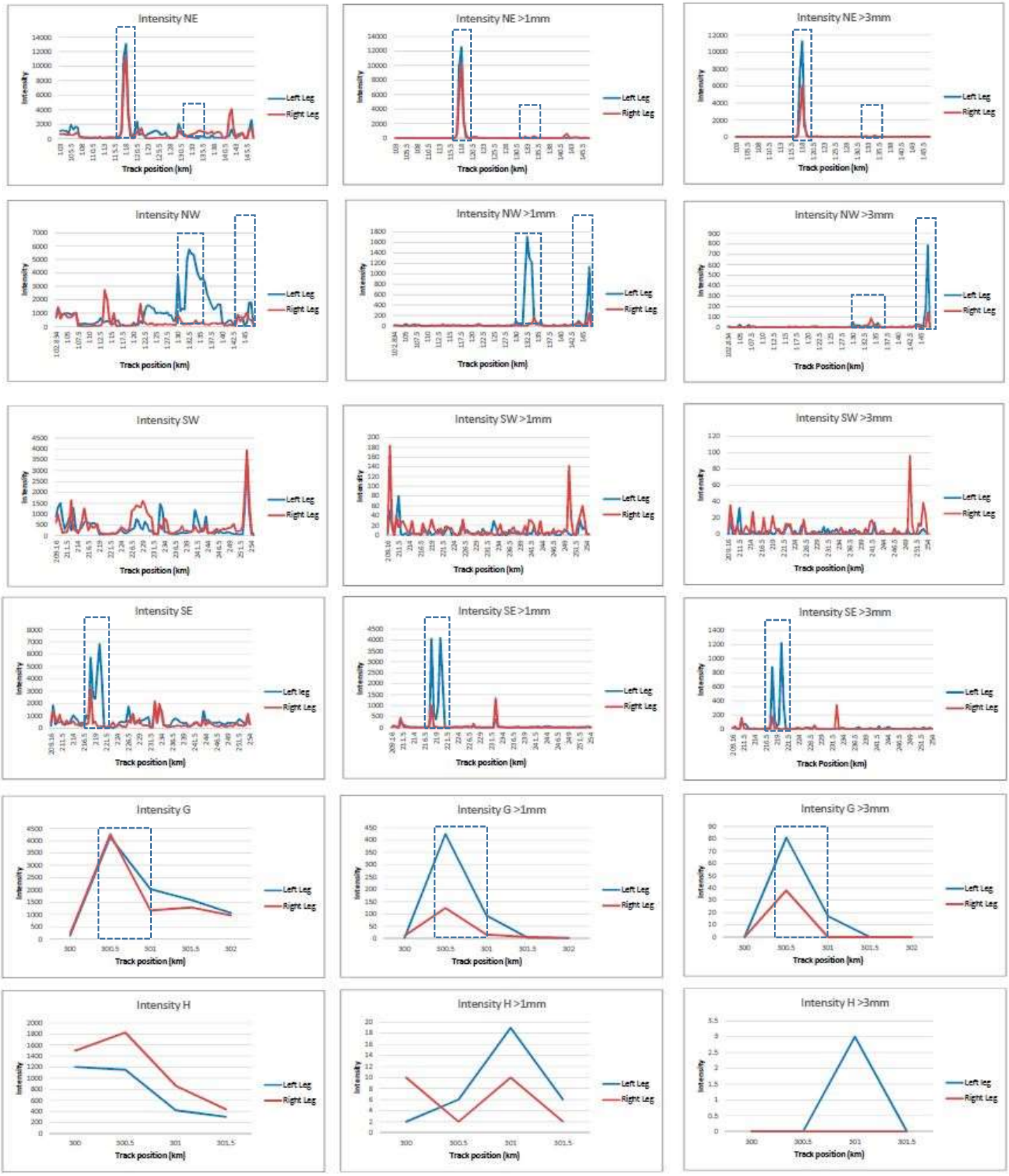

Figure 80: Overview of the different intensity distributions for all the sections of the HSL. The marked areas are the six hotspots.

Appendix D. Traction and breaking forces per axle

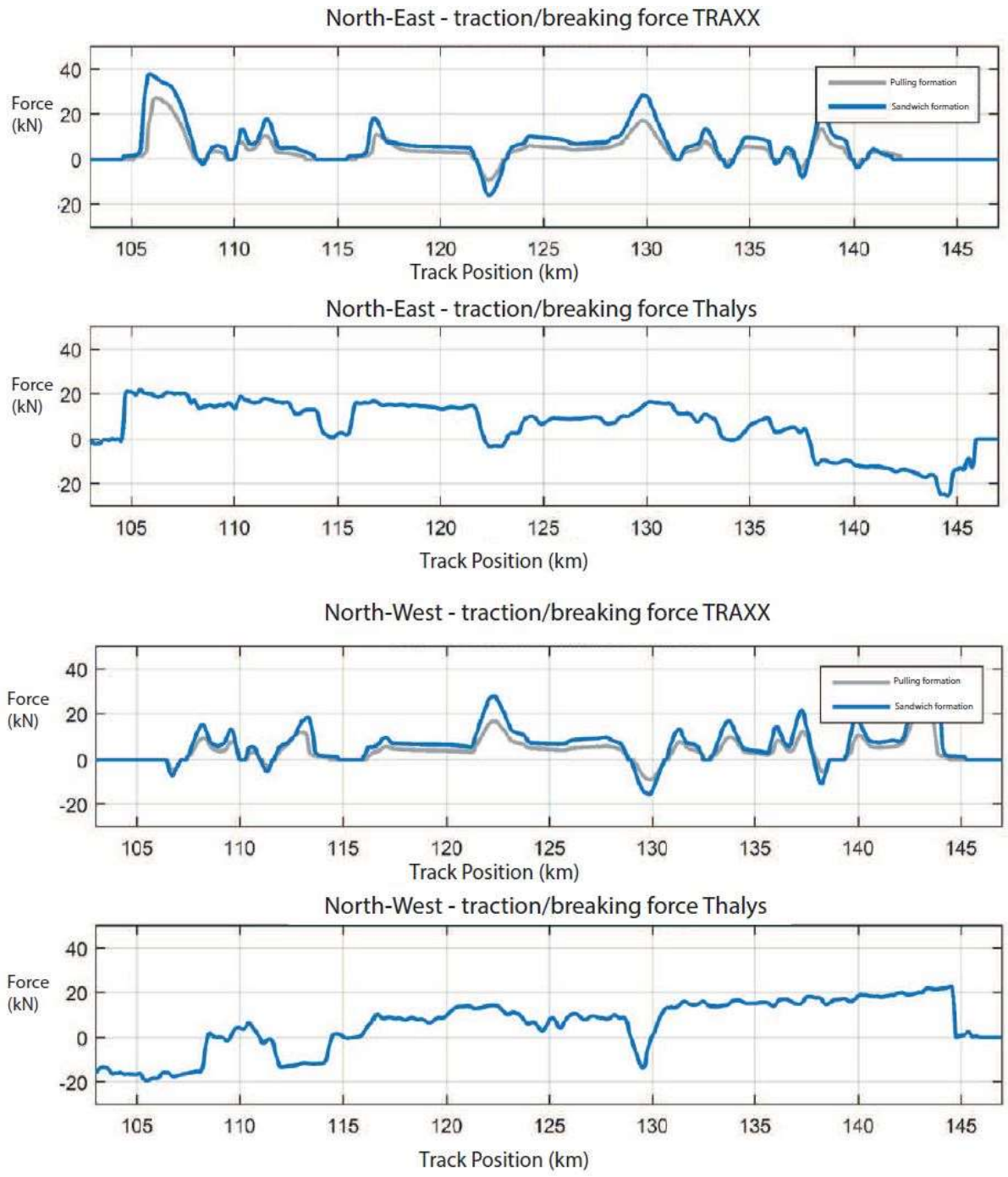

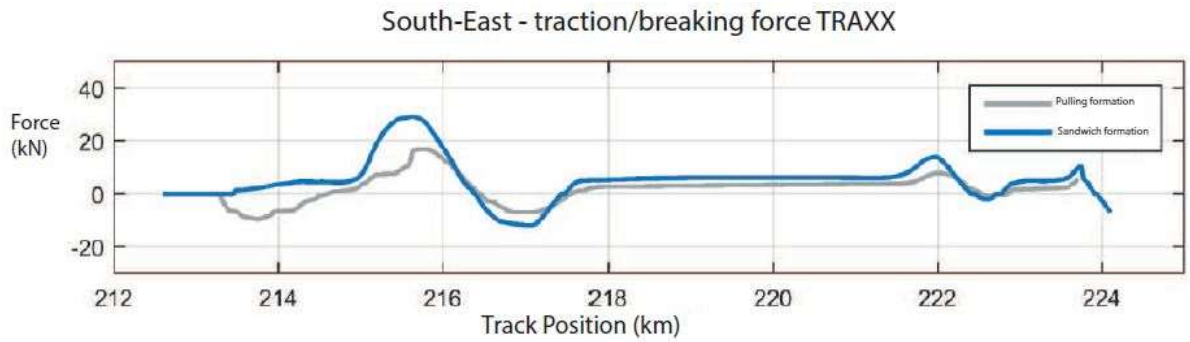
South-East - traction/breaking force TRAXX
Force (kN)
40
20
0
-20
212
214
216
218
220
222
224
Track Position (km)
Pulling formation
Sandwich formation

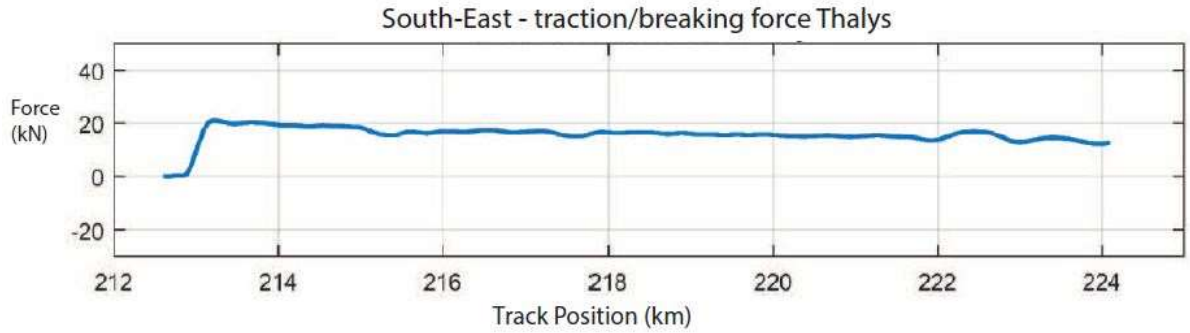
South-East - traction/breaking force Thalys
Force (kN)
40
20
0
-20
212
214
216
218
220
222
224
Track Position (km)

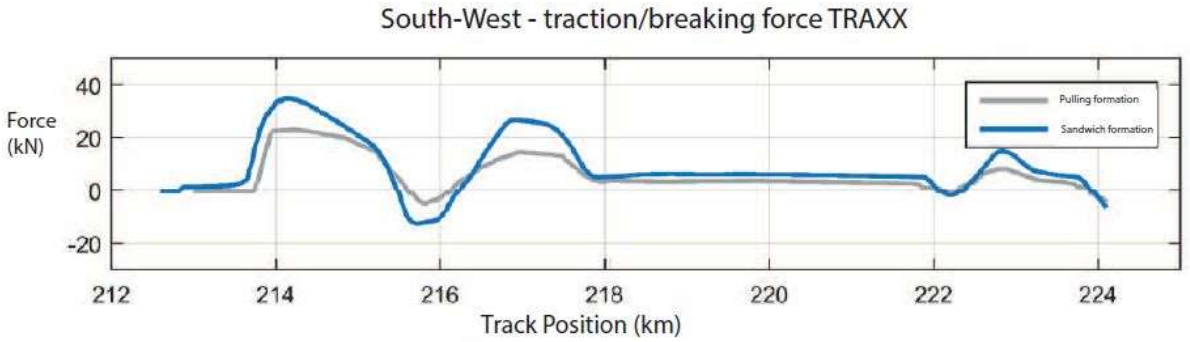
South-West - traction/breaking force TRAXX
Force (kN)
40
20
0
-20
212
214
216
218
220
222
224
Track Position (km)
Pulling formation
Sandwich formation


South-West - traction/breaking force Thalys
Force (kN)
40
20
0
-20
212
214
216
218
220
222
224
Track Position (km)

Appendix E. Cant excess related to ground areas

Cant excess Northeast track

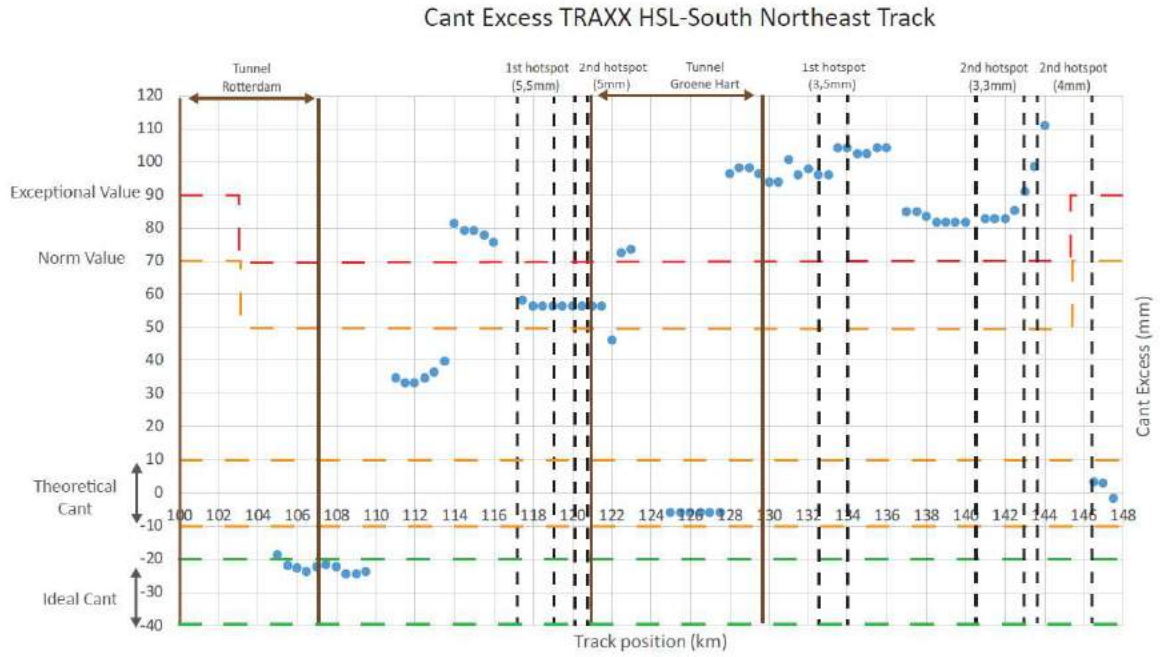

Cant excess Northwest track

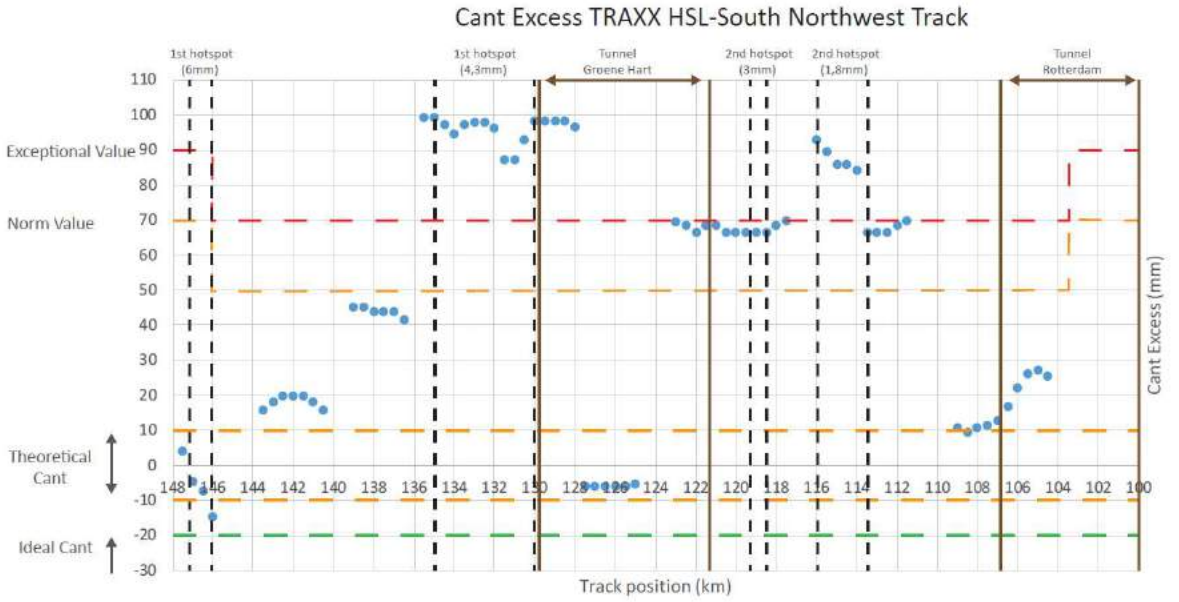

Cant Excess Southeast track

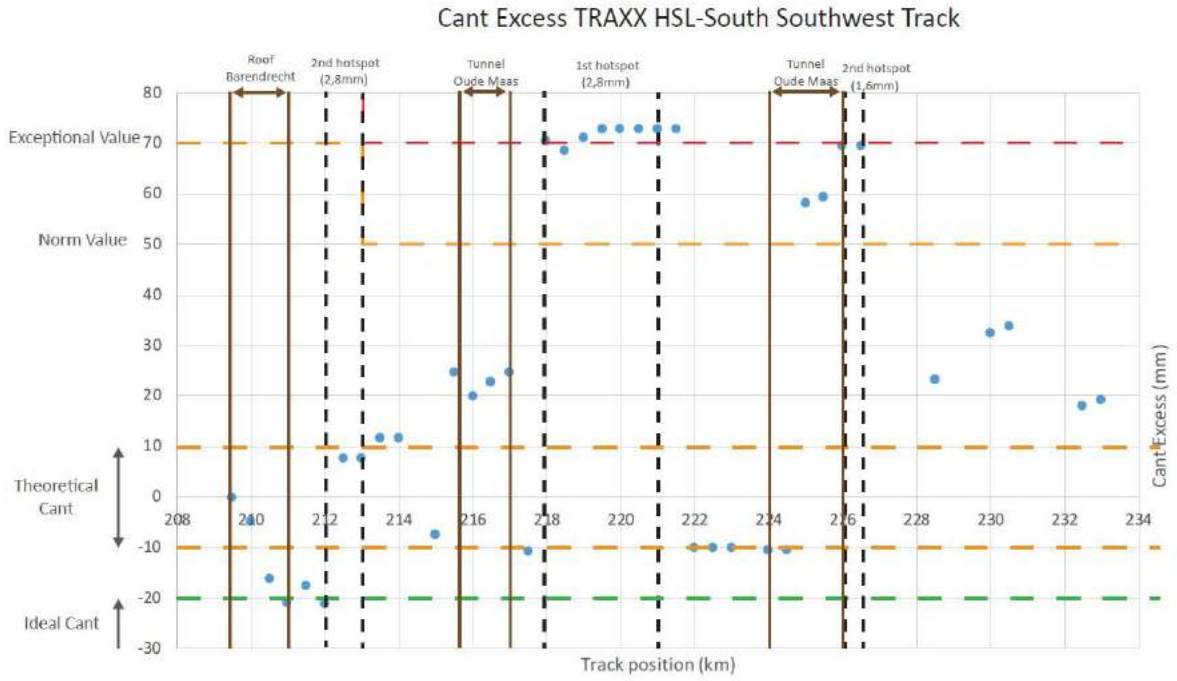

Cant excess Southwest

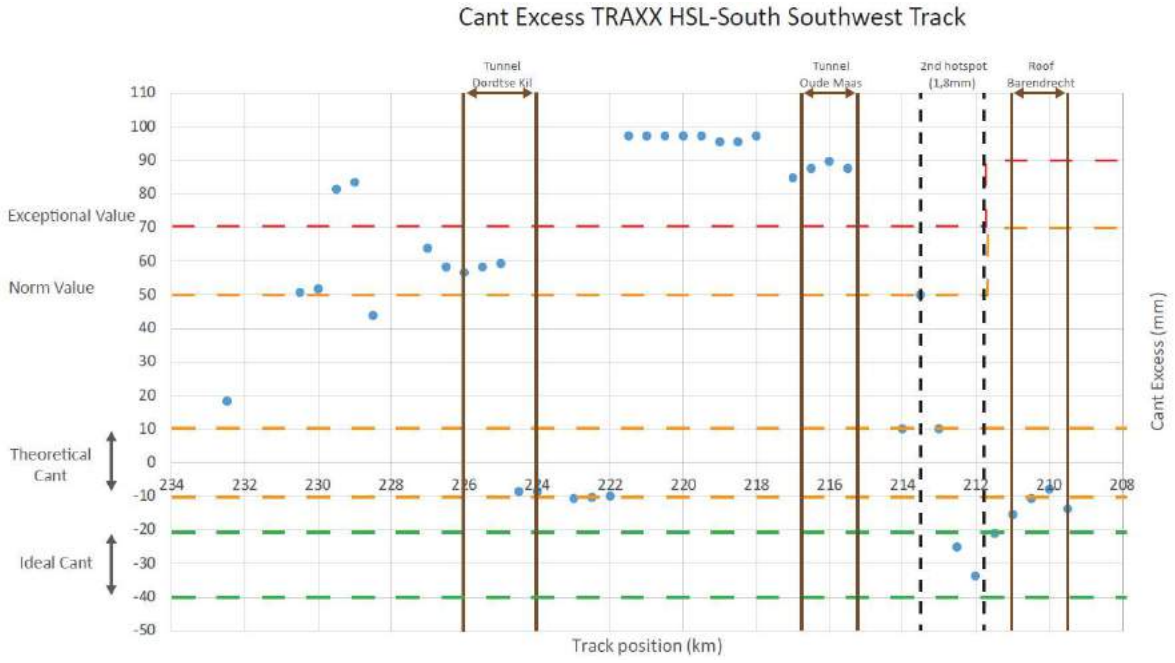

Appendix F. Traction related to ground areas

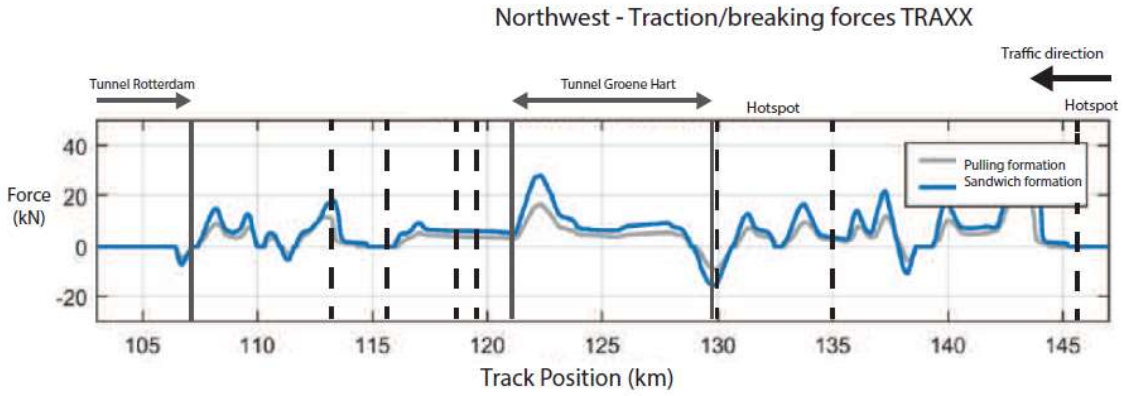

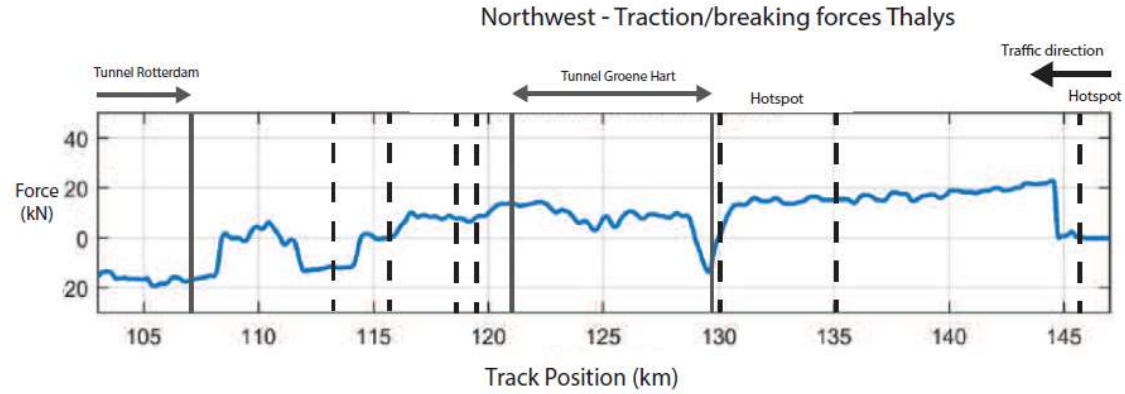

Appendix G. Determining where the damages occur

Open track

Zoetermeer

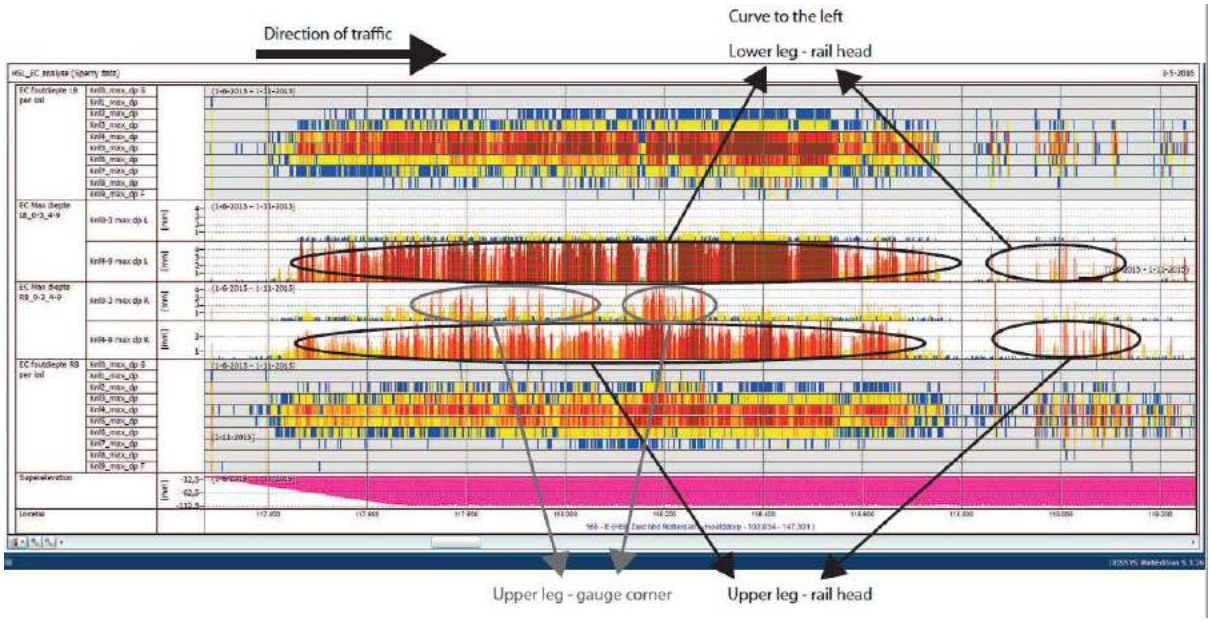

SW 218-221

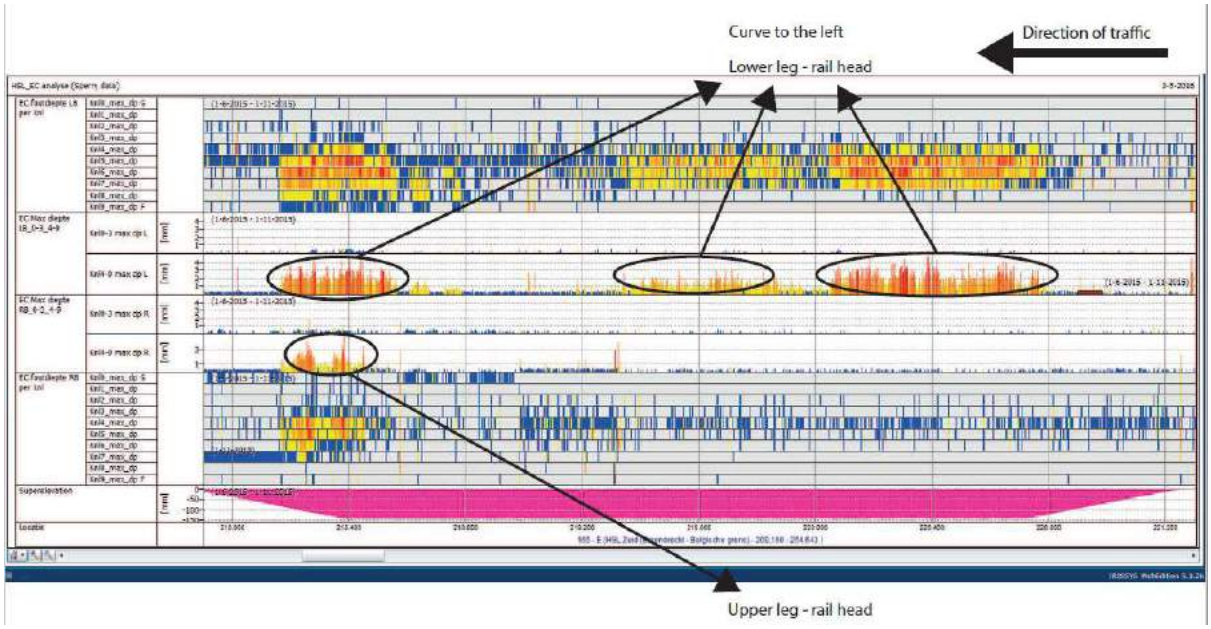

Entry zone

Hoofddorp

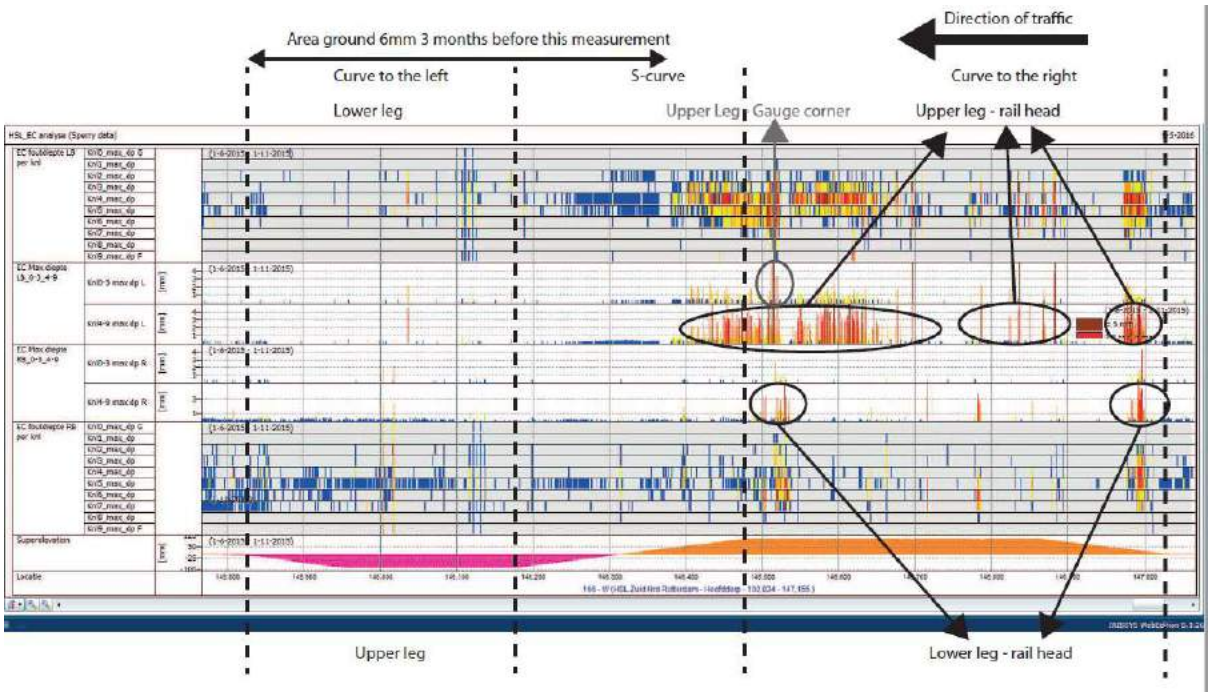

Turnout 300-301

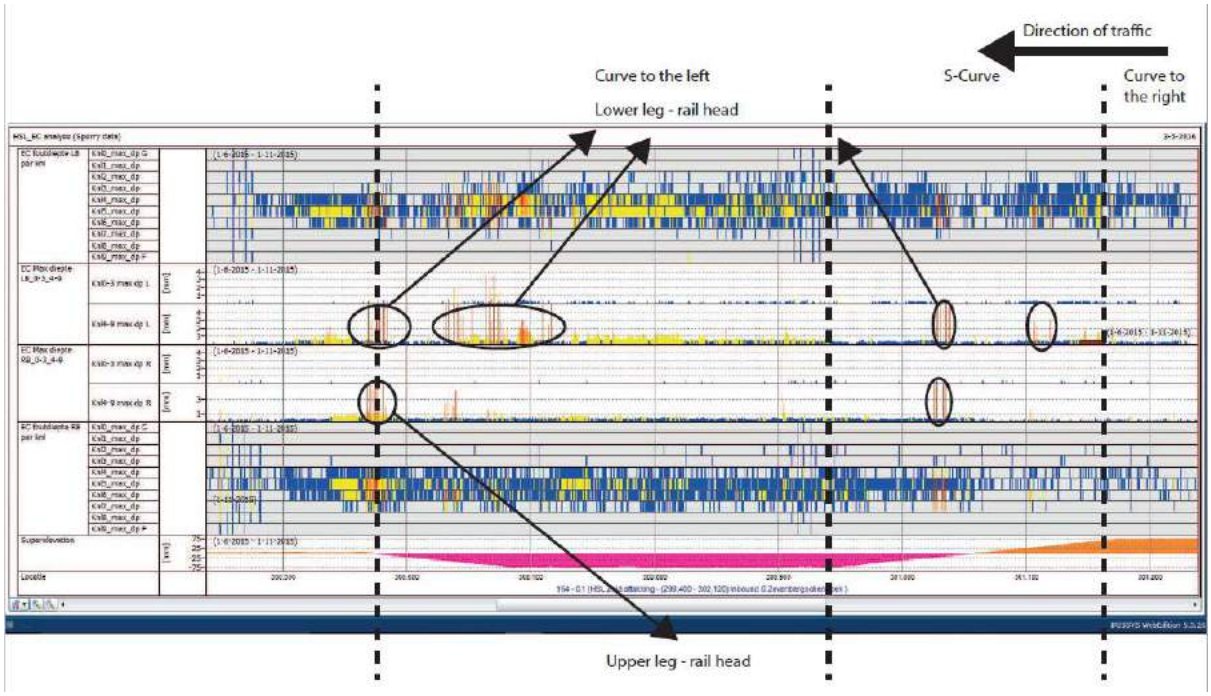

Appendix G. Eddy current measurements hypothesis check

NW 110.781-113.485

No traction by the Thalys present. This can be explained because this curve lies in the rolling out area of the Thalys in the direction of Rotterdam. We see two large damages at the beginning of the curve at the upper leg.

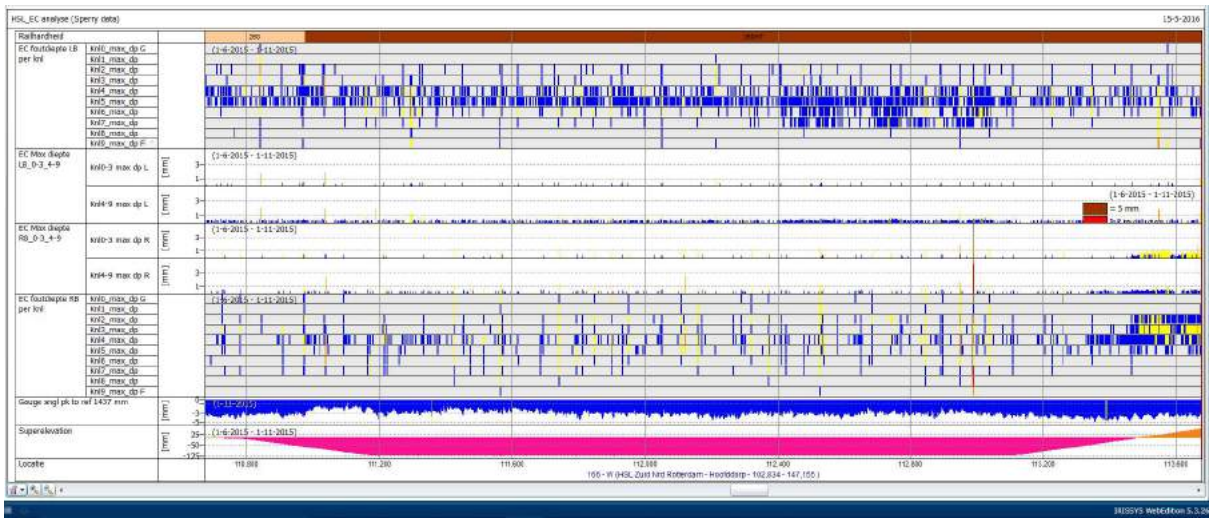

NW 113.485-115.945

At this curve there is no traction from both trains this is because there is a phase lock located around km 115 We see no damages larger than 3mm. Though we see some smaller damages at the beginning and ending of the curve which is concentrated at the lower leg.

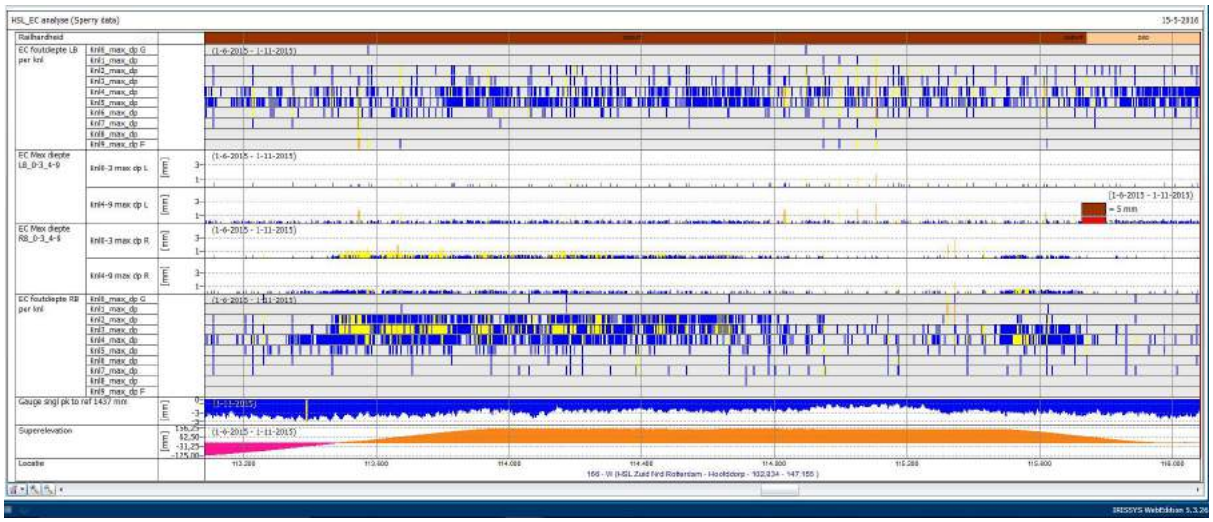

NW 117.216-121.709

Here we see different larger damages at the transition to the full curve, these are mainly located at the upper leg. Also there are more damages at the full curve spread among the upper- and lower leg. At the end of the curve (low km's) the damages mainly occur at the lower leg.

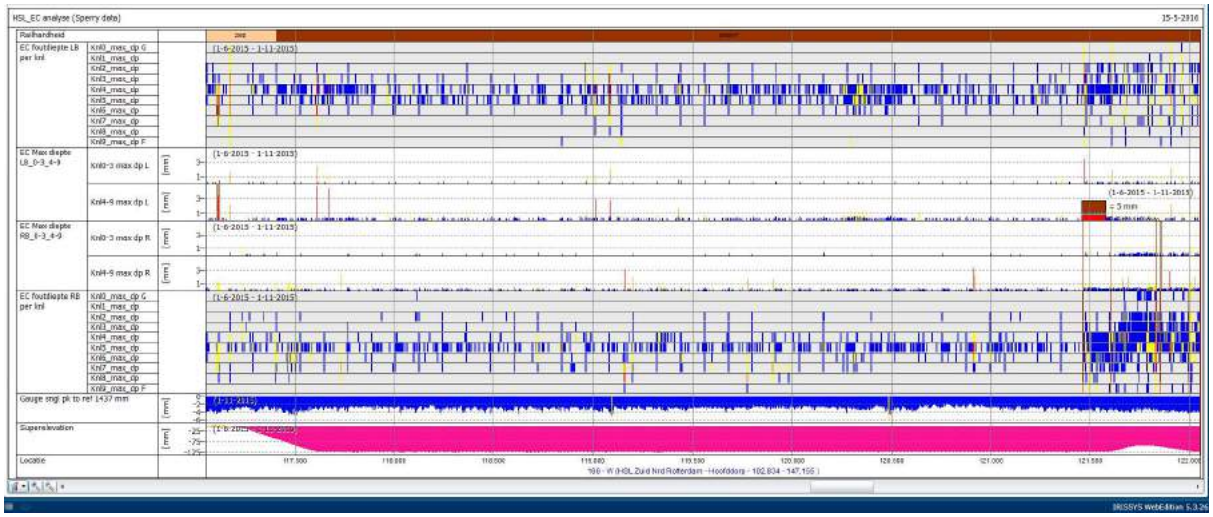

NE 113.485-115.945

No traction by the TRAXX at this hotspot and only traction by the Thalys at the beginning of the curve because of a phase lock which located around km 115. There are 3 damages of more than 3mm among the curve from which 2 lie on the upper leg and 1 on the lower leg of the curve.

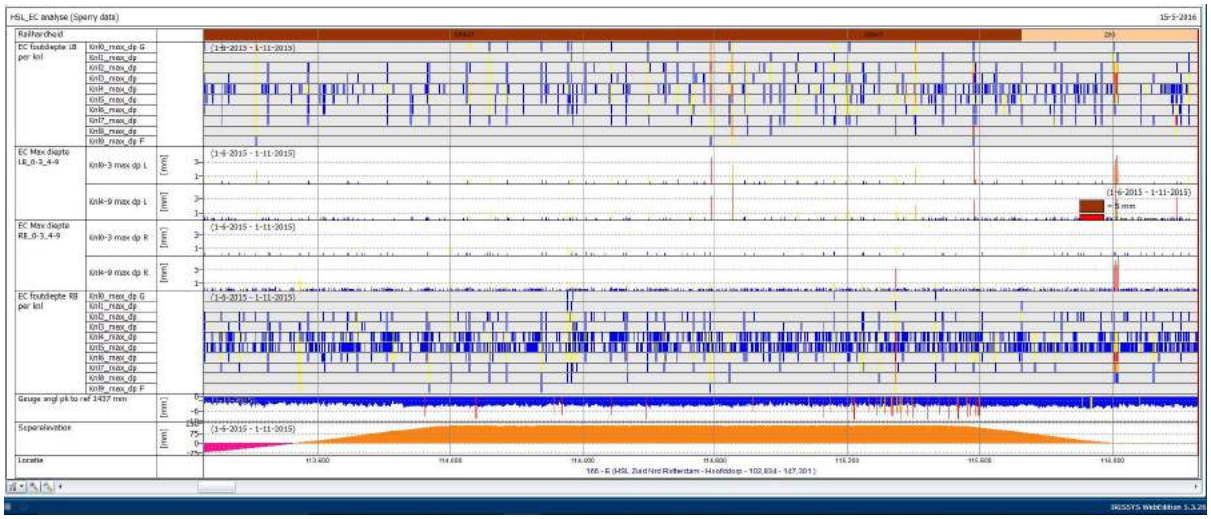

NE 130.399-130.982 & NE 130.982-132.685

4 damages from which 3 are located at the lower leg and 1 on the upper leg of the rails. Also we see different smaller damages at the beginning of the curve. Also we see a sudden transition between the results at the beginning of the curves. This can be explained because the curve has been measured in two series of measurements. The walking stick was probably differently calibrated. Further it strikes that both curves transition into each other there is a very small difference in canting (10mm) and radius (150).

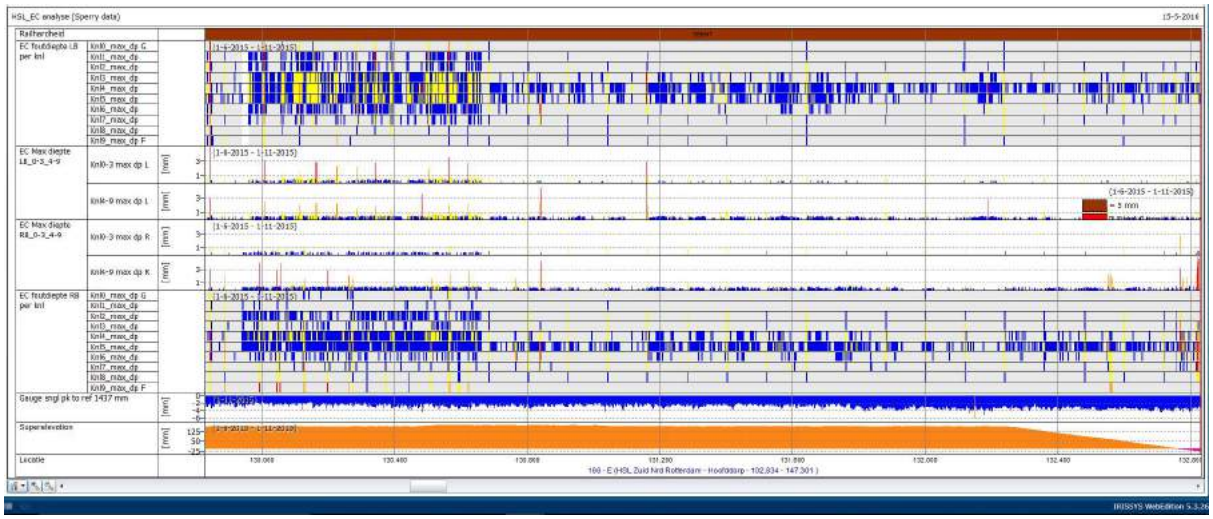

NE 136.375-138.971

No traction by the Thalys is present here. Which can be explained because the Thalys enters the rolling out zone just before this curve. We see 5 larger than 3mm here at the start of the curve from which 3 are located at the upper leg and 2 at the lower leg.

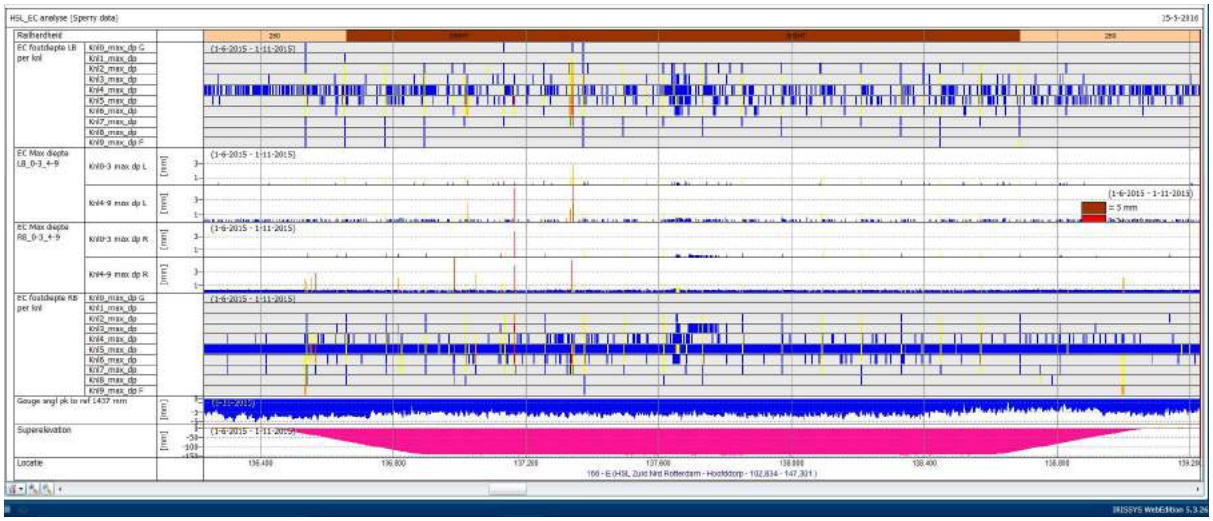

NE 140.028-143.499

Here we have no traction by the Thalys. We see several larger damages at the upper leg at the beginning of the curve. It further is remarkable that halfway the curve there seems to be a larger concentration of (smaller) damages is located at the lower leg. This curve shows much resemblances with other hotspots though the damages seem to be smaller.

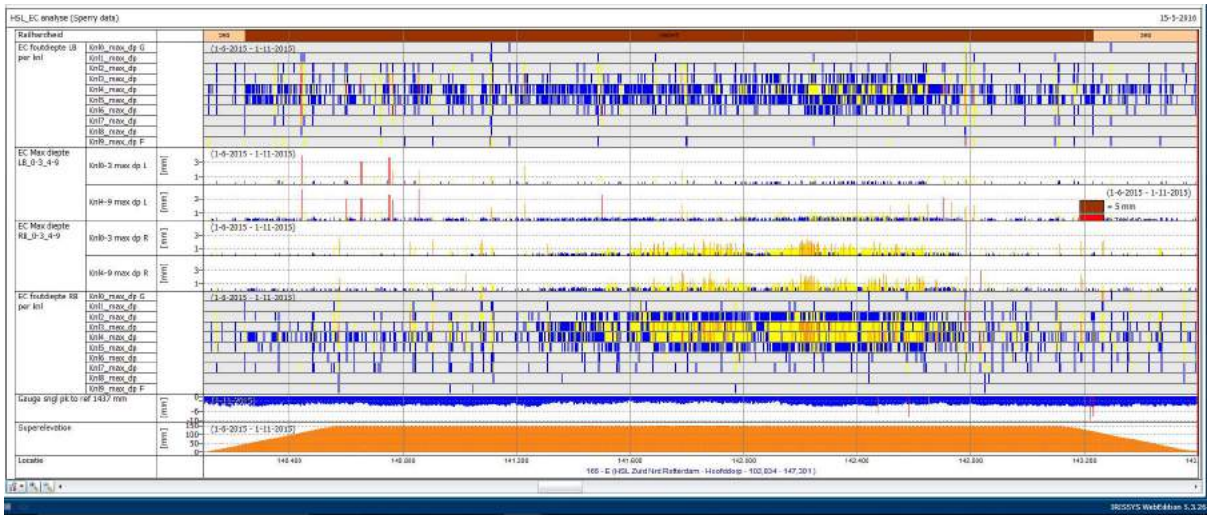

SW 217.896-221.269

Some damages at both the railhead of the lower and upper leg. Especially at the full curve, but way less than at the opposite curve which is a hotspot.

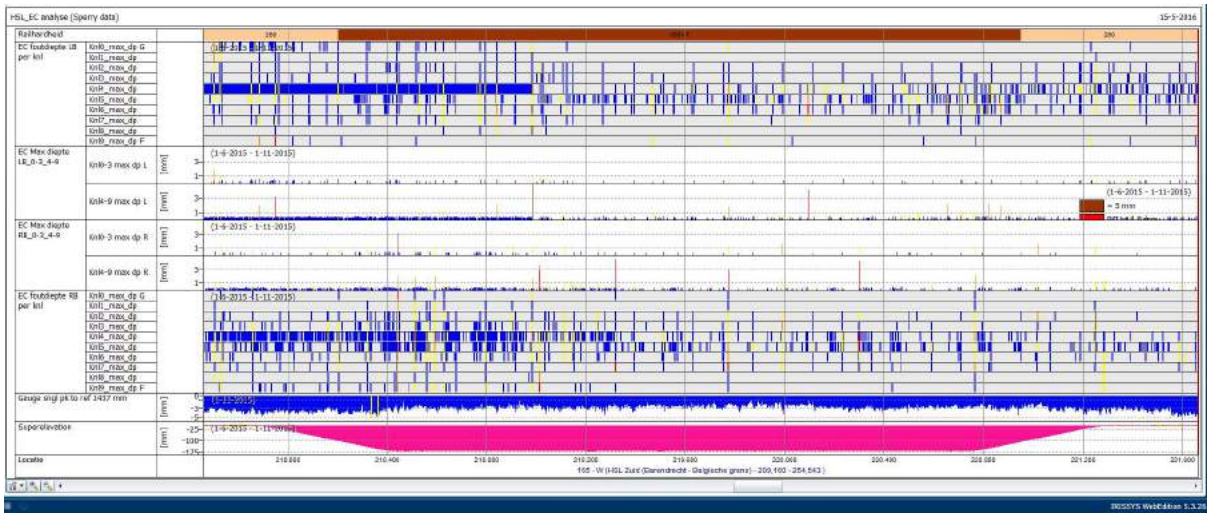

SW 228.817-229.788

One damage at the start of the curve at the lower leg at the railhead. 260 rail grade has been used in this curve. Channel 5 and 7 of the walking stick at the right leg seems to differ in sensitivity compared to the other channels.

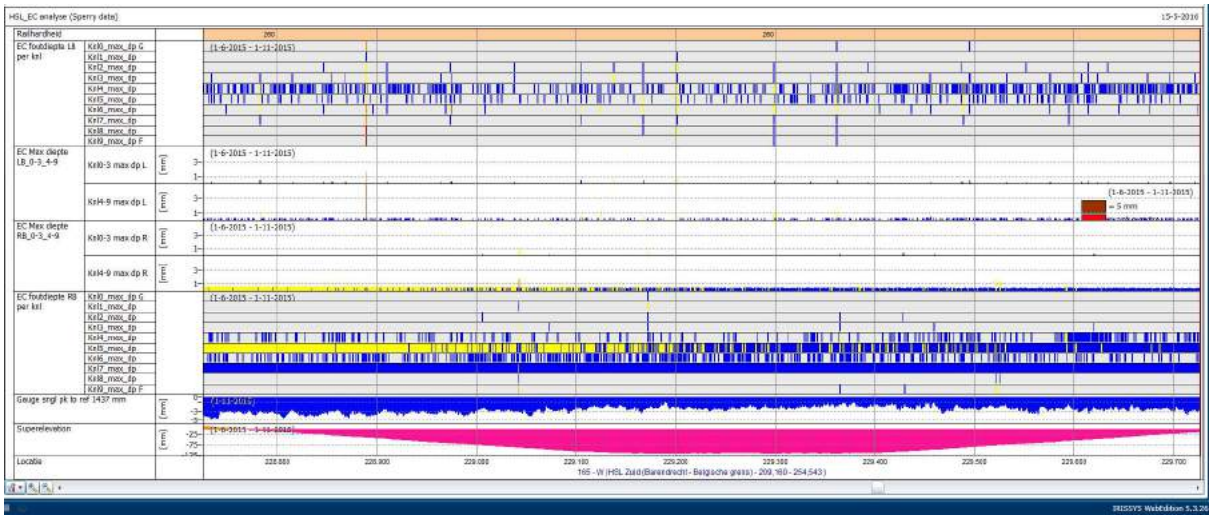

SW 229.788-230.454

The 260 rail grade has been used here, we see no large damages here. Channel 5 and 7 at the right leg of the walking stick seems to differ in sensitivity compared to the rest of the channels.

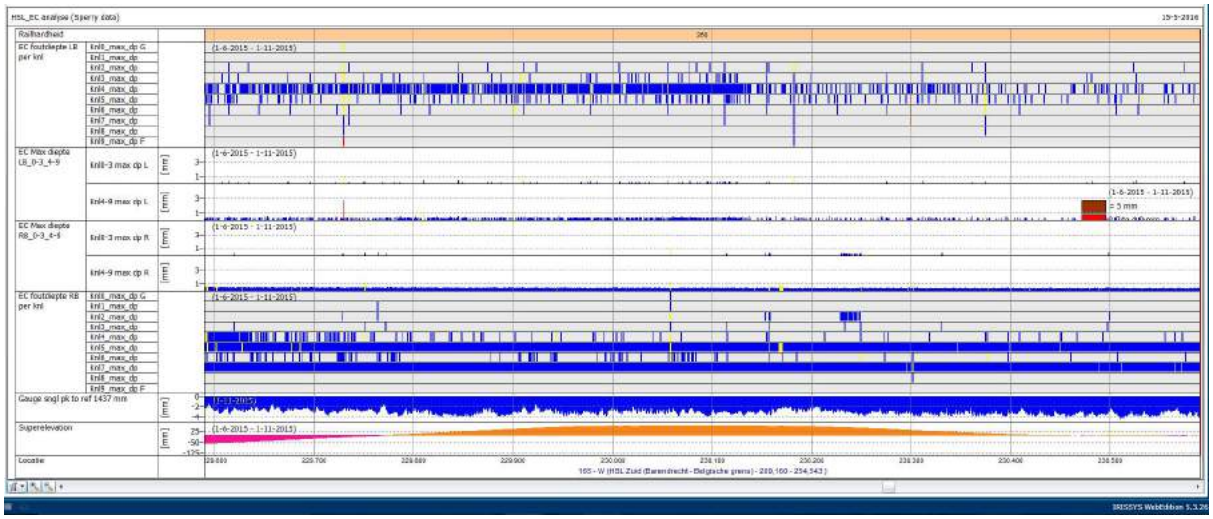

SE 225.889-226.523

Several damages located at the start and the end of the curve.

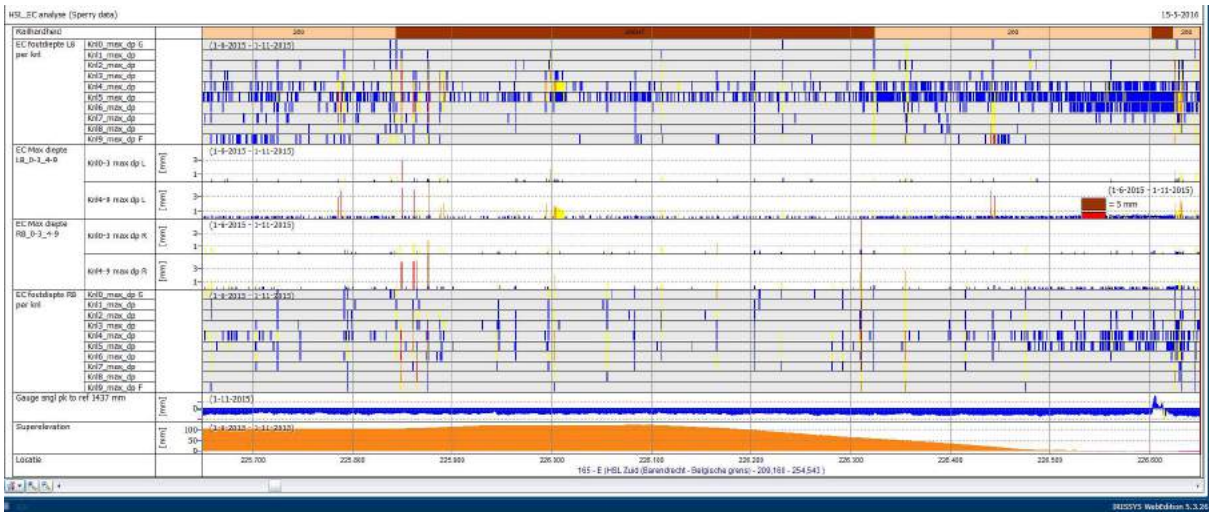

SE 228.118-228.817

No traction by the TRAXX only one damage at the start of the curve on the upper leg.